

# Pellino-2 intracellular localization and inflammasome overactivation in skin and corneal disease

---

Ileana Cristea

Thesis for the degree of Philosophiae Doctor (PhD)  
University of Bergen, Norway  
2021

UNIVERSITY OF BERGEN



# **Pellino-2 intracellular localization and inflammasome overactivation in skin and corneal disease**

Ileana Cristea



Thesis for the degree of Philosophiae Doctor (PhD)  
at the University of Bergen

Date of defense: 17.12.2021

© Copyright Ileana Cristea

The material in this publication is covered by the provisions of the Copyright Act.

Year: 2021

Title: Pellino-2 intracellular localization and inflammasome overactivation in skin and corneal disease

Name: Ileana Cristea

Print: Skipnes Kommunikasjon / University of Bergen

This work is dedicated to:

*Mihai Oancea (†2020)*  
*Ileana Gheorghief (†2020)*  
*Liviu Boşneag (†2021)*



*“There are known knowns; there are things we know we know. We also know there are known unknowns; that is to say we know there are some things we do not know. But there are also un-known unknowns—the ones we don’t know we don’t know.”*

Donald Rumsfeld

*“If we knew what it was we were doing, it would not be called research, would it?”*

Albert Einstein



## Table of contents

<b>SCIENTIFIC ENVIRONMENT</b> .....	<b>III</b>
<b>ACKNOWLEDGMENTS</b> .....	<b>V</b>
<b>LIST OF PUBLICATIONS</b> .....	<b>VII</b>
<b>LIST OF ABBREVIATIONS</b> .....	<b>IX</b>
<b>SUMMARY</b> .....	<b>1</b>
<b>INTRODUCTION</b> .....	<b>3</b>
1.1.    INFLAMMATION .....	3
1.2.    THE IMMUNE SYSTEM .....	4
1.2.1. <i>The innate immune system</i> .....	4
1.2.2. <i>Pattern-recognition receptors (PRRs)</i> .....	6
1.2.2.1.    PRR ligands .....	7
1.2.3. <i>Toll-like receptors (TLRs) signaling</i> .....	7
1.3.    THE PELLINO FAMILY OF PROTEINS .....	8
1.3.1. <i>The role of E3 ubiquitin ligases in ubiquitination</i> .....	11
1.3.2. <i>Pellino-1 and Pellino-3</i> .....	12
1.3.3. <i>Pellino-2</i> .....	14
1.3.3.1.    Localization.....	14
1.3.3.2.    Structure.....	15
1.3.3.3.    Interaction partners .....	16
1.3.3.4.    Function.....	17
1.3.4. <i>Pellino-related diseases</i> .....	18
1.4.    THE NLRP3 INFLAMMASOME .....	19
1.4.1. <i>Priming the NLRP3 inflammasome</i> .....	21
1.4.2. <i>Activating the NLRP3 inflammasome</i> .....	22
1.4.2.1.    K <sup>+</sup> efflux .....	23
1.4.2.1.1.    Intracellular vs extracellular concentrations of K <sup>+</sup> .....	23
1.4.2.1.2.    K <sup>+</sup> in different compartments inside the cell.....	24
1.4.3. <i>Inhibition of the NLRP3 inflammasome</i> .....	24
1.4.4. <i>Regulating the NLRP3 inflammasome</i> .....	25
1.4.4.1.    Ubiquitination.....	26
1.4.4.2.    NLRP3 regulation by interaction partners .....	26
1.4.5. <i>NLRP3-linked diseases</i> .....	27
1.5.    OCULAR PTERYGIUM-DIGITAL KELOIDS DYSPLASIA (OPDKD) .....	29
1.5.1. <i>Disease characteristics</i> .....	29
1.5.1.1.    Pterygium .....	29
1.5.1.2.    Keloids .....	32
1.5.2. <i>OPDKD epidemiology and patient description</i> .....	33
1.5.3. <i>Pathogenesis and pathophysiology of OPDKD</i> .....	34
<b>AIMS</b> .....	<b>37</b>
<b>MATERIALS AND METHODS</b> .....	<b>39</b>
3.1.    ETHICAL CONSIDERATIONS (PAPER 1 & 3) .....	39
3.2.    EXPRESSION VECTORS (PAPER 1, 2 & 3).....	39



3.3. TRIO EXOME SEQUENCING (PAPER 3).....	39
3.4. GENERATION OF TRANSDUCED CELL LINES (PAPER 2 & 3) .....	40
3.5. CELL CULTURE (PAPER 1, 2 & 3).....	40
3.6. DRUG TREATMENTS.....	41
3.6.1. <i>Macrophages (paper 1)</i> .....	41
3.6.2. <i>K<sup>+</sup> efflux (paper 2)</i> .....	41
3.6.3. <i>Cycloheximide chase assay (paper 3)</i> .....	42
3.7. IMMUNOFLUORESCENCE (PAPER 1, 2 & 3) .....	42
3.8. TRANSIENT TRANSFECTION, CELL LYSIS AND CO-IMMUNOPRECIPITATION (PAPER 1, 2 & 3) .....	43
3.9. SUBCELLULAR FRACTIONATION (PAPER 2) .....	43
3.10. YEAST TWO-HYBRID SCREEN (PAPER 2).....	45
3.11. IMMUNOBLOTTING (PAPER 1, 2 & 3) .....	45
3.12. ELISA (PAPER 1 & 3) .....	46
3.13. CELL VIABILITY ASSAY (PAPER 1 & 3).....	46
3.14. LIVE IMAGING (PAPER 2) .....	47
3.15. IMAGE ACQUISITION AND ANALYSIS (PAPER 1, 2 & 3) .....	47
3.16. STATISTICAL ANALYSIS AND REPRODUCIBILITY (PAPER 1, 2 & 3).....	47
<b>RESULTS.....</b>	<b>49</b>
4.1. PAPER 1.....	49
4.2. PAPER 2.....	50
4.3. PAPER 3.....	52
<b>DISCUSSION .....</b>	<b>55</b>
5.1. PELLINO-2 IN NON-IMMUNE CELLS .....	55
5.2. PELLINO-2 IN IMMUNE CELLS .....	56
5.3. PELLINO-2 IS A K <sup>+</sup> SENSOR .....	57
5.4. PELLINO-2 AND NOVEL INTERACTION PARTNERS .....	58
5.5. PELLINO-2 IN DISEASE .....	60
<b>CONCLUSIONS AND FUTURE PERSPECTIVES.....</b>	<b>64</b>
<b>REFERENCES.....</b>	<b>66</b>
<b>APPENDIX .....</b>	<b>82</b>

## **Scientific environment**

The work presented in this thesis was initiated in June 2016 and was conducted at the Department of Clinical Medicine, Faculty of Medicine, University of Bergen, Bergen, Norway.

The main supervisor was Associate Professor Cecilie Bredrup MD PhD, and the co-supervisor was Professor Eyvind Rødahl MD PhD.

The PhD fellowship was funded by grants from the University of Bergen, and I was enrolled as a PhD student in the Postgraduate School of Clinical Medical Research, University of Bergen, Norway.



## Acknowledgments

I wish to extend my sincere gratitude to all those who contributed to the culmination of this work. I wish I had the space to thank everyone by name, who along the course of my life and academic years, have believed in me and encouraged me, from Deva to Cluj to Bonn to Eindhoven to Bergen. Teachers, mentors, family, friends, I have you all in my heart!

I will start by expressing my utmost gratitude to my main supervisor and mentor, assoc. prof. Cecilie Bredrup. Thank you for a lovely PhD project and a lovely PhD experience. Few can honestly say, like me, that they've enjoyed their PhD period. Thank you for sharing your experience with me and helping me make sense of my own experiences, thank you for helping me ask better questions and especially for helping me find my own path. Thank you for your time and dedication to the project, as well as to our relationship. I couldn't have asked for a better mentor!

The next person I wish to convey my gratitude to is prof. Eyvind Rødahl. A treasure chest of knowledge and wisdom, you have always driven me to do better and be better, ask more and look deeper. I am so grateful for the close supervision and the regular discussions on the project, and always having your door open for me.

My particular thanks go to Ove Bruland for sharing his expertise with me all these years, for troubleshooting experiments with me and for much of the experimental work that this project is based on. Furthermore, I would like to thank the Department of Medical Genetics, at Haukeland University Hospital, Bergen for providing their scientific, personal and technical support.

Next on the list is Anne Mellgren, and whoever knows Anne, knows she is Wonder-Woman: co-author, colleague, friend, head of the super-mom club, shoulder to cry on and chocolate supplier, Anne has done it all for me. And for all that, I really have no words to thank you!

Another special “thank you!” goes to Unni Larsen, for her help in day-to-day experiments, for making my laboratory work as painless as possible, and all her support and kindness till the end of the project.

Many thanks go to all the coauthors who have had valuable contributions to the papers included in this thesis. Especially Ingvild Aukrust has been a trusted collaborator.

Additionally, prof. Jaakko Saraste, from the Molecular Imaging Center, Department of Biomedicine, Faculty of Medicine, has been a close collaborator to the project and has had invaluable input for the experiments presented in the thesis. A special thanks to Hege Dale and Endy Spriet at MIC for their assistance and fruitful discussions.

I would like to thank the staff and students at the Ophthalmogenetics Research Group: Linda, Titas, Roya, Ida, for your friendship, hiking trips and lovely discussions about everything from academics to immigration regulations.

To all the staff at the Department of Ophthalmology, at Haukeland University Hospital, Bergen, and especially to Kjetil Sævartveit, Frank Jenssen and Ragnhild Wivestad Jansson, thank you for a lovely work environment, for the technical support, and for the cake parties and pølse parties ever so often!

I also wish to thank my friends for their moral support: Viorela and Andrei, Yiommo and Tommy, Sadaf and Novin, Flavia and Buz, Nigar, Alexandra, Henriette, Raquel, Ewa, Ingebjørg and Stig. Thank you for being my family away from home.

I am also grateful to my parents and relatives, especially Angelica and her loving family, for their support and help throughout the whole of my life!

Lastly, the most important for me, my husband and daughter: I want to thank you for your understanding during these recent stressful times. You mean the world to me!

## **List of publications**

### **Article I**

#### **K<sup>+</sup> regulates relocation of Pellino-2 to the site of NLRP3 inflammasome activation in macrophages**

Authors: Ileana Cristea, Ove Bruland, Eyvind Rødahl, Cecilie Bredrup

Publication: FEBS Letters - doi.org/10.1002/1873-3468.14176

### **Article II**

#### **Pellino-2 in nonimmune cells: novel interaction partners and intracellular localization**

Authors: Ileana Cristea, Ove Bruland, Ingvild Aukrust, Eyvind Rødahl, Cecilie Bredrup

Publication: FEBS Letters – doi.org/10.002/1873-3468.14212

### **Article III**

#### **A *de novo* PELI2 variant associated with constitutive NLRP3 inflammasome activation**

Authors: Ileana Cristea, Hugo Abarca, Anne EC Mellgren, Roya Mehrasa, Gunnar Houge, Raoul CM Hennekam, Eyvind Rødahl, Ove Bruland, Cecilie Bredrup

Publication: manuscript

*The published article is reprinted with permission from the publisher.*



## List of abbreviations

Å	angstrom ( $10^{-10}$ m)
AIM-2	absent in melanoma 2
ADP	adenosine diphosphate
Ala	alanine amino acid
Arg	arginine amino acid
Asn	asparagine amino acid
AP1	activating protein 1
ASC	apoptosis-associated speck-like protein
ATP	adenosine triphosphate
ATPIF1	ATPase inhibitory factor 1
BCL10	B-cell lymphoma/leukemia 10
BHB	beta-hydroxy-butyrate
BMDMs	bone marrow derived macrophages
Ca <sup>2+</sup>	calcium ions
CAPS	cryopyrin-associated periodic syndrome
CARD	caspase activation and recruitment domain
CCP110	centriolar coiled-coil protein of 110 kDa
cDNA	complementary deoxyribonucleic acid
CINCA	chronic infantile neurological cutaneous and articular syndrome
CLRs	C-type lectin receptors
CO	carbon monoxide
COPs	CARD-only proteins
CREB	cAMP response element-binding protein
Cys	cysteine amino acid
DAMPs	danger-associated molecular patterns
DDR2	discoidin domain-containing receptor 2
DUBs	deubiquitinating enzymes
DVL-2	dishevelled homolog 2
EAE	experimental autoimmune encephalomyelitis



ELISA	enzyme-linked immunosorbent assay
ELK1	ETS Like-1 protein
ERKs	extracellular signal-regulated kinases
FCAS	familial cold autoinflammatory syndrome
FBXL2	F-box/LRR-repeat protein 2
FHA	fork-head associated domain
FMD2	frontometaphyseal dysplasia 2
GFP	green fluorescent protein
HECT	homologous to the E6-AP carboxyl terminus
HEK293	human embryonic kidney cells 293
HEK293-EBNA1	HEK293 cells stably expressing the Epstein-Barr virus nuclear antigen-1
HIF-1 $\alpha$	hypoxia inducible factor 1 $\alpha$
His	histidine amino acid
HMGB1	high mobility group box 1 protein
IFN	interferons
IKK	inhibitor of nuclear factor-kB (NF-kB) kinase
IL-1 $\beta$	interleukin 1 $\beta$
IL-6	interleukin 6
IL-8	interleukin 8
IL-1R	interleukin 1 receptor
Ile	isoleucine amino acid
IRAK-1	interleukin-1 receptor associated kinase 1
IRAK-4	interleukin-1 receptor associated kinase 4
IRS-1	insulin receptor substrate 1
JNKs	c-Jun N-terminal kinases
K <sup>+</sup>	potassium ions
K <sub>ATP</sub>	ATP-sensitive potassium channel
KCl	potassium chloride
KFH	keratoendoteliitis (keratitis) fugax hereditaria
K <sub>v</sub> 1.3	potassium voltage gated channel 1.3

LAMP1	lysosomal-associated membrane protein 1
LC3B	microtubule-associated proteins 1A/1B light chain 3B
LPS	lipopolysaccharide
LRRs	leucine-rich repeats
Lys	lysine amino acid
MAD	multiwavelength anomalous dispersion
MAP3K7	mitogen-activated protein kinase kinase kinase 7
MAPKs	mitogen-activated protein kinases
Met	methionine amino acid
mitoK <sub>ATP</sub>	mitochondrial ATP-sensitive potassium channel
miRNA	micro ribonucleic acid
mM	millimolar
MMPs	matrix metalloproteases
mRNA	messenger ribonucleic acid
MWS	Muckle-Wells syndrome
MyD88	myeloid differentiation primary response protein 88
NACHT/NBD	nucleotide binding domain
NEK7	NIMA related kinase 7
NEK9	NIMA related kinase 9
NF-κB	nuclear factor-κB
NLRs	NOD-like receptors
NO	nitric oxide
NOD	nucleotide-binding oligomerization domain
OPDKD	ocular pterygium-digital keloid dysplasia
PAMPs	pathogen-associated molecular patterns
PB	phosphate buffer
PBS	phosphate buffer saline
PCNA	proliferating cell nuclear antigen
PDGFRβ	platelet-derived growth factor receptor β
PHD	plant homeo-domain
Phe	phenylalanine amino acid

PLC $\gamma$	phospholipase C gamma
PML	promyelocytic leukemia bodies
POPs	PYD-only proteins
PP2A	protein phosphatase 2A
PRRs	pattern recognition receptors
pThr	phosphor-threonine amino acid
PTPN22	protein tyrosine phosphatase, non-receptor type 22
PYD	pyrin domain
RING	really interesting new gene zinc finger domain
RIP1	receptor-interacting serine-threonine kinase 1
RLRs	retinoic acid-inducible gene (RIG)-like receptors
RNAi	RNA interference
ROBO-1	roundabout homolog 1
ROS	reactive oxygen species
RTK	receptor tyrosine kinase
Ser	serine amino acid
siRNA	small interfering RNA
SNPs	single nucleotide polymorphisms
STAT1	signal transducer and activator of transcription 1
TAB1	TGF-activated protein kinase 1 binding protein 1
TAB2	TGF-activated protein kinase 1 binding protein 2
TAK-1	transforming growth factor $\beta$ (TGF $\beta$ )-activated kinase 1
TEA	tetraethylammonium
TEWL	trans-epidermal water loss
TGF $\beta$	transforming growth factor beta
Thr	threonine amino acid
TIMPs	tissue inhibitors of matrix metalloproteases
TIR	toll-interleukin-1-receptor resistance domain
TLRs	toll-like receptors
TMEM175	transmembrane protein 175
TNF $\alpha$	tumor necrosis factor alpha

TNFR	tumor necrosis factor receptor
TOMM20	translocase of outer mitochondrial membrane 20
TRAF6	tumor necrosis factor receptor (TNFR)-associated factor 6
TRAF7	tumor necrosis factor receptor (TNFR)-associated factor 7
TRIC	trimeric intracellular cation
TRIF	TIR-domain-containing adapter-inducing interferon- $\beta$
TWIK2	two-pore domain K <sup>+</sup> channel
Tyr	tyrosine amino acid
UV	ultraviolet



## Summary

**Background:** Ocular pterygium-digital keloids dysplasia (OPDKD) is a rare, genetic disorder characterized by early onset corneal overgrowth and later development of keloids on distal limbs. We identified a *de novo* *PELI2* germline mutation in a family with OPDKD. Pellino-2 is part of the Pellino family of E3 ubiquitin ligases, involved in the innate immune system. Pellino-2 has been linked to the activation of the NLRP3 inflammasome.

**Objectives:** Little was known about Pellino-2 at the beginning of this project. The overall aim of this thesis has been to examine Pellino-2 in greater detail with particular focus on how the identified mutation could lead to OPDKD.

Aims paper 1: To analyze the interplay between Pellino-2 and NLRP3 in the activation of the NLRP3 inflammasome.

Aims paper 2: To identify novel interaction partners of Pellino-2 and characterize Pellino-2 localization in non-immune cells.

Aims paper 3: To report and characterize the *PELI2* variant in an OPDKD patient.

## Methods:

Paper 1: Immunofluorescence, ELISA, immunoblotting

Paper 2: Yeast two-hybrid, co-immunoprecipitation, subcellular fractionation, immunoblotting, immunofluorescence, live cell imaging

Paper 3: Trio exome sequencing, immunofluorescence, co-immunoprecipitation, cycloheximide chase assay, ELISA, cell viability assay

## Results:

Paper 1: Pellino-2 was constitutively expressed in THP1-derived macrophages. Pellino-2 changed intracellular localization upon NLRP3 inflammasome activation, and co-localized with both NLRP3 protein and ASC protein in the late stages of inflammasome assembly. The interaction between Pellino-2 and NLRP3 and ASC, and thus NLRP3

inflammasome activation, was initiated by low levels of extracellular  $K^+$ . The relocation of Pellino-2 and the NLRP3 inflammasome activation was blocked by various  $K^+$  channel blockers.

Paper 2: Six novel interaction partners of Pellino-2 were identified: ROBO-1, DVL-2, NEK9, IRS-1, cyclin F and TRAF7. Pellino-2 intracellular localization was proven to be dependent on  $K^+$  efflux, also in non-immune cells. Live cell imaging confirmed that Pellino-2 is a dynamic protein, that can change intracellular localization. This provides an explanation for its interaction partners being located in various intracellular compartments.

Paper 3: In an OPDKD patient, a *de novo* *PELI2* variant c.770C>T p.(Thr257Ile) was identified. The substitution did not affect Pellino-2 intracellular localization, its binding to its interaction partners, or its stability. However, in U87MG cells transduced with the Thr257Ile variant, a constitutive activation of the NLRP3 inflammasome was observed.

### **Conclusions:**

In this thesis, we characterized endogenous Pellino-2 in immune and non-immune cells. We showed that Pellino-2 acts as a potential  $K^+$  sensor that changes intracellular localization following  $K^+$  efflux. In immune cells, Pellino-2 relocates to the activated NLRP3 inflammasome, and in non-immune cells, to the nucleus.

Further, we expanded the list of interaction partners of Pellino-2, opening new avenues of research for Pellino-2 and the signaling pathways in which these proteins are involved: cell migration via ROBO-1, epithelial-mesenchymal transition via DVL-2, insulin signaling via IRS-1, or cell division via cyclin F and NEK9. Our data suggest that Pellino-2 is a dynamic protein that can move within the cell to reach its interaction partners.

Lastly, we reported a novel mutation in *PELI2* that appears to constitutively activate the NLRP3 inflammasome. This provides a potential mechanism for inflammation and tissue overgrowth in OPDKD.

## Introduction

The theoretical background of this thesis is focused on ocular pterygium-digital keloid dysplasia (OPDKD) and the involvement of innate immunity in disease development. Pellino-2, an E3 ubiquitin ligase involved in toll-like receptor (TLR) signaling, and the NLRP3 inflammasome, involved in secretion of pro-inflammatory cytokines, are extensively presented.

### 1.1. Inflammation

Inflammation is a defense mechanism vital for health (1). Following infection or injury, tissue structure and function must be restored, and inflammation is the restorative response to such challenges (2). As a protective mechanism, a successful inflammatory response can clear an infection, eliminate a trigger and repair tissue damage, leading to the resolution of the acute inflammation (3). However, a persistent trigger or a faulty inflammatory response can lead to chronic inflammation (3). In essence, inflammation has beneficial effects on structural and functional recovery, but can also become detrimental when excessively activated.

Inflammation takes many shapes and different mechanisms govern its induction, regulation and resolution. There are four components of the inflammatory pathway: inducers, sensors, inflammatory mediators and target tissues. Combinations of these components play a role in distinct inflammatory pathways. The inducers of inflammation are either infectious (pathogens: components of bacteria, viruses, and other microorganisms), or non-infectious (biological signals from damaged cells and chemical signals from toxic compounds). The sensors that detect the inducers are components of the immune system, both innate and acquired. Inflammatory mediators are induced by the sensors (e.g. pro-inflammatory cytokines, chemokines, histamine, bradykinin, eicosanoids etc). Lastly, target tissues are affected by the inflammatory mediators (e.g. liver, skin, blood) (3).

At tissue level, immune, vascular and inflammatory responses lead to changes in vascular permeability, leucocyte migration and accumulation, followed by the release of inflammatory mediators (1).



In case of infection, the inflammatory response is mediated by the immune system upon activation of its two branches, innate and acquired immunity, with the aim of eliminating the pathogens. In case of sterile tissue injury, the inflammatory response is triggered by molecules released from dying cells or breakdown products of the extracellular matrix. This promotes tissue repair and prevents infections with opportunistic pathogens.

However, persistent antigenic stimulus, autoimmunity, long term exposure to irritants or a faulty inflammatory response can lead to chronic inflammation. The consequences of chronic inflammation are tissue damage, misdirected and incomplete repair, and cancer.

## 1.2. The immune system

The immune system represents a set of defense mechanisms against disease, integrated in a complex, dynamic and highly regulated process. The immune system can be divided, based on the speed and duration of the initial response and the specificity against the target, into two categories: the innate and the acquired immune system, equally important, but with distinct characteristics (Fig. 1).

The innate immune system is more primitive and gives a rapid and non-specific response when activated. In contrast, the acquired immune system is more sophisticated and produces a unique set of specific immune responses (antibodies and sensitized immune cells) against each individual pathogen it encounters. Thus, the function of the innate immune system is complemented and enhanced by the adaptive immunity.

### 1.2.1. The innate immune system

Innate immunity is considered the first-line barrier, providing a rapid response mechanism against invading microorganisms (viruses, bacteria, fungi, parasites). Its components are germline-encoded and are directed against molecules expressed only by microorganisms, thus differentiating them from the organism's own structures. The innate immune response is acute and is generated within 6-12 hours after exposure to the pathogen.

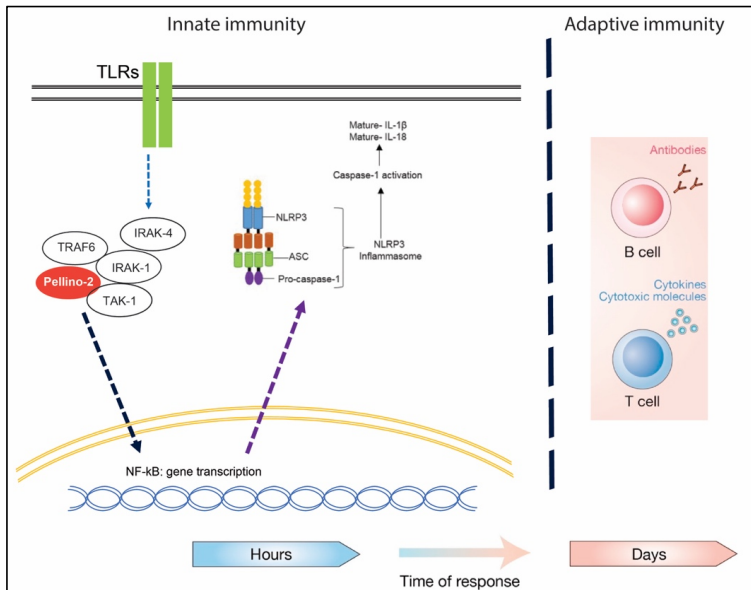


**Figure 1. The two distinct types of immune response: innate and adaptive immunity.**

As part of the innate immune system, toll-like receptors (TLRs) rapidly recognize pathogens and activate intracellular signaling cascades. Downstream of TLRs is the Pellino-2 protein, as well as the NLRP3 inflammasome, both being the focus of this thesis. Responses of the adaptive immune system include specific antibody production by B cells against target antigens, as well as secretion of cytokines and cytotoxic molecules by T cells, that help eliminate the pathogens. The abbreviations can be found in the list of abbreviations. Figure partially adapted from (4, 5). Reprinted with permission from publishers.

The components of innate immunity include a vast array of cells, receptors and molecules that work together to eliminate the pathogens, as well as a similar array of components that work together towards restoring the body's baseline physiology.

Below is an overview of the components of the innate immune system:

- Physical or surface barriers that prevent pathogens from entering the body including skin, epithelial and mucous cells, as well as blood vessel endothelial cells (6-8).
- Phagocytes (neutrophils, monocytes, macrophages) and other cells that release mediators of the inflammatory response (dendritic cells, natural-killer cells, mast cells, innate lymphoid cells) (9).
- Inflammation-related serum proteins including the complement system, acute-phase proteins (e.g. C-reactive protein) and lectins (10).

- Antimicrobial peptides (defensins, cathelicidins etc) on cell surfaces and inside phagocytic granules, as well as antimicrobial enzymes produced by epithelial and phagocytic cells (e.g. lysozyme).
- Signaling proteins that mediate immunity and inflammation: cytokines, chemokines, interferons, lymphokines, tumor necrosis factor (TNF $\alpha$ ).

Activation of the innate immune system begins in macrophages, epithelial, mast and innate lymphoid cells at the site of insult. If pathogens manage to evade the physical barriers, these cells recruit other cells into the inflamed tissue (such as neutrophils, platelets, monocytes, dendritic cells). In addition to providing a first line of defense against microbes, the innate immune system also activates and instructs adaptive immune responses. It also regulates immunologic homeostasis by balancing the pro-inflammatory mechanisms of host defense and the anti-inflammatory processes that restore the physiological baseline.

### 1.2.2. Pattern-recognition receptors (PRRs)

The innate immune system can induce a rapid immune response that directly attacks the invading pathogens due to a family of germline-encoded receptors, called pattern recognition receptors (PRRs). PRRs are also expressed by cells of the adaptive branch of the immune system (11) and can be activated by pathogenic or endogenous ligands. Pathogen-associated molecular patterns (PAMPs) are displayed on the cell surface of bacteria, fungi or viruses, while damage-associated molecular patterns (DAMPs) are molecules released from host cells undergoing necrosis.

The host organism must be able to recognize a diverse array of PAMPs and DAMPs, and several PRR classes of receptors have been identified (12):

- Membrane receptors: toll-like receptors (TLRs), C type lectin-like receptors.
- Cytosolic receptors: nucleotide binding and oligomerization domain leucine-rich repeat receptors (NLRs), retinoic acid-inducible gene (RIG)-I-like receptors (RLRs).
- DNA sensors: absent in melanoma (AIM)-2, a cytoplasmic protein that recognizes double-stranded DNA of microbial origin.

The activation of these receptors leads to different intracellular cascades that activate various transcription factors and influence gene expression, by upregulating pro-inflammatory cytokines, interferons, chemokines and other antimicrobial proteins. These molecules thus stimulate an inflammatory environment at the infection site that will later on direct the adaptive immune response against the pathogens.

#### 1.2.2.1. PRR ligands

As mentioned above, PRRs specifically recognize pathogen-associated molecular patterns (PAMPs) on the cell surface of microorganisms, that are absent in the host organism. Such molecules are peptidoglycans, like lipopolysaccharide (LPS) in the cell wall of Gram-negative bacteria (13), flagellin, the major protein component of mobile bacteria displaying flagellum (14), but also viral, single or double stranded DNA or RNA (15).

In addition, PRRs are also effective detectors of misplaced or altered host molecules that signal tissue damage or cell death. Endogenous ligands, known as “alarmins” or damage-associated molecular patterns (DAMPs), are nuclear, mitochondrial or cytosolic molecules, released from host cells that have undergone infection, injury or inflammation. DAMPs bind specific receptors both inside and outside the cells to activate inflammation.

Once released in the extracellular environment, DAMPs are recognized by PRRs expressed by cells of the innate immune system and promote immune and inflammatory responses (16). Some examples of DAMPs include proteins like heat-shock proteins, high-mobility group box 1 (HMGB1), amyloid  $\beta$ , S100 proteins, cytokines e.g. interferons (IFNs), but also non-protein DAMPs, like uric acid, mitochondrial DNA, extracellular ATP, heparan sulfate (16).

#### 1.2.3. Toll-like receptors (TLRs) signaling

TLRs are transmembrane receptors, that contain an N-terminus extracellular domain, a single pass transmembrane region and a C-terminus cytosolic domain. The extracellular domain contains leucine-rich repeats (LRRs) that recognize extracellular PAMPs and

DAMPs; the transmembrane region continues with an intracellular domain containing a Toll-Interleukin 1 receptor Resistance (TIR) signaling domain.

Upon ligand binding, the receptors dimerize and TIR domains are brought together to form docking sites for adapter proteins. Myeloid differentiation primary response protein 88 (MyD88) is a common TLR adapter protein that interacts with an interleukin-1 receptor associated kinase, IRAK-4. Recruitment of IRAK-4 leads to its auto-phosphorylation (17, 18). IRAK-1 then binds to the protein cluster and is phosphorylated by IRAK-4. Activation of IRAK-1 also requires ubiquitination by the Pellino family of E3 ubiquitin ligases (Pellino-1, -2 and -3a, -3b), followed by recruitment of TNFR-associated factor 6 (TRAF6). IRAK-1 and TRAF6 then dissociate from the TIR-MyD88-IRAK-4 complex, in order to interact with TGF-activated kinase 1 (TAK-1) and TGF-activated protein kinase 1 binding proteins 1 and 2 (TAB1 and TAB2) (17, 19, 20). Phosphorylation of TAK-1 and TAB2 induces the activation of mitogen-activated protein kinases (MAPKs) and inhibitor of nuclear factor- $\kappa$ B (NF- $\kappa$ B) kinase (IKK) complex. This activates transcription factors that increase the production of inflammatory cytokines, interferons, chemokines to further activate inflammatory cascades and autophagy processes (Fig. 2).

### 1.3. The Pellino family of proteins

The Pellino proteins are E3 ubiquitin ligases with important function in TLR signaling. The Pellino protein was initially identified in 1999 in *Drosophila*, in a yeast-two hybrid screen as an interaction partner of Pelle, a serine-threonine kinase involved in the toll receptor signaling pathway (21). Invertebrates rely entirely on innate immunity to protect them from harmful stimuli and only express one transcript of the Pellino protein. However, mammals possess a more intricate immune system and express four different Pellino proteins that are highly conserved and similar in size: Pellino-1 (22), Pellino-2 (23), and the splice variants Pellino-3a and Pellino-3b (24).

The relative expression levels of mammalian Pellino mRNAs differ remarkably in different organs, suggesting tissue-specific functions for the different Pellino proteins (25). Pellino-1 is the only family member that is highly expressed both by T and B cells (26). While B cells also have substantial levels of Pellino-3, T cells only express a

negligible level of Pellino-2 and Pellino-3 compared to the strikingly high level of Pellino-1.

However, it has been suggested that the Pellino proteins may have overlapping roles and/or that other mediators in the TLR signaling cascade can complement the E3 activity of Pellinos. For instance, TRAF6, Pellino-1 and Pellino-2 appear to have redundant E3 ubiquitin ligase functions in IL-1 $\beta$ -dependent MyD88 signaling, by generating Lys63-mediated poly-ubiquitin chains (27).

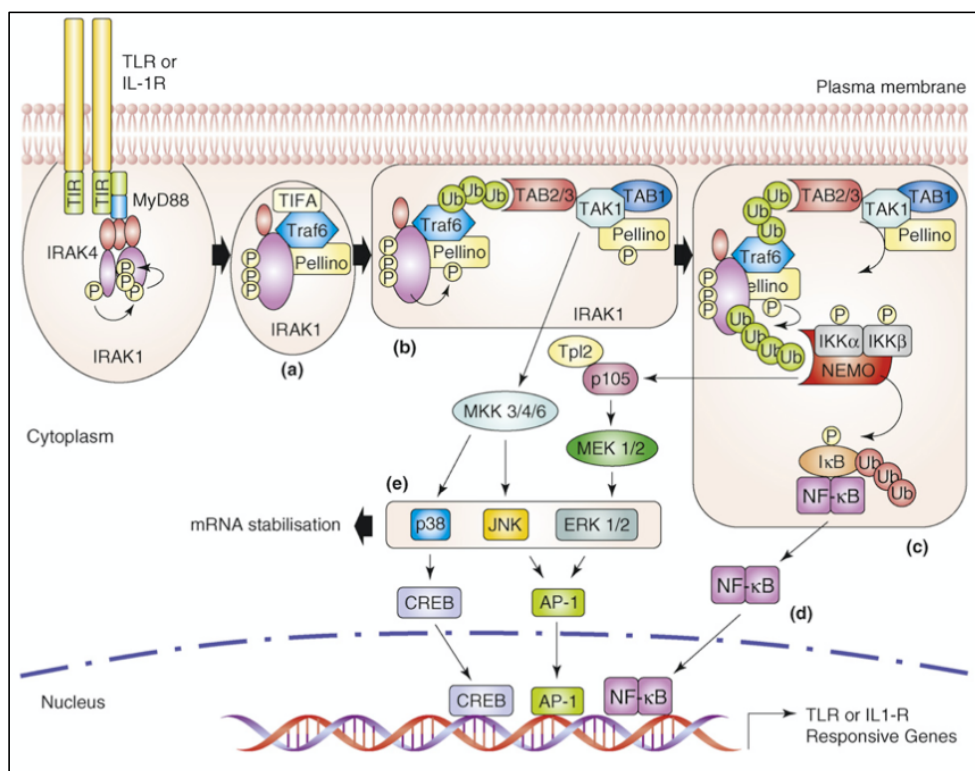


**Figure 2. TLR- and IL-1R-dependent activation of NF- $\kappa$ B and MAPK pathways.**

Upon stimulation, receptor dimerization occurs and intracellularly, MyD88 is recruited to the plasma membrane. Binding of IRAK-4 and autophosphorylation is followed by recruitment of IRAK-1 and its autophosphorylation. E3 ubiquitin ligases (e.g. Pellinos, TRAF6) are required for full activation and recruitment of TAK-1, along TAB1 and TAB2. MAPK pathway and NF- $\kappa$ B complex are activated, and transcription factors relocate to the nucleus, followed by upregulation of nuclear encoded pro-inflammatory cytokines (28). The abbreviations can be found in the list of abbreviations. Reprinted with permission from publisher.

Due to their high homology and degree of conservation across different species, these proteins are thought to possess an important biological role (25). However, before the characterization of functional or catalytic domains, the Pellinos were only considered scaffolding proteins (24). They were thought to serve simply as docking site for multiple protein partners in TLR downstream signaling, such as IRAK-1 (29-31), IRAK-4 (29, 31), TAK-1 (32) and TRAF6 (24, 33). Then, structural analysis of the Pellino proteins revealed the presence of an N-terminal Fork-Head Associated (FHA) domain (34), and a C-terminal Really Interesting New Gene (RING)-like domain (35).

The FHA domain binds phospho-threonine epitopes on target proteins (34). However, two atypical insertions (of 45 and 26 amino acids, respectively) in the FHA module initially prevented the recognition of the FHA core in Pellino sequences (34) (Fig. 3). FHA-containing proteins have been implicated in DNA damage repair and signaling (as transcription factors), vesicular transport and even protein degradation (36).

RING-like domains are a characteristic feature of E3 ubiquitin ligases that mediate ubiquitination of target proteins (37). A classical RING domain contains a His and seven Cys residues that coordinate two zinc atoms needed for RING domain function (Cys3-His-Cys4). The Pellinos contain a closely related RING-like motif, Cys-His-Cys2-Cys-His-Cys2, with two His and six Cys residues that coordinate two zinc atoms (35) (Fig. 3 and Fig. 4b).

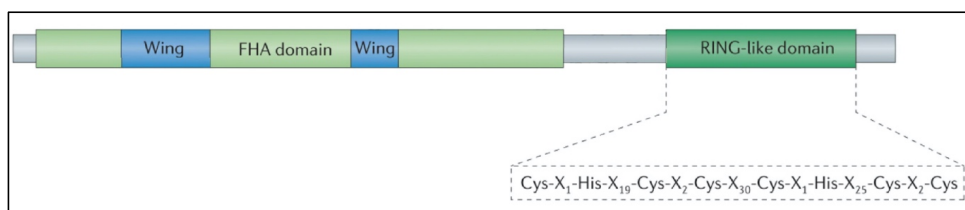


**Figure 3. Schematic representation of Pellino functional domains.**

Pellino proteins contain a forkhead-associated (FHA) domain with two additional inserts in the core of the FHA domain that form a “wing”. In the C-terminal part, Pellino proteins have a Really Interesting New Gene (RING)-like domain with cysteine (Cys) and histidine (His) amino acids in a Cys-His-Cys2-Cys-His-Cys2 pattern. Figure adapted from (19). Reprinted with permission from publisher.

The first direct evidence that Pellino proteins are E3 ligases was illustrated in an *in vitro* ubiquitination assay, where all three Pellino proteins catalyzed poly-ubiquitination (31). Ubiquitination occurs on lysine (Lys) residues, as described in detail below. Ubiquitination studies usually involve mutant forms of ubiquitin, in which Lys residues are replaced with arginine. Using recombinant mutant forms of ubiquitin with Lys48 mutated to arginine (Lys48Arg) or Lys63 mutated to arginine (Lys63Arg), Butler and colleagues showed that each of the Pellino proteins lost all ability to catalyze poly-ubiquitination when Lys63Arg ubiquitin was used as the substrate. This proved that Pellino proteins are E3 ligases that catalyze Lys63-linked ubiquitination (31). Several E2 ubiquitin conjugating enzymes have later been shown to form ubiquitination complexes with Pellinos, mediating *in vitro* both Lys-63 and Lys-48 linked poly-ubiquitination (38), thus implicating Pellino proteins in a range of cellular signaling processes.

### 1.3.1. The role of E3 ubiquitin ligases in ubiquitination

Ubiquitination is a major regulatory cellular system that coordinates complex protein signaling pathways, including the innate immune response. Ubiquitin is the central element of this process and is a 76 amino acid polypeptide expressed in all eukaryotic cells (39). A ubiquitin-activating enzyme (E1) triggers the cascade by binding ubiquitin to its active site. This activated ubiquitin molecule is then transferred to the active site of a ubiquitin-conjugating enzyme (E2). Lastly, the E2-ubiquitin complex is brought in close proximity to the substrate of the ubiquitination process by an ubiquitin-ligase protein (E3), which enables the transfer of ubiquitin on the target protein (40).

So far two ubiquitin E1 enzymes, forty-fifty E2 conjugating enzymes and hundreds of E3 ubiquitin ligases have been described in humans (41). The E3 ubiquitin ligases mediate substrate specificity, while the E2 conjugating enzymes mediate the type of ubiquitin chains on the target protein (42).

Proteins can undergo ubiquitination at a single lysine residue (mono-ubiquitination) (43), at multiple lysine residues simultaneously (multi-ubiquitination) (44) or ubiquitin chains can be formed by covalent binding of new ubiquitin molecules on another ubiquitin's lysine residue (poly-ubiquitination) (45). Mono-ubiquitination targets



receptor proteins and leads to internalization and endocytosis (43), but also gene silencing (46) and protein trafficking (47). Poly-ubiquitin chains can be formed on the seven lysine residues of the ubiquitin molecule (Lys6, 11, 27, 29, 33, 48, 63), as well as the N-terminal methionine residue (Met1) (48). The most studied poly-ubiquitination processes are Lys48- and Lys63-linked, the former targeting proteins for degradation, while the latter modulates protein signaling and function (49). Ubiquitination on other lysine residues has yet to be fully elucidated.

### 1.3.2. Pellino-1 and Pellino-3

Pellino-1 is the most studied of the Pellino family members, for which several approaches have been employed: overexpression, RNA interference (RNAi), generation of knock-in and knock-out mice, as well as studies of Pellino-1 genetic mutations.

By inducing poly-ubiquitination of IRAK-1 and IRAK-4 in the TLR and IL-1R pathways, human Pellino-1 was shown to be specifically involved in NF- $\kappa$ B activation (31, 35). Overexpression of Pellino-1 led to an increase in basal NF- $\kappa$ B activation, while a decrease in Pellino-1 expression (RNAi) led to a decrease in IL-1-induced NF- $\kappa$ B activation (50). In line with Pellino-1 involvement in the innate immune system, Pellino-1 levels can be upregulated upon stimulation with lipid A (a major constituent of bacterial LPS) (51).

Pellino-1 induces *in vitro* poly-ubiquitination with five different E2 conjugating complexes. In the presence of Ubc13–Uev1a, Pellino-1 induced the formation of Lys63-poly-ubiquitin chains, while, in the presence of UbcH3, Lys48-poly-ubiquitin chains were formed specifically. In the presence of UbcH4, UbcH5a and UbcH5b, the poly-ubiquitin chains formed were linked via Lys48 and Lys11, with minor ubiquitination via Lys63. This suggests that E2 conjugating complexes direct the specificity of poly-ubiquitin chain formation (38).

*In vivo* experiments with Pellino-1-deficient mice indicated that Pellino-1 was not compulsory for IL-1R signaling, but rather for TRIF-dependent TLR signaling by binding and facilitating RIP1 poly-ubiquitination (52). By 6 months of age, Pellino-1-deficient mice developed multi-organ inflammation and auto-antibody production

because Pellino-1-deficient T cells become hyperactive (26). Together, these data suggest that Pellino-1 is required to prevent autoimmunity.

In contrast to this, a different role of Pellino-1 in autoimmunity was reported by Xiao et al (2013), investigating the pathogenesis of multiple sclerosis. Abundantly expressed in microglia, Pellino-1 promotes the induction of chemokines and proinflammatory cytokines during the development of experimental autoimmune encephalomyelitis (EAE). In contrast, Pellino-1-deficient mice display reduced neuroinflammation, being protected from developing the disease (53).

Pellino-3 proteins have an extra N-terminal 27 amino acid sequence compared to Pellino-1/2. Pellino-3a consists of 7 exons and Pellino-3b only 6, missing exon 2 due to an in-frame deletion of 24 amino acids. Pellino-3a and Pellino-3b are widely expressed, with highest expression levels in the human heart, brain and testes (24). Interaction partners of Pellino-3 include IRAK-1, TRAF6 and TAK-1 upon IL-1R activation (24). In reporter assays, Pellino-3 leads to activation of c-Jun and Elk-1, but not NF- $\kappa$ B (24).

Knockdown studies of Pellino-3 (by siRNA) have shown increases in cytokine IL-8 production (54) and decreases in cytokine IL-1 $\beta$  secretion (30). Conversely, the overexpression of Pellino-3 induced p38 phosphorylation, which in turn activated the transcription factor CREB (30).

Pellino-3 knockout mice have normal growth and viability. While type I interferons (INF) expression was increased in these animals, this was not the case for other proinflammatory cytokines (55).

Pellino-3 has been shown to negatively regulate the expression of pro-IL-1 $\beta$ , via destabilization of the transcription factor hypoxia-inducible factor 1 $\alpha$  (HIF-1 $\alpha$ ) and suppression of gene transcription (56). This suggests an anti-inflammatory effect of Pellino-3.

### 1.3.3. Pellino-2

The human Pellino-2 protein is the lesser-investigated member of the Pellino family. The *PELI2* gene is located at chromosome 14 and encodes a 420 amino acid protein (23).

A yeast two-hybrid screen using full length human IRAK-4 (as bait) and a HeLa cDNA library (as target) first identified human Pellino-2 as a binding partner of IRAK-4 (29). However, under overexpression conditions in HEK293 cells, the interaction between Pellino-2 and IRAK-1 was significantly stronger than the interaction with IRAK-4 (29). Additionally, co-expression of Pellino-2 and IRAK-1 led to high molecular weight species of IRAK-1, suggesting increased ubiquitination of IRAK-1 (29). This was not the case for IRAK-4. *In vitro* kinase assays with recombinant Pellino-2 and IRAKs showed that both IRAK-4 and IRAK-1 were able to efficiently phosphorylate Pellino-2 (29). Thus, the interactions between Pellino-2 and the IRAK-4 kinase have been extensively studied, but have shown conflicting findings.

Furthermore, in overexpression experiments, Pellino-2 did not induce the transcriptional activity of NF- $\kappa$ B and AP-1 (29). However, others studies reported that downregulation of mouse Pellino-2 reduced IL-1-dependent activation of the NF- $\kappa$ B-dependent IL-8 gene promoter (57). Furthermore, Pellino-2 can be involved in signaling sub-pathways that specifically lead to the activation of transcription factors AP-1 (the c-Jun subunit) and Elk-1 (32).

Some of these differences could be explained by species- and cell type-specific functions of Pellino-2. However, also differences in experimental procedures and assays could induce bias and conflicting data (25). Taken together however, current literature suggests that Pellino-2 is an integral part of TLR pathways, but it is less clear which transcriptional elements are activated by Pellino-2.

#### 1.3.3.1. Localization

Little is known about the localization of human Pellino-2. In mice, Pellino-2 mRNA expression analysis, using northern blot, indicated that it is found in the developing mouse embryo, as well as in the adult mouse. Mouse Pellino-2 was found in abundance in mouse liver and skin – tissues central in innate immunity response. In contrast, low

mRNA expression or no expression of mouse Pellino-2 was found in thymus and spleen, organs that predominate in adaptive immune responses (57).

### 1.3.3.2. Structure

In 2008, the X-ray crystal structure of the N-terminal region of Pellino-2 was determined by multiwavelength anomalous dispersion (MAD) down to 1.8 Å resolution (34). Pellino-2 N-terminal domain consists of a single globular domain. There are 17 β strands that form 4 distinct β sheets, similar to the forkhead-associated (FHA) domain, a well-known and extensively characterized phosphothreonine (pThr)-binding module. Two insertions (of 45 and 26 amino acids, respectively) in the FHA module constitute a “wing” or appendage on the FHA domain structure (Fig. 4a) (34, 58).

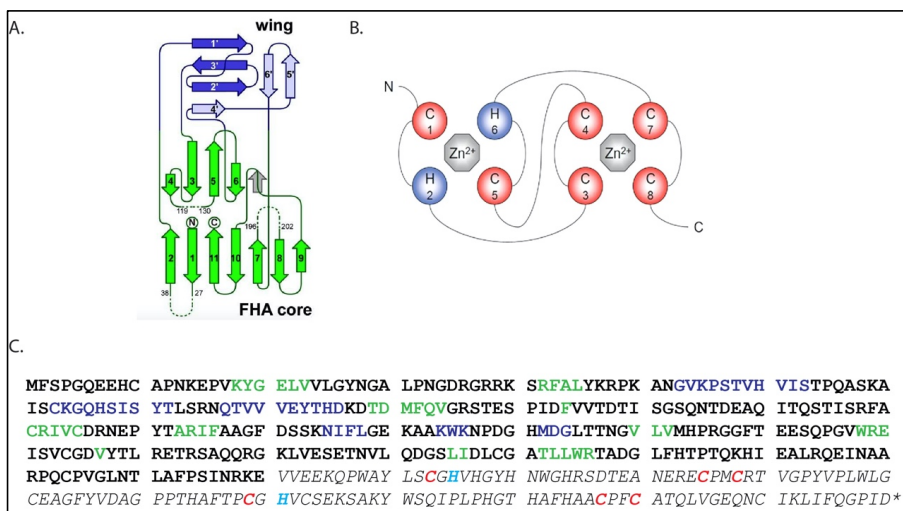


**Figure 4. Human Pellino-2 structure.**

A. Schematic representation of the N-terminal FHA domain of Pellino-2: green labeling of the 11 β sheets comprising the FHA core; blue labeling of the 6 β sheets comprising the additional wing.

B. Schematic representation of the CHC2CHC2 RING-like domain of Pellino-2: red labeling of the cysteine amino acids; light blue labeling of the histidine amino acids.

C. Amino acid sequence of human Pellino-2 (FHA domain in bold letters, RING domain in italic letters), with color representation of the corresponding amino acids for the structures illustrated in A. and B.

The abbreviations can be found in the list of abbreviations. Adapted from (34, 59). Reprinted with permission from publishers.

Additionally, key residues in the Pellino-2 structure were identified, such as Arg106, Ser137, Arg138, Thr187 and Asn188, that contribute directly to pThr-dependent binding of Pellino-2 to IRAK-1. When IRAK-1 was dephosphorylated enzymatically, the ability to interact with Pellino-2 was abolished (34), indicating that IRAK-1 phosphorylation is critical for interaction with Pellino-2 FHA core.

A striking feature of the Pellino-2 FHA core is the increased length of many of the loops separating strands in the  $\beta$  sandwich compared with the short connecting loops typically seen in canonical FHA domains. These loops are not well conserved between Pellino proteins and the differences in these three loops might dictate binding selectivity (and thus different substrate and signaling specificities) for these proteins (34). Thus, local differences in the Pellinos sequence may be responsible for different substrate specificities (33).

In the appendage wing of the FHA domain, phosphorylation sites critical for Pellino-2 activation by IRAK-1 and IRAK-4 were identified: Ser78, Ser80, Thr82, Ser84, Thr88. In addition, two other sites are located at Thr290, Ser295, in the N-terminal part of the RING-like domain with E3 ligase activity (60).

The RING-like domain in the structure of Pellino-2 follows the same Cys-His-Cys<sup>2</sup>-Cys-His-Cys<sup>2</sup> pattern as the other Pellino proteins. The E3 ubiquitin ligase activity of Pellino-2 depends on this C-terminal RING-like domain. Mutations of two key residues (Cys397Ala and Cys400Ala) in this domain abolished the capability of Pellino-2 to promote the poly-ubiquitination of IRAK-1 (61).

#### 1.3.3.3. Interaction partners

As mentioned above, Pellino-2 has been shown to associate with several signaling proteins involved in the TLR pathways, including IRAK-1 (29, 33-35, 57, 61), IRAK-4 (29, 31), TAK-1 (32, 61) and TRAF6 (32, 33, 61).

Overexpression of mouse IRAK-1 and Pellino-2 in HEK293-EBNA cells led to the immunoprecipitation of a protein complex between the two proteins (57). However, when only mouse Pellino-2 was overexpressed, mouse IRAK-1 immunoprecipitated with mouse Pellino-2 only when the HEK293-EBNA cells were treated with IL-1 $\beta$  (57).

This suggests that under steady-state conditions, the two proteins do not form a complex, but that complexes are formed in response to IL-1 $\beta$  signaling (57).

While some reported that the FHA domain is the binding site of phosphorylated IRAK-1, (33, 34), others showed that efficient binding of Pellino-2 to IRAK-1 requires the C-terminal RING domain (35). In addition, binding of Pellino-2 to IRAK-1 required IRAK-1 kinase activity and was associated with Pellino-2 phosphorylation (29, 35). The functional consequence of this phosphorylation is enhancement of Pellino E3 ligase activity, leading to ubiquitination of both Pellino-2 and IRAK-1 (38). This suggests that poly-ubiquitination of Pellino proteins is a functional consequence of IRAK-induced phosphorylation of these proteins (31, 38).

Using mass spectrometry, it was shown that the poly-ubiquitin chains attached to IRAK-1 were almost exclusively linked via Lys63, with only traces of IRAK-1 being linked via Lys48 (38).

In contrast to what is seen for IRAK-1, IRAK-4 co-expression promoted strong ubiquitination of Pellino-3, and a very weak ubiquitination of Pellino-1 and Pellino-2. Pellino-3 also interacted more strongly with IRAK-4, than Pellino-1 or Pellino-2 (31). Further, overexpression of wild-type IRAK-4 caused the degradation of all three Pellino proteins. In IRAK-1-deficient cells, kinase-active IRAK-4 was still capable of degrading the Pellino proteins. Taken together, these data suggest that IRAK-4 directly binds Pellino proteins, but with different specificity (31).

Mouse Pellino-2 has been shown to interact with BCL10 (B cell lymphoma/leukemia 10). This important molecule for T cell receptor function mediates LPS-TLR4 signaling leading to NF- $\kappa$ B activation (62, 63). Pellino-2 was detected in both the membrane-bound and cytosolic TAK-1 complexes in conjunction with BCL10, following LPS stimulation (63). Following dissociation from IRAK-1, BCL10 translocated into the cytosol along with TRAF6 and TAK-1, bridged by a direct BCL10-Pellino-2 interaction (63).

#### 1.3.3.4. Function

Initial studies of Pellino-2 were hampered by proteolytic degradation when expressed in *E. coli* (34, 38). Butler and colleagues succeeded in purifying Pellino-2 in Rosetta

cells to perform *in vitro* ubiquitination assays and show that Pellino-2 has the biological function of a E3 ubiquitin ligase (31).

Results from Kim et al. (2012) indicated that the E3 ubiquitin ligase Pellino-2 is required for TAK-1-dependent NF- $\kappa$ B activation, as well as the activation of JNK and ERK, mitogen-activated protein kinases that maintain the stability of pro-inflammatory transcripts, such as IL-8, IL-6, TNF $\alpha$  (61).

In 2018, the first mouse model of a constitutive Pellino-2 knockout was described, along with the first indications of a physiological role of Pellino-2. While Pellino-2-deficient mice are viable and develop normally, Pellino-2-deficient bone marrow-derived macrophages (BMDMs) present impaired activation of NLRP3, clearly indicating a critical role for Pellino-2 in NLRP3 inflammasome biology (64). A marker for NLRP3 inflammasome activation, IL-1 $\beta$  protein levels were significantly reduced in Pellino-2-deficient BMDMs, suggesting an important role for Pellino-2 in the pathway controlling the production of mature IL-1 $\beta$ . The activation of the NLRP3 pathway was shown to be dependent on full-length Pellino-2. Mutants lacking either the FHA or the RING-like domain could not facilitate NLRP3 inflammasome activation (64).

Similar findings were made in a human monocytic THP-1 cell line where Pellino-2 knockdown also led to a reduction of secreted, mature IL-1 $\beta$ , consistent with less processing of pro-IL-1 $\beta$  by caspase-1 (64).

Furthermore, Lys63-linked poly-ubiquitination of NLRP3 was promoted by LPS and mediated by Pellino-2, in an indirect manner, by targeting IRAK-1 that regulates NLRP3. Humphries and colleagues proposed that IRAK-1 is binding to NLRP3, to suppress its ubiquitination and priming. When Pellino-2 ubiquitinates IRAK-1, this leads to dissociation of IRAK-1 from NLRP3 and ubiquitination of NLRP3 in a Pellino-2 dependent manner (64).

#### 1.3.4. Pellino-related diseases

The Pellino proteins have been implicated in various diseases, where protein levels were either significantly increased or decreased compared to healthy controls. To this date, neither germline nor somatic mutations have been reported in Pellino-related human diseases. Table 1 summarizes the involvement of Pellino proteins in various diseases.

**Table 1. Expression of Pellinos in various disorders.**

<b>Pellino-1</b>	<b>Pellino-2</b>	<b>Pellino-3</b>
Multiple sclerosis, autoimmune encephalomyelitis (53).	Elevated in kidney transplant recipients experiencing acute rejection (65).	Reduced in colon samples from Crohn's disease patients (66).
Risk of coronary artery lesions in children with Kawasaki disease (67, 68).	Potential therapeutic target for postmenopausal osteoporosis with kidney-Yin deficiency (69).	
Elevated in patients with asthma (70).	Elevated in acute respiratory distress syndrome; reduced by miR-802 (71).	
Proangiogenic during ischemia in skin flap survival (72) or myocardial infarction (73, 74).	Elevated in gastric cancer cells (75).	
Elevated in human psoriatic skin lesions and murine psoriasis-like models (76).	Elevated in acute lung injury; reduced by miR-128-3p (77).	

Abbreviations: miR=micro RNA

#### 1.4. The NLRP3 inflammasome

Inflammasomes represent an intracellular mechanism of the innate immune system, that respond to cellular damage or microbial infection, via PRRs/TLRs, leading to secretion of pro-inflammatory cytokines. The activation of the inflammasomes is triggered by a variety of molecular and cellular events, however it is not yet well understood how these signaling events lead to the assembly and activation of inflammasomes.

Inflammasomes are intracellular multimeric protein complexes, that consist of a sensor protein, an adaptor protein and pro-caspase-1 (78). The five types of inflammasomes characterized so far take their names from their sensor proteins: nucleotide-binding domain, leucine-rich repeat-containing proteins (NLRs): NLRP1, NLRP3 and NLRC4; absent-in-melanoma 2 (AIM2); and pyrin (79).

In the case of NLRP1, NLRP3, AIM2 and pyrin, the recruitment of pro-caspase-1 to the inflammasome is facilitated by the adaptor protein apoptosis-associated speck-like (ASC). ASC is composed of two domains, the N-terminal PYD domain facilitating the interaction with NLRP3 and the C-terminal CARD domain facilitating the interaction with pro-caspase-1 (80). Upon recruitment to the inflammasome, pro-caspase-1 is



activated by proximity-induced autocleavage, and active caspase-1 is released. In turn, caspase-1 cleaves precursors of the inflammatory cytokines IL-1 $\beta$  and IL-18 into mature and biologically active peptides (81).

NLRP3 is a multidomain protein, consisting of an N-terminal pyrin domain (PYD), a central nucleotide-binding and oligomerization domain (NACHT/NBD) and a C-terminal leucine-rich repeat domain (LRR) (82). The danger signal is sensed by the C-terminal LRR domain, leading to the interaction of the pyrin domain of NLRP3 with ASC in the initiation phase of the inflammasome assembly (83). The NBD domain has ATPase activity required for NLRP3 oligomerization (84).

There are conflicting reports regarding both the localization and the assembly of the NLRP3 inflammasome (85). For instance, in resting state, NLRP3 has been found both in the cytosol (86, 87) or the endoplasmic reticulum (88, 89). Further, while the mitochondria seem to assist in the assembly of the inflammasome as a scaffold (86, 88, 90), other studies have found that it is rather the Golgi apparatus that has a scaffolding role (91). Finally, others have found that there is no association of the inflammasome with major organelles at all (92).

Although the NLRP3 protein is the sensor protein of the inflammasome, it is not directly activated by all the potential inflammasome stimuli. The structurally and chemically diverse stimuli of NLRP3 include immune activators, such as bacteria and bacterial products (LPS, bacterial muramyl dipeptide, bacterial RNA), viruses and fungi. In addition, activators not related to infection, such as pore-forming toxins, particulate matter, reactive oxygen species (ROS), nitric oxide (NO) and gout-associated uric acid crystals can trigger inflammasome assembly (93-96).

It is assumed that NLRP3 senses a common cellular event induced by all these stimuli and that this leads to NLRP3 activation through a two-step model (Fig. 5).

The first step, or the priming step, consists of an extracellular signal from microbial components that activates the transcription factor NF- $\kappa$ B, leading to subsequent upregulation of NLRP3, pro-IL-1 $\beta$  and pro-IL-18. In a second step, the activating step, a second signal from extracellular ATP, pore-forming toxins or particulate matter activate the NLRP3 inflammasome (97).

### 1.4.1. Priming the NLRP3 inflammasome

Resting macrophages do not constitutively express proinflammatory cytokines and NLRP3 levels are too low for initiating inflammasome assembly (98), therefore a priming signal is required for the activation of the NLRP3 inflammasome. Ligands for TLRs activate the transcription factor NF- $\kappa$ B. This in turn upregulates NLRP3 and pro-IL-1 $\beta$  expression but does not affect the expression levels of ASC, pro-caspase-1 and pro-IL-18 (98).

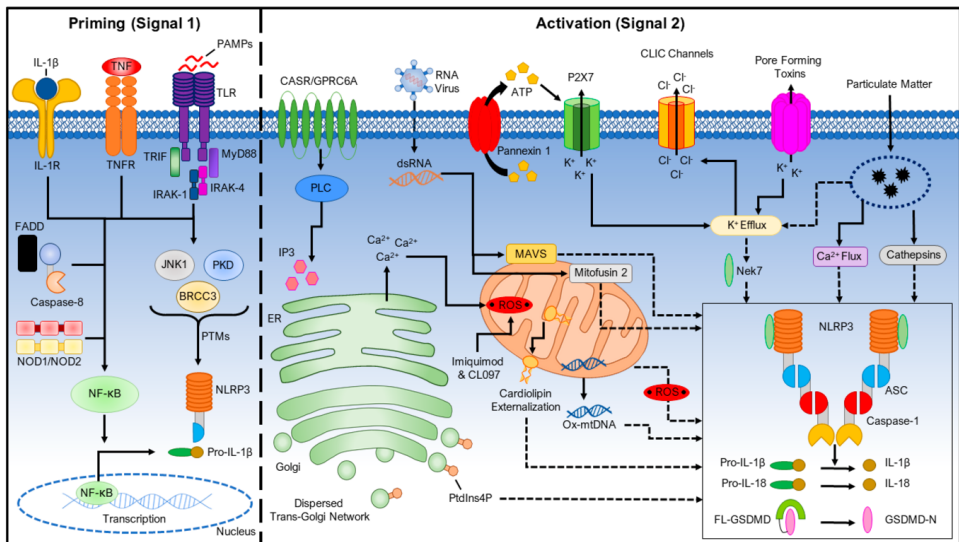


**Figure 5. The proposed two-step model of activating the NLRP3 inflammasome.**

The first signal (the priming step) is initiated by extracellular stimuli that act on membrane receptors to upregulate gene expression of important components of the NLRP3 inflammasome complex.

The second signal (activation of the NLRP3 inflammasome) consists of a second extracellular stimulus that activates multiple intracellular events, leading to secretion of pro-inflammatory cytokines (97). Reprinted with permission from publisher.

However, there have also been reports of NLRP3 inflammasome activation in the absence of NLRP3 induction, using only acute LPS stimulation (99). This rapid transcription-independent priming of NLRP3 is mediated by phosphorylated IRAK-1 and is independent of downstream NF- $\kappa$ B signaling (100). This has led to suggestions that the priming step may also have other unknown regulatory functions.

#### 1.4.2. Activating the NLRP3 inflammasome

Following the priming step, a second signal is required to assemble the proteins into a mature NLRP3 inflammasome complex that further cleaves precursor cytokines into active, pro-inflammatory effectors. A wide range of stimuli have been characterized for the assembly of the inflammasome, including ATP, K<sup>+</sup> ionophores, heme, particulate matter, pathogen-associated RNA, bacterial and fungal toxins, monosodium urate, alum, silica, asbestos,  $\alpha$ -synuclein (101), amyloid- $\beta$  (102), cholesterol crystals (103) and calcium crystals. As mentioned above, NLRP3 does not directly interact with all these; the current supposition is that they trigger a common intracellular event to which NLRP3 is sensitive (Table 2).

**Table 2. Known activators and inhibitors of the NLRP3 inflammasome.**

Activators of the NLRP3 inflammasome	Inhibitors of the NLRP3 inflammasome
Increased intracellular Ca <sup>2+</sup> (104), as a result of endoplasmic reticulum stress (105).	Ca <sup>2+</sup> chelators (106) e.g. BAPTA-AM (107).
Na <sup>+</sup> influx (108).	Nitric oxide (NO) (109, 110).
Cl <sup>-</sup> efflux (111).	Carbon monoxide (CO) (112).
ROS and mitochondrial dysfunction (113).	ROS inhibitors (114).
Mitochondrial proteins mitofusin 2 (115) and cardiolipin (116) .	
Knockdown of autophagy proteins LC3B and beclin-1 (117).	Autophagy (118); autophagy/degradation of ASC aggregates (119) or pro-IL-1 $\beta$ (120).
Low levels of lysosomal damage by lysosomal enzymes: cathepsin B (121), other cathepsins (122).	Extensive levels of lysosomal disruption (123).
miR-17, miR-137, miR-150; downregulation of miR-330 (124).	miR-7 (125), miR-9 (126), miR-223 (127).
K <sup>+</sup> efflux (108, 128) and K <sup>+</sup> ionophores (107).	PYD-only proteins (POPs) and CARD-only proteins (COPs) (129-131).
	Immune cells and immune molecules, such as activated T cells (132), neutrophils (133), type I interferons (134, 135).

Abbreviations: miR=micro RNA

#### 1.4.2.1. K<sup>+</sup> efflux

A common trigger for NLRP3 inflammasome activation, upon treatment with various NLRP3 stimuli, is the depletion of cytosolic K<sup>+</sup>. Several studies have shown that K<sup>+</sup> efflux mediates IL-1 $\beta$  maturation in response to ATP or nigericin. Further, K<sup>+</sup> efflux alone can activate the NLRP3 inflammasome and high extracellular K<sup>+</sup> concentrations inhibit the activation of the NLRP3 inflammasome (108, 128, 136).

Intracellular hypokalemia also impairs the mitochondrial function. This leads to the release of cytoplasmic and mitochondrial DNA ROS, that also activate the NLRP3 inflammasome (88, 137). This suggests that K<sup>+</sup> efflux is an upstream event of mitochondrial dysfunction. Depleted cytosolic K<sup>+</sup> concentrations mobilize the K<sup>+</sup> from the mitochondria, resulting in mitochondrial damage (138).

K<sup>+</sup> efflux has also been shown to induce NEK7-NLRP3 interactions, essential for the inflammasome activation (139, 140).

However, this mechanism may not be as straightforward as initially thought. Recently, a study using small molecules targeting the mitochondria proved that the NLRP3 inflammasome can be activated in a K<sup>+</sup> efflux-independent manner (141). Additionally, the disease-causing mutation in the *NLRP3* gene p.(Arg260Trp) occurring in Muckle-Wells syndrome has been shown to activate the inflammasome after stimulation with only LPS and without any depletion of the cytosolic K<sup>+</sup>. This is caused by a lowered activation threshold of the inflammasome (142).

Together, these observations indicate that K<sup>+</sup> efflux is sufficient, but not necessary, for the activation of the NLRP3 inflammasome and that there may also be other pathways, independent of K<sup>+</sup> efflux, for triggering the NLRP3 inflammasome.

##### 1.4.2.1.1. Intracellular vs extracellular concentrations of K<sup>+</sup>

The human body has very tightly regulated mechanisms that preserve the gradient of K<sup>+</sup> concentrations between the intracellular (140 mM) and extracellular (5 mM) compartments. While only 2% of total body K<sup>+</sup> is found extracellularly, high levels of intracellular K<sup>+</sup> are critical for many functions, among others protein synthesis (143) and cell volume regulation (144). The steep transmembrane K<sup>+</sup> gradient creates a membrane potential that is used to drive action potentials in neuronal, cardiac and

muscular tissue, and as an energy source for other ion transporters. The active process of pumping  $K^+$  into the cells is performed by the ubiquitous plasma membrane enzyme  $Na^+/K^+$ -ATPase. Against concentration gradients, the ATP-driven pump takes up  $K^+$  into the cell, while pumping out  $Na^+$  (145). The physiological function of intracellular  $K^+$  is to regulate volume changes, create a pH gradient in the electron transport chain, compensate for electrical charges during  $Ca^{2+}$  transport and regulate mitochondrial ROS production for the purpose of cell signaling (e.g. gene transcription) (146).

At the same time, the  $Na^+/K^+$ -ATPase is tightly regulated by circulating hormones, such as mineralocorticoids (aldosterone), catecholamines or insulin, via feedforward control mechanisms that clear  $K^+$  from the extracellular space by cell uptake or renal excretion (147).

#### 1.4.2.1.2. $K^+$ in different compartments inside the cell

While the plasma membrane maintains  $K^+$  homeostasis on both sides of the membrane, inside the cells,  $K^+$  localization and concentration are also tightly regulated, via multiple types of  $K^+$  channels expressed on various organelles. BK channels and TMEM175 can be found in the lysosomal membrane (148, 149),  $K_{ATP}$  and TRIC channels in the endoplasmic reticulum (150),  $K_v1.3$  channels in the cis-Golgi membrane (151) and in the nuclear membrane (152), and  $mitoK_{ATP}$  and  $K^+/H^+$ -antiporter are located in the mitochondrial inner membrane (153). In other organisms, where intracellular  $K^+$  concentrations were studied at the organelle level, it has been shown that different intracellular compartments have different concentrations of  $K^+$  (154, 155).

#### 1.4.3. Inhibition of the NLRP3 inflammasome

NLRP3 inflammasome activation is tightly regulated. In addition to positive regulation of the inflammasome, there are also inactivators of the NLRP3 inflammasome. The fine balance between activation and inhibition prevents exacerbated inflammatory responses that could lead to chronic inflammation.

An overview of the cellular and molecular mechanisms inhibiting the NLRP3 inflammasome activation are listed in Table 2. Additionally, there are pharmacological inhibitors that either suppress the NLRP3 protein directly, inhibit the inflammasome

activation, block upstream signals, inhibit caspase-1 activation or neutralize the inflammatory cytokines released by NLRP3 inflammasome (156).

- a.** Glyburide is a sulfonylurea drug, used in the treatment of type 2 diabetes. By inhibiting ATP-sensitive  $K^+$  channels, glyburide acts downstream of the P2X7R receptor and inhibits ASC aggregation (157).
- b.** Quinine inhibits NLRP3 inflammasome activation by inhibiting  $K^+$  efflux via the two-pore domain potassium channel TWIK2 (158).
- c.** FC11A-2 is a synthetic small molecule that hinders the proximity-induced autocleavage of procaspase-1, leading to reduced amounts of active caspase-1, thus inhibiting the NLRP3 inflammasome (159).
- d.** Parthenolide is a naturally occurring compound with anti-inflammatory properties: as a lactone, it alkylates Cys residues of both caspase-1 and the ATPase domain of NLRP3 (160).
- e.**  $\beta$ -hydroxy-butyrate (BHB) lowers the production of IL-1 $\beta$  and IL-18 by inhibiting  $K^+$  efflux from macrophages and blocking ASC aggregation (161).
- f.** MCC950 is a direct inhibitor of the NLRP3 protein, binding directly to its NBD domain, blocking ATP hydrolysis and the NLRP3 inflammasome activation (162).
- g.** Tranilast is a tryptophan metabolite analog that binds to the NLRP3 NBD domain and prevents NLRP3 oligomerization within the inflammasome (163).

#### 1.4.4. Regulating the NLRP3 inflammasome

Post-translational modifications are the most common way of regulating the activity of a protein. NLRP3 can undergo multiple types of post-translational modifications, including phosphorylation, ubiquitination, sumoylation and S-nitrosylation.

NLRP3 phosphorylation by protein kinase A prevents the activation of the NLRP3 inflammasome (164), while protein kinase D and JNK1-mediated phosphorylation of NLRP3 promotes inflammasome assembly and activation (87, 165).

Phosphorylation can also have inhibitory effects on the activation of NLRP3 inflammasome, suggesting that protein phosphatases may also regulate the NLRP3 inflammasome activation. Both protein tyrosine phosphatase non-receptor 22 (PTPN22) and protein phosphatase 2A (PP2A) have been shown to dephosphorylate

residues in the NLRP3 (Tyr861 and Ser5, respectively). This step is required for the activation of the NLRP3 inflammasome (166, 167). Together these data suggest that phosphorylation can have both a positive and negative influence on NLRP3 inflammasome activation, depending on the kinase involved and the specific amino acid residue undergoing phosphorylation.

NLRP3 inflammasome activation is also regulated by other post-translational modifications: S-nitrosylation (110) and sumoylation (168) negatively regulate NLRP3 inflammasome activation, while ADP-ribosylation by a *Mycoplasma pneumoniae* toxin promotes the activation of the NLRP3 inflammasome (169).

#### 1.4.4.1. Ubiquitination

There are conflicting reports also on the biological significance of NLRP3 ubiquitination. The Lys-63-specific deubiquitinase BRCC36 was identified as the enzyme responsible for deubiquitinating NLRP3 during the priming step (92), and several inhibitors of deubiquitinases (DUBs) have been shown to inhibit the activation of the NLRP3 inflammasome (170, 171). This suggests that ubiquitination has an inhibitory role in the activation of the NLRP3 inflammasome.

Several E3 ubiquitin ligases have been shown to induce Lys-48-mediated polyubiquitination of NLRP3 and target it for degradation, including FBXL2 (172), MARCH7 (173), TRIM31 (174) and ARIH2 (175). In contrast, the E3 ubiquitin ligase Pellino-2 has been shown to facilitate the Lys-63-mediated polyubiquitination of NLRP3, and in this way promote the NLRP3 inflammasome canonical activation (64). Taken together, these findings suggest that ubiquitination can have both a positive and negative influence on NLRP3 inflammasome activation, depending on the enzyme and the type of ubiquitin chains formed.

#### 1.4.4.2. NLRP3 regulation by interaction partners

There have been several reports of multiple interaction partners of NLRP3 that mediate activation of the inflammasome. One example is NEK7, a kinase involved in cell division and mitotic progression, that has been shown to interact with NLRP3 and activate inflammasome assembly, by promoting NLRP3 oligomerization (139, 176-

178). NEK7 interacts with the NOD and LRR domains of NLRP3 via its catalytic domain (178). Interestingly, K<sup>+</sup> efflux was recently identified as a requirement for the binding of NEK7 to NLRP3, and this interaction could be blocked by high extracellular K<sup>+</sup> concentration (>50 mM) (139).

To summarize, presently, there is no consensus with regards to the mechanism of activation of the NLRP3 inflammasome. There is a wide array of stimuli that trigger, or inhibit, the inflammasome via various signaling and cellular events. The efflux of K<sup>+</sup> seems to be a unifying mechanism by which the NLRP3 inflammasome is activated, although there are several other regulatory mechanisms that influence this.

#### 1.4.5. NLRP3-linked diseases

Well-regulated NLRP3 inflammasome activation has been shown to have protective effects against keratitis and corneal neovascularization (179) and to be required in burn wound healing (180) and skin wound healing in mice (181). However, abnormal activation of the NLRP3 inflammasome has been linked to the pathogenesis of several diseases such as atherosclerosis, gout, myocardial ischemia, cardiomyopathy, ischemic stroke, hypertension, obesity, diabetes, cancers, as well as renal, hepatic, autoimmune and neurodegenerative diseases (182).

In eye diseases, involvement of NLRP3 has been seen in acute glaucoma (183), age-related macular degeneration (184), uveitis (185) and Behcet's syndrome (186). Table 3 addresses further pathologies of the eye or skin, in which NLRP3 has been implicated.

In addition, there are also rare, inherited, monogenic conditions in which *NLRP3* variants cause disease. There have been 65 germline mutations reported in *NLRP3* and 8 of them have been identified also in a mosaic state (187). For instance, keratoendotheliitis (keratitis) fugax hereditaria (KFH) is associated with a missense substitution in the first exon of *NLRP3* c.61G>C, p.(Asp21His), exclusively diagnosed in the Finnish population (188). This heterozygous mutation results in the replacement of a negatively charged aspartic acid with a positively charged histidine. This is thought to cause altered protein folding and function, leading to aberrant activation of the NLRP3 inflammasome (189).



**Table 3. Pathologies associated with NLRP3 inflammasome activation, affecting the eye or the skin**

Eye diseases		Skin diseases	
Cornea	Pterygium	General	Keloids
Dry eye disease (190)	Pterygium (191)	<i>P. acnes</i> infection (192, 193)	Increased NLRP3 protein levels (194)
<i>S. pneumoniae</i> keratitis (195, 196)			Increased active caspase-1, IL-1 $\beta$ and IL-18 (181)
Delayed diabetic wound healing (197, 198)			
Corneal inflammation by airborne particulate matter (199)			

*S. pneumoniae* = *Staphylococcus pneumoniae*, *P. acnes*=*Propionibacterium acnes*.

Patients with KFH experience, several times a year and in one eye at the time, recurring attacks of conjunctival redness, ocular pain, transient corneal endothelial edema and photophobia. After several attacks, permanent corneal opacities, consisting of extracellular lipid deposits (200), may lead to visual impairment (201). These attacks appear to follow after periods of physical or mental stress, but low temperature or draughts have also been hypothesized (201).

KFH presents only with eye symptoms (188), but other germline *NLRP3* variants have been associated with systemic symptoms. Heterozygous, gain-of-function mutations of *NLRP3* cause a group of diseases named auto-inflammatory cryopyrin-associated periodic syndromes (CAPS). These conditions manifest on the skin as urticaria-like lesions, papules or plaques. In the eye, corneal vascularization and corneal opacification, dry eye, and conjunctivitis are the most common manifestations, but significant visual loss can occur in severely affected individuals (202).

In general, CAPS are divided into three subtypes although many patients present clinical features that overlap more than one subtype. Familial cold auto-inflammatory syndrome (FCAS) is the mild form and symptoms include urticarial-like rash, limb pain, and fever following generalized cold exposure. Muckle–Wells syndrome (MWS) is the intermediate form, characterized by recurrent episodes of rash, limb pain, and fever. Chronic infantile neurological cutaneous and articular syndrome (CINCA) is the most

severe form of CAPS. Patients experience chronic, severe, urticarial-like rash, pain, and fever with developmental delay, seizures and physical disability (203).

These diseases are now recognized as a severity spectrum rather than separate entities (204). Cold exposure (less than 22 °C) triggers noticeable symptoms within a few hours of exposure, that may last less than a day in FCAS patients, but up to 1-3 days for MWS patients (203).

In addition to germline mutations, also somatic/mosaic *NLRP3* variants can give CAPS phenotypes. Over 100 pathogenic *NLRP3* mutations have been reported in CAPS patients. Also non-affected, asymptomatic individuals have been found to carry low-penetrance *NLRP3* missense substitutions. Eye symptoms are less common, rather the clinical manifestations include fever and gastrointestinal symptoms (205). This suggests that other factors are involved in disease manifestations.

Most CAPS mutations are found in the NOD domain of NLRP3 and cause constitutive activation of the NLRP3 inflammasome, even in the absence of the two-signal activation. Peripheral blood leukocytes isolated from CAPS patients and stimulated with LPS without ATP present increased ASC speck formation, caspase-1 cleavage and IL-1 $\beta$  release (206), while monocytes from FCAS, but not MWS or CINCA patients, produce IL-1 $\beta$  when cultured at 32 °C without LPS (207). CAPS are characterized by excessive release of IL-1 $\beta$  and patients respond very well to IL-1 targeted therapy, such as anakinra, riloncept and canakinumab (202).

## **1.5. Ocular pterygium-digital keloids dysplasia (OPDKD)**

### **1.5.1. Disease characteristics**

Ocular pterygium-digital keloid dysplasia (OPDKD) presents in the first few years of life with ocular pterygium and, later in young adulthood, with keloid scars on fingers and toes (Fig. 6). Patients are otherwise healthy (208, 209).

#### **1.5.1.1. Pterygium**

Ocular pterygium is a vascularized overgrowth of the conjunctiva that gradually covers the cornea (210). This conjunctival ingrowth usually occurs in both eyes and starts on



**Figure 6. OPDKD clinical manifestations.**

a. Pterygium-like changes in OPDKD Norwegian patient (left) and in OPDKD Peruvian patient (right).

b. Finger keloids in OPDKD Norwegian patient (left) and toe keloids in OPDKD Peruvian patient (right).

Adapted from (208, 209). Reprinted with permission from publishers.

the nasal side. Typical symptoms include redness, swelling, irritation, itchiness, and pain. In severe cases, it can cross the visual axis and lead to reduced vision.

Pterygium development has been commonly attributed to environmental factors, such as chronic exposure to ultraviolet (UV) light, heat, dust, and smoke (211). There is also a genetic predisposition to pterygium development, as well as an ethnic predisposition, predominantly in Hispanic, Asian and black populations (212). Treatment is challenging, but surgical excision in combination with a conjunctival graft has led to fewer recurrences (210).

Pterygium develops as a result of processes involved in abnormal wound healing, such as excessive fibroblast proliferation and reduced matrix degradation, alongside abnormal angiogenesis (213). At a molecular level, pterygium shares many similarities with UV-related ocular surface squamous neoplasia and skin cancers. Exposure to UV light leads to cellular damage that disrupts biochemical pathways and can cause DNA damage. In response, cellular repair mechanisms are activated, alongside cellular adaptations, but also autophagy and apoptosis (210). This results in structural changes

of the cell and overgrowth. In contrast to the UV-related cancers, pterygium remains superficial and localized.

The innate immune system has been implicated in the pathogenesis of pterygium. Central players of the innate system, such as TLR2, 3, 4, 5 and 7 are expressed by conjunctival, limbal and corneal epithelial cells (213). A recent study has shown that, upon UVB exposure, pterygial conjunctival cells have increased expression of TLR3 and increased levels of phosphorylated, nuclear NF- $\kappa$ B in superficial layers of the conjunctiva (214). This indicates that there is a correlation between UV exposure, TLR3 expression and downstream signaling. It has been suggested that TLR3 may recognize noncoding RNAs released from necrotic cells damaged by UV light, induce nuclear translocation of NF- $\kappa$ B, and thus promote uncontrolled proliferation of pterygial cells (214). This increased TLR3 signaling seems specific, as for instance TLR5 expression does not correlate with pterygium development (215) and similar levels of TLR5 were found in pterygial and healthy cells.

In the conjunctiva, TLRs can be activated by the calcium-binding protein S100A (216). S100 proteins are ubiquitously expressed, and among others regulate intracellular calcium ( $\text{Ca}^{2+}$ ) concentrations so that they are sufficient for cell metabolism, yet preventing accumulation (217). Intracellularly, in addition to regulating  $\text{Ca}^{2+}$  homeostasis, S100 proteins bind to enzymes, cytoskeletal proteins receptors, transcription factors, and nucleic acids, to mediate among others proliferation and inflammation (217, 218).

In the extracellular space and in bodily fluids, S100 proteins are usually an indication of disease, with some of them being considered biomarkers for atherosclerosis (219) or stroke (220). What causes the release of S100 proteins from cells has not been completely elucidated, however their secretion occurs either passively, due to cell damage, or actively following cell activation mechanisms (221). However, it is clear that once released, S100 proteins trigger immune responses by activating TLRs and other cell surface receptors (222).

In pterygium tissues, S100A proteins are thought to increase cell adhesion and migration, and contribute to inflammation, angiogenesis and fibrosis (216). In particular S100A6, S100A8 and S100A9 proteins are highly upregulated, at both transcript and

protein levels, particularly in the superficial layers of pterygial epithelium (223). S100A8 and S100A9 were also found highly upregulated in the tears of patients with pterygium (224), suggesting a role for these S100A proteins in ocular inflammation and corneal neovascularization.

NLRP3, caspase-1 and IL-1 $\beta$  mRNA and protein levels are much higher in pterygium tissue compared to normal conjunctival tissue (191), suggesting a role for NLRP3 inflammasome activation in the development of pterygia. Local injections with mitomycin C have been shown to inhibit the activation of the NLRP3 inflammasome pathway, reduce the levels of secreted IL-1 $\beta$  and decrease the recurrence rate of pterygium postoperatively (225).

#### 1.5.1.2. Keloids

Under physiological conditions, the wound healing process is assisted by a host of mechanisms. In the acute inflammatory phase, macrophages and other inflammatory cells are recruited. In the proliferative phase, contractile fibroblasts are mobilized, and the extracellular matrix of the granulation tissue is formed. In the final stage, matrix metalloproteinases (MMPs) and their inhibitors (tissue inhibitor of metalloproteinases [TIMPs]) replace the granulation tissue with collagen type I and elastin (226). When this process is exacerbated, excessive scar tissue formation occurs and keloid-like scars form.

Keloids proliferate into normal adjacent areas, are elevated above skin level, and do not respect the original borders of the wounds. Prevalence of keloids is much higher in populations with pigmented skin (e.g. Hispanics, African-Americans, Asians) (227). Keloids rarely occur in syndromes and when they do, they are usually located on the earlobes, upper arms, shoulders and torso (227). Typical keloid symptoms include discomfort, pain, itching, stiffness, restricted joint movement, (228), as well as depression (227).

Keloid formation is attributed to the accumulation of extracellular matrix components and collagen, as well as abnormal proliferation and failure of apoptosis of myofibroblasts, leading to atypical fibroblasts deposition (226).

Similarly to what is reported for pterygium, the innate immune system has been implicated also in the pathogenesis of keloids. At a molecular level, TLR6, 7 and 8 are highly upregulated in keloid scars, at both mRNA and protein level (229). In contrast, a more recent study reported downregulation of TLR7, suggesting a more complex picture. In addition, upregulation of TLR4 was found, that increases connective tissue growth factor (CTGF) and collagen accumulation within keloids (230). It has been reported that in keloids, TLR4 can be activated by hypoxia-inducible factor 1 $\alpha$  (HIF-1 $\alpha$ ). This factor is expressed at a significantly higher level in keloid tissue as it is a hypoxic microenvironment (231).

In the acute inflammatory phase of the wound healing process, NLRP3 inflammasome activation occurs (180). While this is beneficial for wound healing, persistent activation of the NLRP3 inflammasome has been seen in keloid tissue. The levels of NLRP3 (194), caspase-1 and IL-1 $\beta$  (181) are highly increased in keloid samples compared to normal or burn skin.

Elevated levels of trans-epidermal water loss (TEWL) have been observed in keloids (232). Reduced hydration in these tissues increases the expression levels of several S100 proteins in the epidermis: S100A8, A9 (233) and A12 (234). These S100 proteins then activate dermal fibroblasts via TLR4, thus promoting fibrosis (233).

Keloid cells have similar pathological behavior to cancer cells. They undergo metabolic reprogramming from oxidative phosphorylation to aerobic glycolysis, known as the “Warburg effect”, characterized by high glucose uptake and increased lactate production (235). In line with this, the glucose transporter Glut1 is overexpressed in keloid tissue, suggesting that glucose uptake into the cells is an indicator for increased keloid risk (181).

#### 1.5.2. OPDKD epidemiology and patient description

There are only a few families with OPDKD described in the literature: a Norwegian family spanning 3 generations (208, 209, 228), a Peruvian patient (209) and a Saudi Arabian family with 3 members affected over 2 generations (211).

The Norwegian proband and her oldest son developed conjunctival ingrowth by the age of 2, that progressed rapidly. Despite multiple surgical interventions, the changes

progressed, leading to visual loss. The younger son developed corneal changes somewhat later, at the age of 6. All patients developed keloids on their fingers in their early 20s, and later on their toes (209). The third generation OPDKD patient presented a corneal nodule in one eye at the age of 3, which has become vascularized (208). Otherwise, the patients are healthy.

In 2014, Abarca and coworkers reported a new case of OPDKD in a Peruvian patient (209). By age 7, he had been diagnosed with pterygium in his right eye and in his left at age 9. He underwent surgery in both eyes, but the changes recurred soon after (209). On his toes, he had keloid formation after surgery for ingrown nails, but also other keloids that appeared spontaneously. At the age of 19, he presented small keloids on fingers (209).

In a report of familial pterygium, two siblings presented with aggressive pterygium development at the age of 4 and 6, respectively (211). Their maternal aunt had pterygium diagnosed at the age of 20. Although all three patients underwent surgical resections followed by adjuvant therapy with mitomycin C, they all had unusually aggressive recurrences. No skin changes were reported.

In addition, there are other hereditary diseases that present with pterygium-like changes and/or keloids. One such condition is Penttinen type of premature aging syndrome. This condition is characterized by translucent skin, delayed bone maturation and dental development, progressive lipodystrophy, pronounced acro-osteolysis (236, 237), pronounced connective tissue destruction, in addition to corneal vascularization (238). Penttinen syndrome has been associated with missense mutations in *PDGFRB* (238, 239). Warburg-Cinotti syndrome also presents with corneal neovascularization and keloids, chronic skin ulcers, wasting of subcutaneous tissue and acro-osteolysis. This disabling condition is associated with missense variants in the discoidin domain receptor tyrosine kinase 2 (*DDR2*) (240).

### 1.5.3. Pathogenesis and pathophysiology of OPDKD

Genetic analysis of the Norwegian family identified an autosomal dominant variant in *PDGFRB* p.(Asn666Tyr), that co-segregated with the disease in the family. It was found to occur as a *de novo* mutation in the first generation (208). This variant leads to an

amino acid change in the highly conserved autoinhibitory domain of the receptor tyrosine kinase (RTK) PDGFR $\beta$ . Other, non-synonymous variants in this particular codon have been associated with both Penttinen syndrome (238) and somatic infantile myofibromatosis (241).

This *PDGFRB* mutation is temperature sensitive, causing significant constitutive activation of PDGFR $\beta$  and downstream ligands, particularly at the physiological lower temperatures of the cornea (208). At ambient temperatures (20 °C), the measured temperature of the corneal surface is approximately 32 °C (242). Similarly, distal limbs are regions with physiologically lower temperature. These body parts are constantly exposed to lower and more variable temperatures, than the core temperature of 37 °C. This observation is important for understanding why these body parts are most affected in *PDGFRB*-associated OPDKD (208).

In contrast, the p.(Asn666Ser) mutation associated with Penttinen syndrome leads to highly activated PDGFR $\beta$  regardless of temperature. However, at reduced temperature, increased levels of P-STAT1 were observed. STAT1 is important for tissue wasting (243), possibly explaining the chronic ulcers on feet in these patients (208).

Bredrup and colleagues found that the p.(Asn66Tyr) *PDGFRB* variant was sensitive to treatment with imatinib, an RTK inhibitor, *in vitro*. However, when a patient was treated off-label with this drug, no improvement was observed and the medication was discontinued after 10 months (208).





## **Aims**

The main goal of this thesis has been to characterize the Pellino-2 protein and a novel c.770C>T, p.(Thr257Ile) *PELI2* variant associated with OPDKD.

## **Objectives**

**Paper 1:** Following previous reports that Pellino-2 mediates NLRP3 inflammasome activation, we aimed to elucidate the role of Pellino-2 in the activation of NLRP3 inflammasome and secretion of interleukin-1 $\beta$ .

**Paper 2:** We aimed to identify novel interaction partners of Pellino-2 and characterize Pellino-2 intracellular localization in non-immune cells.

**Paper 3:** We aimed to report and characterize the *PELI2* variant associated with OPDKD.



## Materials and Methods

This section describes the methods and techniques used in preparation of this thesis.

### 3.1. Ethical considerations (paper 2 & 3)

The study was approved by the Regional Committee for Medical and Health Research Ethics, Western Norway (IRB.no.00001872, project number 2014/59). Informed written consent was obtained from the affected individual and healthy family members prior to collection of blood samples and skin biopsies. The study thus adhered to the Tenets of the Declaration of Helsinki.

### 3.2. Expression vectors (paper 1, 2 & 3)

Human *PELI2* cDNA encoding full-length human Pellino-2 (UniProt ID: Q9HAT8) was subcloned from a pLenti-Peli2-myc-DDK vector (RC203409L1, OriGene, Rockville, USA) into a pQCXIH/pQCXIP retroviral expression vector (Clontech, California, USA), using BamHI and EcoRI restriction enzymes. Apart from the FLAG tag, several other molecular tags were cloned on the Pellino-2 sequence: an N-terminal or C-terminal GFP tag, respectively, were inserted, alongside a linker between the GFP and Pellino-2, consisting of six amino acids (Ser-Gly-Leu-Arg-Ser-Ala) (244). An additional plasmid was generated by inserting a C-terminal HA tag.

HA-IRS-1 (vector ID: VB170108-1009arr) and TRAF7-HA (vector ID: VB160907-1025yut) encoding plasmids were purchased from VectorBuilder Biosciences (Guangzhou, China) Inc. The HA tag was also changed to a myc tag. All constructs were subsequently verified by Sanger sequencing.

### 3.3. Trio exome sequencing (paper 3)

DNA extracted from peripheral blood from the affected individual and his parents was subjected to Whole Exome Sequencing (WES), performed by HudsonAlpha (HudsonAlpha Genomic Services Laboratory, Huntsville, AL, USA) using NimbleGen v3 exome capture and sequenced on Illumina HiSeq with 2 x 100 bp reads and an estimated median coverage of 75x. Illumina BCL-files were converted to fastq-files by HudsonAlpha. Trimming (Trimmomatic-0.33), alignment (bwa-0.6.2) to GRCh37.1,

realignment, and variant calling (picard-tools-1.129 and GenomeAnalysisTK-2.7.4) (245) were performed following the Broad recommended best practice guidelines (246). Vcftools v.0.1.9 was used for filtering variants (247), and Annovar (248) was used for annotation.

#### 3.4. Generation of transduced cell lines (paper 2 & 3)

Transduced HEK293 and U87MG cells, stably overexpressing *PELI2* (NM\_021255.3) c.wt and c.770C>T, p.(Thr257Ile) variants with a C-terminal HA tag, as well as transduced BJ-5ta immortalized fibroblasts, stably overexpressing *PELI2* c.wt with an N-terminal GFP tag, were generated by transduction with the constructs described above (249). Virus production was performed by transfecting Phoenix-AMPHO packaging cells (CRL-3213, ATCC, Manassas, VA) as described previously (250). Two days after transfection, the medium was harvested and the immortalized cell lines HEK293 (ATCC CRL-1573™), U87MG (ATCC HTB-14™) and BJ-5ta immortalized fibroblasts (ATCC, CRL-4001™) were transduced following standard protocols (251). The cells were grown in DMEM containing 10% fetal calf serum. Two days post-infection, stably transduced cells were selected by adding 1 ng/ml puromycin (cat# ant-pr-1, InvivoGen, San Diego, CA) to the culture medium, and kept thereafter in selection medium for additional 14 days.

#### 3.5. Cell culture (paper 1, 2 & 3)

Normal rat kidney (NRK) cells stably expressing GFP-Rab1 (NRK-GFP-Rab1 cells) (244), along with human embryonic kidney (HEK) 293 cells, HeLa cells and human fibroblasts were cultured in Dulbecco's Modified Eagle Medium (DMEM), high glucose (4500 mg/L), supplemented with 10% fetal bovine serum (FBS), penicillin 100 U/mL, streptomycin 100 µg/mL and L-glutamine 2 mM.

U87MG glioblastoma cells were grown in DMEM medium, high glucose, supplemented with 10% FBS, penicillin 100 U/mL, streptomycin 100 µg/mL, L-glutamine 2 mM, non-essential amino acids (NEAA) 0.3 mM and plasmocin 10 µg/mL.

LNCaP cells (ATCC CRL-1740™) were cultured in Roswell Park Memorial Institute (RPMI) 1640 medium, supplemented with 10% FBS, penicillin 100 U/mL, streptomycin 100 µg/mL and L-glutamine 2 mM.

THP-1 cells (ATCC TIB-202™) were cultured in RPMI-1640 medium, supplemented with 10% FBS, penicillin 100 U/mL, streptomycin 100 µg/mL, L-glutamine 2 mM and 2-mercapto-ethanol 0.05 mM. Cells were cultured for no longer than 15 passages.

THP-1 monocytes were gradually transitioned for cultivation in Dulbecco's Modified Eagle Medium (DMEM), high glucose (4500 mg/L), supplemented with 10% fetal bovine serum (FBS), penicillin 100 U/mL, streptomycin 100 µg/mL L-glutamine 2 mM and 2-mercapto-ethanol 0.05 mM.

### 3.6. Drug treatments

#### 3.6.1. Macrophages (paper 1)

THP-1 monocytes were differentiated into adherent macrophages, as previously described (252), using 200 nM phorbol-12-myristate-13-acetate (PMA, #4174S, Cell Signaling) for 3 days, followed by a 5-day resting period (THP1PMA cells).

Following differentiation into macrophages, the THP1PMA cells were primed with 100 ng/mL LPS (E. coli O111:B4, #LPS25, Sigma-Aldrich) for 4 h and activated with 5 mM ATP (#R0441, Thermo Scientific) for 15 min, before fixation.

In order to block the activation of the NLRP3 inflammasome, THP1PMA cells were treated with either 10 µM quinine (#ab141247, Abcam), 30 mM KCl or 50 µM glyburide (#15009, Cayman Chem) for 30 min, before priming with LPS and activation with ATP, as described above.

#### 3.6.2. K<sup>+</sup> efflux (paper 2)

HEK293 cells were treated with 10 mM tetraethylammonium chloride (TEA) before fixation for 30 min using 3% PFA in PBS or with 10 µM nigericin for 1 h before fixation for 30 min using 3% PFA in PB. The staining procedure was performed as described.

### 3.6.3. Cycloheximide chase assay (paper 3)

Transduced HEK293 cells stably overexpressing wild type and mutant Pellino-2 with a C-terminal HA tag were seeded in 6-well dishes at  $5 \times 10^5$  cells/well. At 70-80% confluency, the cells were treated with 10  $\mu\text{g}/\text{mL}$  cycloheximide (Sigma-Aldrich, #C4859-1ML) for the indicated time points, followed by cell lysis and immunoblotting.

### 3.7. Immunofluorescence (paper 1, 2 & 3)

Fixation was performed at room temperature for 30 min, with 3 % paraformaldehyde (PFA) in 0.1 M phosphate buffer pH=7.2 or 1x PBS pH=7.4 prewarmed at 37 °C, followed by 3 quick washing steps with 0.2 % BSA (#9998S, Cell Signaling Technology) in PBS, supplemented with 0.02 % sodium azide (wash solution). Permeabilization was done with 0.2 % saponin (#47036, Sigma-Aldrich) in wash solution, for 5 min at room temperature. Unspecific antibody binding sites were blocked with the permeabilization solution supplemented with 5 % normal goat serum (#ab7481, Abcam), filtered through 0.2  $\mu\text{m}$  sterile filter. Incubation with primary antibody properly diluted in block solution was performed at room temperature, for 2 h. The cells were thoroughly washed 3 times with wash solution, followed by a long overnight washing step at room temperature on a rocking platform. The secondary antibody incubation was performed for 2 h, at room temperature, in block solution. The cells were washed 3 times with wash solution, followed by a long washing step at room temperature on a rocking platform, followed by a final rinse in PBS and  $\text{dH}_2\text{O}$ , before mounting the coverslips on glass slides with ProLong® Gold Antifade Reagent with DAPI (#8961, Cell Signaling).

Double labeling immunofluorescence analysis was performed using antibodies against Pellino-2 (#HPA053182, Sigma-Aldrich), NLRP3 (#ALX-804-819-C100, Enzo) ASC (#sc-514414, Santa Cruz), GM130 (#610823, BD Transduction Laboratories), acetylated  $\alpha$ -tubulin (#T6793, Sigma Aldrich), LAMP-1 (#sc-18821, Santa Cruz), TOMM20 (#WH0009804M1, Sigma Aldrich), proteasome 19S S5A/ASF (#ab20239, Abcam), LC3 (#SAB1305552, Sigma Aldrich), ATP synthase subunit IF1 (ATPIF1, #A-21355, ThermoFischer Scientific), splicing factor SC-35 (gift from prof. Karl-

Henning Kalland, University of Bergen), PML nuclear bodies (#sc-966, Santa Cruz), and proliferating cell nuclear antigen PCNA (#2586, Cell Signaling).

Goat anti-rabbit IgG Alexa Fluor® 488 and goat anti-mouse IgG Alexa Fluor® 594 (#111-546-144 and #115-586-146, both from Jackson Laboratories) were used as secondary antibodies.

### 3.8. Transient transfection, cell lysis and co-immunoprecipitation (paper 1, 2 & 3)

For transient transfection, 8  $\mu$ L Lipofectamine 2000 reagent (Invitrogen, Waltham, Massachusetts, USA) and 2  $\mu$ g plasmid DNA were added to HEK293 cells upon 60-70 % confluency. Cells were harvested after 40 h in cold lysis buffer and after 20 min incubation on ice, the cells were gently lysed on a rotor for 45 min, then centrifuged at 21250 g and 4 °C for 10 min.

Co-immunoprecipitation with anti-FLAG M2 magnetic beads (#M8823, Merck) was performed for 90 min at room temperature, followed by four washing steps with PBS + 0.5 % Triton-X100.

Co-immunoprecipitation with anti-HA magnetic beads (#88837, Thermo Fischer) was performed according to manufacturer's instructions: inputs were aliquoted before cell supernatants were incubated with anti-HA magnetic beads for 30 min at room temperature. The beads were washed 4x 3 min with washing buffer, before boiling the samples with Bolt LDS sample buffer (#B0007, Thermo Fischer) and Bolt sample reducing agent (#B0009, Thermo Fischer) at 98 °C for 10 min.

The exact composition of the lysis buffer and the washing buffer for each individual interaction partner studied can be found in Table 4.

### 3.9. Subcellular fractionation (paper 2)

HEK293 cells were seeded on 10-cm dishes ( $10^6$  cells/dish) and grown until 70-80 % confluency. Prior to harvesting, the cells were washed 2 times with cold, serum-free medium. The cells were scraped and collected in 9 mL cold, serum-free medium. The cells were centrifuged for 5 min at 900 g and 4 °C and washed two more times with 5 mL of cold, serum-free medium, before resuspending the cells in 500  $\mu$ L cold



**Table 4.** Components of the lysis buffer and washing buffer used for co-immunoprecipitation of target proteins

Target protein	Lysis buffer	Washing buffer
Cyclin F	50 mM Tris HCl pH 7.5, 200 mM NaCl, 5 mM EDTA, 0.1 % NP40, 0.5 % Tween20, 1 mM PMSF, Complete protease inhibitors (Roche)	Lysis buffer diluted 1/10 with dH <sub>2</sub> O
DVL2	50 mM Tris HCl pH 7.5, 200 mM NaCl, 5 mM EDTA, 0.1 % NP40, 0.5 % Tween20, 1 mM PMSF, Complete protease inhibitors (Roche)	Lysis buffer diluted 1/5 with dH <sub>2</sub> O
IRAK-1 (p <sub>i</sub> =5.87)	Citric acid-Na <sub>2</sub> HPO <sub>4</sub> buffer pH=5.87, 200 mM NaCl, 5 mM EDTA, 0.1 % NP40, 0.5 % Tween20, 1 mM PMSF, 5% Triton-X100, Complete protease inhibitors (Roche)	Lysis buffer
IRAK-4 (p <sub>i</sub> =5.23)	Citric acid-Na <sub>2</sub> HPO <sub>4</sub> buffer pH=5.23, 200 mM NaCl, 5 mM EDTA, 0.1 % NP40, 0.5 % Tween20, 1 mM PMSF, Complete protease inhibitors (Roche)	Lysis buffer
NEK-9	50 mM Tris HCl pH 7.5, 200 mM NaCl, 5 mM EDTA, 0.1 % NP40, 0.5 % Tween20, 1 mM PMSF, Complete protease inhibitors (Roche)	Lysis buffer diluted 1/15 with dH <sub>2</sub> O
ROBO-1	50 mM Tris HCl pH 7.5, 200 mM NaCl, 5 mM EDTA, 0.1 % NP40, 0.5 % Tween20, 1 mM PMSF, 5% Triton-X100, Complete protease inhibitors (Roche)	Lysis buffer
TAK-1 (p <sub>i</sub> =6.23)	Citric acid-Na <sub>2</sub> HPO <sub>4</sub> buffer pH=6.23, 200 mM NaCl, 5 mM EDTA, 0.1 % NP40, 0.5 % Tween20, 1 mM PMSF, 5% Triton-X100, Complete protease inhibitors (Roche)	Lysis buffer
TRAF6 (p <sub>i</sub> =6.1)	Citric acid-Na <sub>2</sub> HPO <sub>4</sub> buffer pH=6.1, 200 mM NaCl, 5 mM EDTA, 0.1 % NP40, 0.5 % Tween20, 1 mM PMSF, 5% Triton-X100, Complete protease inhibitors (Roche)	Lysis buffer
TRAF7 (p <sub>i</sub> =6.1)	Citric acid-Na <sub>2</sub> HPO <sub>4</sub> buffer pH=6.1, 600 mM NaCl, 5 mM EDTA, 0.1 % NP40, 0.5 % Tween20, 1 mM PMSF, 5% Triton-X100, Complete protease inhibitors (Roche)	Lysis buffer

homogenization buffer (10 mM HEPES pH 7.4, 50 mM sucrose, 1 mM PMSF, 1 µg/mL aprotinin, supplemented with Complete protease inhibitors Roche). The cells suspension was homogenized 20 times with the cell homogenizer (Isobiotec, Heidelberg, Germany) using the 8-µm clearance ball and two 1-mL syringes. Afterwards, 500 µl cold homogenization buffer was added and the cells were homogenized 40 times more.

The cell lysate was centrifuged at 4 °C and 2,000 g for 10 min. The pellet (nuclear fraction) was resuspended in homogenization buffer. The supernatant (cytoplasmic fraction) was centrifuged at 100,000 g at 4 °C for 60 min. After resuspension in homogenization buffer and centrifugation at 100,000 g at 4 °C for 15 min, the pellet (membranous fraction) was resuspended in homogenization buffer. Acetone precipitation was performed on all three fractions and resuspended in equal amount of sample buffer for immunoblot analysis.

For the detection of Na<sup>+</sup>/K<sup>+</sup>-ATPase, the nuclear, cytoplasmic and membranous fractions were resuspended in RIPA buffer (25 mM Tris HCl pH 7.6, 150 mM NaCl, 1 % NP40, 1 % Na deoxycholate, 0.1 % SDS, supplemented with Roche protease inhibitors) and directly added to the gel, without boiling them.

### 3.10. Yeast two-hybrid screen (paper 2)

The yeast two-hybrid screen was performed by Hybrigenics Services (Paris, France). Briefly, full-length human *PELI2* cDNA in an N-LexA-bait-C fusion vector was used as bait, and a human lung cancer random primed cDNA fragment library as prey. The number of analyzed interactions was 98.1 million. The positive clones were isolated and their corresponding prey fragments were Sanger-sequenced and identified using the NCBI GenBank Database. A predicted biological score (PBS) was calculated for each candidate, assessing the reliability of each protein-protein interaction (highest probability of specificity: score A; lowest probability of specificity: score E).

### 3.11. Immunoblotting (paper 1, 2 & 3)

The protein samples were resolved on Bolt® 4-12% Bis-Tris Plus gels, at 200 V for 38 min, in 1x Bolt® MES SDS Running Buffer. Separated proteins were transferred onto nitrocellulose membrane at 10 V for 1 h, at 4 °C, in 1x Bolt® Transfer Buffer, supplemented with 10 % methanol.

On a rocking platform, the membranes were incubated with blocking solution (5 % non-fat dry milk) for 1 h, followed by 3x5 min washing steps with TBST. The membranes were incubated at 4 °C overnight with the primary antibody (dilution in 5 % BSA in TBST). After 3x5 min washing with TBST, the membranes were incubated for 1 h at room temperature with HRP-linked anti-rabbit IgG secondary antibody (Cell Signaling, #7074) or HRP-linked anti-mouse IgG secondary antibody (Cell Signaling, #7076), 1:2,000 dilution in 5 % non-fat dry milk in TBST. The final washing steps of 3x5 min were performed with TBST, followed by enhanced chemiluminescent detection on a ChemiDoc Touch Imaging System (Biorad).

Proteins were visualized using the Super Signal West Pico system alone or with added Super Signal West Femto Maximum Sensitivity Substrate (Thermo Fisher Scientific,

Rockford, IL). A protein standard (MagicMark; Thermo Fisher Scientific) was used as a molecular weight marker.

Antibodies used were targeting Pellino-2 (#HPA053182, Sigma-Aldrich), HA tag (#71-5500, Thermo Scientific), GFP tag (JL-8, #632381, Clontech Labs), GAPDH (#G9545, Sigma-Aldrich), Na<sup>+</sup>/K<sup>+</sup>-ATPase (#ab76020, Abcam), IRAK-1 (#4504, Cell Signaling), IRAK-4 (#4363, Cell Signaling), TRAF6 (#8028, Cell Signaling),  $\alpha$ -tubulin (#3873, Cell Signaling), HP1 $\alpha$  (#2616, Cell Signaling) and TAK-1 (#4505, Cell Signaling). DVL-2 (#3216, Cell Signaling), NEK9 (#ab138488, Abcam), ROBO-1 (#ab7279, Abcam) and cyclin F (#sc-952, Santa Cruz) were detected as previously described (240).

### 3.12. ELISA (paper 1 & 3)

Polystyrene 96-well plates (Thermo Scientific™) were pre-coated overnight at 4 °C with specific IL-1 $\beta$  capture antibody, then blocked with ELISA/ELISASPOT diluent for 1 hour at RT, and incubated with standard IL-1 $\beta$  dilutions and cell cultures media (100  $\mu$ L, undiluted) overnight at 4 °C followed by washes with PBS plus 0.05 % Tween-20, and incubation with biotinylated detection antibody for 1 hour at RT. The plates were incubated with avidin-HRP for 30 min at RT and washed again. The signal was developed after addition of tetramethylbenzidine (TMB) for 15 min and the reaction was stopped by 1 M H<sub>2</sub>SO<sub>4</sub>. BioTek Synergy™ HT microplate reader was used to detect the signals with 450 nm and correction at 470 nm. The detection range of IL-1 $\beta$  ELISA was 2-150 pg/ml.

### 3.13. Cell viability assay (paper 1 & 3)

Cell proliferation/viability following NLRP3 inflammasome activation was assessed by WST-1 assay. Twenty-four hours after inflammasome activation, the WST-1 reagent (#5015944001, Roche) was added into the wells at a 1:10 dilution and incubated for an additional 4 h at 37 °C. The optical density (OD) was measured at wavelength 440 nm with correction at 650 nm, using a BioTek Synergy™ HT microplate reader.

### 3.14. Live cell imaging (paper 2)

Transgenic immortalized fibroblasts stably overexpressing Pellino-2 with an N-terminal GFP tag were seeded in 35 mm culture dishes (#P35G-1.5-14-C, MatTek, no. 1.5 coverslip, 14 mm glass diameter, uncoated) for live cell imaging. The Andor Dragonfly 505 confocal spinning disk system was used, under temperature and CO<sub>2</sub> control (37 °C and 5% CO<sub>2</sub>).

### 3.15. Image acquisition and analysis (paper 1, 2 & 3)

Images were acquired using Leica SP5 and SP8 confocal laser-scanning microscopes (Leica Microsystems). The Z-stack function was used to enhance resolution and allow for 3D examination, in order to confirm co-localization. Post-processing of images was performed using the integrated adaptive deconvolution module Lightning (Leica Microsystems). Images were prepared for publication using Adobe Photoshop and Illustrator.

### 3.16. Statistical analysis and reproducibility (paper 1, 2 & 3)

Statistical analysis was performed using the software Prism 9. All results have been replicated in at least 3 independent experiments.



## **Results**

### 4.1. Paper 1

#### **K<sup>+</sup> regulates relocation of Pellino-2 to the site of NLRP3 inflammasome activation in macrophages**

##### **Background**

The Pellino proteins have been identified as key E3 ubiquitin ligases that mediate innate immune responses. More precisely, Pellino-2 has been shown to be involved in the activation of the mouse Nlpr3 inflammasome by indirectly promoting Lys-63-linked poly-ubiquitination of NLRP3 in the priming step.

##### **Methodology**

In human THP-1 monocytes differentiated into macrophages using phorbol-12-myristate-13-acetate (PMA) and primed with LPS and activated with ATP, we performed indirect immunofluorescence against endogenous Pellino-2, NLRP3 and ASC, in order to examine the relationship between Pellino-2 and NLRP3 inflammasome activation. The macrophages were also cultured in K<sup>+</sup>-free medium and treated with K<sup>+</sup> channel blockers. To confirm the activation of NLRP3 inflammasome, ELISA analysis of secreted IL-1 $\beta$  was performed in parallel.

##### **Summary of results**

In resting THP1-derived macrophages, Pellino-2 was endogenously expressed throughout the cytoplasm. NLRP3 and ASC proteins were upregulated upon LPS priming and ATP activation. Following NLRP3 inflammasome activation, Pellino-2 changed intracellular localization and co-localized with both the NLRP3 protein and ASC protein, in the late stages of inflammasome assembly.

Given the role of K<sup>+</sup> efflux in NLRP3 inflammasome activation, we next studied the effect of extracellular K<sup>+</sup> levels on Pellino-2 localization by maintaining the cells in K<sup>+</sup>-free medium, without LPS and ATP-induced activation. The co-localization of Pellino-2 with NLRP3 and ASC was also seen in these cells when maintained in K<sup>+</sup>-free

medium, suggesting that low levels of extracellular  $K^+$  alone are sufficient to activate the NLRP3 inflammasome and also to initiate the interaction of Pellino-2 with NLRP3 and ASC.

We next blocked the efflux of  $K^+$  ions from THP1-derived macrophages by incubating them with quinine, KCl or glyburide prior to their activation. Upon treatment with these compounds, Pellino-2 did not change localization under activating conditions or by cultivation in  $K^+$ -free medium. This suggests that Pellino-2 localization is directly sensitive to  $K^+$  efflux from the cells. In line with this, significantly reduced levels of IL-1 $\beta$  secretion were observed, indicating that NLRP3 inflammasome activation had not been fully completed, in the absence of Pellino-2 relocation to the inflammasome.

We observed that when replacing a fixation buffer with physiological  $K^+$  concentration (phosphate buffer saline (PBS)) with phosphate buffer (PB) which does not contain  $K^+$ , this affected Pellino-2 localization. In THP1-derived macrophages primed with LPS before PB-fixation, Pellino-2 presented in the nucleus instead of the cytoplasm as seen with PBS-fixation. Otherwise, priming and activation of the NLRP3 inflammasome, as well as relocation of Pellino-2 intracellularly and its co-localization with NLRP3 after culturing the cells in  $K^+$ -free culture medium were similar in PB- and PBS-fixed cells. In conclusion, we showed that Pellino-2 is a crucial element in the assembly and activation of the NLRP3 inflammasome, and that  $K^+$  efflux has an essential role in Pellino-2 intracellular localization.

#### 4.2. Paper 2

### **Pellino-2 in nonimmune cells: novel interaction partners and intracellular localization**

#### **Background**

In immune cells,  $K^+$  ions influence the intracellular localization of Pellino-2 and its function in the assembly and activation of the NLRP3 inflammasome.

Classically, the Pellino proteins have been identified as substrates or binding partners of proteins involved in the TLR pathway. While Pellino-1 and Pellino-3 have been well

characterized, no extensive studies of Pellino-2 have been performed in non-immune cells, in terms of intracellular localization and interaction partners.

### **Methodology**

To identify novel interaction partners of Pellino-2, we performed yeast two-hybrid screening, followed by co-immunoprecipitation experiments. To visualize the intracellular localization of Pellino-2, we performed indirect immunofluorescence against endogenous Pellino-2 in a variety of cell lines, as well as subcellular fractionation. Live cell imaging was also employed, in GFP-tagged Pellino-2 stably transfected fibroblasts.

### **Summary of results**

Following a yeast two-hybrid screen, we identified several novel protein-protein interactions: Pellino-2 interacts with cyclin F, DVL-2, TRAF7 and ROBO-1 with very high confidence, IRS-1 and NEK9 with high confidence, as well as other proteins, with lower confidence interaction score. These data were confirmed in co-immunoprecipitation experiments. These novel interaction partners are found in different cellular compartments and have diverse functions in intracellular signaling cascades.

In immunofluorescence experiments, we observed that Pellino-2 was localized in the cytoplasm, when using phosphate buffer saline (PBS) as fixation buffer with physiological concentration of  $K^+$  ions. In contrast, when phosphate buffer (PB) that does not contain  $K^+$  was used as fixation buffer, Pellino-2 relocated to the nucleus. Treatment with the potassium ionophore nigericin resulted in nuclear localization of Pellino-2, which was reversed by the potassium channel blocker TEA.

In subcellular fractionation experiments, Pellino-2 was recovered in the membranous fraction of the cytoplasm. In double immunofluorescence against Pellino-2 and a variety of organelle markers, we saw no colocalization between Pellino-2 and any of the examined protein markers: GM130, acetylated  $\alpha$ -tubulin, TOMM20, ATP synthase subunit IF1, LAMP-1, LC3, proteasome 19S S5A/ASF and RAB1, splicing factor SC-35, PML nuclear bodies, and proliferating cell nuclear antigen PCNA.



In immortalized fibroblasts stably overexpressing GFP-tagged Pellino-2, the protein was observed in advancing and retracting membrane protrusions (ruffles), as well as in mobile protein aggregates. Overexpressed Pellino-2 was very dynamic in nature, as it condensed in aggregates that appeared and disappeared at different locations inside the cells, as well as traveling to different parts of the cell.

#### 4.3. Paper 3

### ***A de novo PELI2* variant associated with constitutive NLRP3 inflammasome activation**

#### **Background**

Ocular pterygium-digital keloid dysplasia is characterized by early onset corneal neovascularization causing reduced visions. Patients later develop keloids on digits. A temperature-sensitive activation mutation *PDGFRB* has been associated with OPDKD. In this study, a family with an adolescent boy suffering from OPDKD underwent genetic analysis to identify the variant associated with the disease.

#### **Methodology**

Trio exome sequencing followed by Sanger sequencing were used to identify novel, potentially disease-causing mutations. ELISA analysis and cell viability assays were conducted on stably transfected U87MG cells, overexpressing the WT or the Thr257Ile Pellino-2 amino acid substitution.

Immunofluorescence of endogenous Pellino-2 was performed on the patient fibroblasts and age- and sex-matched controls.

In stably transfected HEK293 cells carrying wild type or the Thr257Ile Pellino-2 substitution, protein-protein interactions were examined using co-immunoprecipitation. Lastly, protein stability was studied using a cycloheximide chase assay.

#### **Summary of results**

*A de novo* variant in *PELI2*, g.C770T p.(Thr257Ile) was identified and predicted to be damaging.

The Pellino-2 OPDKD variant did not affect the binding of the Pellino-2 protein to its interaction partners (IRAK-1, TAK-1, TRAF6, ROBO-1, NEK9, DVL2, cyclin F, TRAF7), nor did it affect the stability and turnover of the protein compared to the wild type protein. The novel variant also did not impact the ability of Pellino-2 to change intracellular localization upon  $K^+$  efflux.

In transgenic U87MG cells stably overexpressing Thr257Ile Pellino-2, much higher baseline levels of IL-1 $\beta$  secretion was observed in non-activated cells (NT or LPS priming), compared to cells overexpressing WT Pellino-2. This suggests that the mutation leads to a constitutive activation of the NLRP3 inflammasome. Furthermore, IL-1 $\beta$  secretion was significantly increased in activated cells overexpressing the Thr257Ile Pellino-2, compared to wild type.



## Discussion

The focus of this thesis has been the lesser studied isoform of the Pellino family of E3 ubiquitin ligases, the Pellino-2 protein. Our work started with a Peruvian patient that presented with an OPDKD-like phenotype: ocular pterygium due to corneal neovascularization, and keloids on hands and feet. At the time, the disease-causing mutation of this condition was not known. As we already had under our care a Norwegian family with this condition, our idea was to examine the two families looking for mutations in a common gene. However, no such gene was identified in our analysis and we later showed that the disease-causing variant in the Norwegian family was *PDGFRB* c.1996A>T, p.(Asn666Tyr) (208). While no *PDGFRB* mutation was found in the Peruvian patient, data analysis revealed that a *de novo* mutation in *PELI2* could be the likely candidate for causing OPDKD.

At the time, there were conflicting and few reports on Pellino-2 function. Most studies performed on Pellino-2 had been done in overexpression conditions, usually transient transfection (29, 32, 35, 57). This leads to high protein expression and may be prone to artefacts (25). At the beginning of this project, the only knowledge on Pellino-2 was that it most likely had an E3 ubiquitin ligase function, due to a RING-like domain discovered in the C terminus of the protein (35, 38). Additionally, a forkhead-associated (FHA) domain had also been characterized for Pellino-2 (34). The function of the FHA domain had been described as binding phospho-Thr residues located in the substrates that Pellino-2 binds to (34).

Therefore, before performing any extensive analysis of the OPDKD variant, first we had to characterize Pellino-2 in more depth.

### 5.1. Pellino-2 in non-immune cells

Before the initiation of this thesis, studies on Pellino-2 had been conducted in non-immune cells, but under overexpression conditions, using transfected Pellino-2 tagged with a variety of recombinant epitopes. However, no localization study had been performed on endogenous Pellino-2.

We therefore began by investigating the intracellular distribution of endogenous Pellino-2 in a variety of non-immune cell lines, to obtain information that is not confined to an individual cell type. We used cancerous, as well as non-cancerous cell lines, immortalized cell lines, as well as primary cultures. In immunofluorescence experiments, we noticed a striking difference in the subcellular localization of Pellino-2, depending on the buffer used for dissolving the paraformaldehyde for fixation.

Using a fixation buffer lacking  $K^+$  ions, Pellino-2 had a nuclear localization in all cells with the exception of HeLa cells. However, when the fixation buffer contained a concentration of  $K^+$  similar to physiological extracellular  $K^+$  concentration, Pellino-2 was localized in the cytoplasm of all tested cells. HeLa cells again stood out in the amount of expressed Pellino-2 and the distribution pattern: while most studied cells have a punctate pattern for Pellino-2 distribution, HeLa cells expressed an abundant amount of Pellino-2.

The influence of  $K^+$  ions on Pellino-2 localization was further confirmed in experiments using either  $K^+$  channel blockers to prevent  $K^+$  efflux from the cells, or ionophores that increase the efflux of  $K^+$  ions from within cells.

The finding that  $K^+$  ions have such a clear effect on Pellino-2 intracellular localization was very intriguing for us. PubMed searches on “potassium” or “potassium efflux” at the time were only limited to immune cells, in relation to another element of the innate immune system, the NLRP3 inflammasome. Then in 2018, Humphries and colleagues published the first *PELI2* knockout mouse model which indicated that Pellino-2 played a role in the activation of the NLRP3 inflammasome and secretion of IL-1 $\beta$  (64).

## 5.2. Pellino-2 in immune cells

Pellino-2 is classically involved in TLR signaling. As an E3 ubiquitin ligase, it can ubiquitinate TLR downstream kinases, such as IRAK-1 and IRAK-4, and at the same time be a substrate for phosphorylation by these kinases (29, 38). Pellino-2 involvement leads to NF- $\kappa$ B activation and upregulation of pro-inflammatory cytokines, such as IL-6, IL-8, and TNF $\alpha$  (61).

Interestingly, while Pellino-3 has been shown to temper the inflammatory response (56), Pellino-2 seems to act in a pro-inflammatory way. In their 2018 study, Humphries

and colleagues showed that Pellino-2 is tightly involved in the secretion of IL-1 $\beta$ , by indirectly mediating NLRP3 poly-ubiquitination during the priming step of NLRP3 inflammasome activation (64). IL-1 $\beta$  is a key cytokine, that can further trigger the secretion of other pro-inflammatory cytokines, therefore it is also called an “early responsive cytokine” (253).

We therefore continued the explorations of Pellino-2 and K<sup>+</sup> efflux, using the NLRP3 inflammasome activation as a study system. We were able to show that Pellino-2 colocalizes with NLRP3 and ASC proteins during inflammasome assembly and is a crucial element in the assembly of the inflammasome and secretion of IL-1 $\beta$ . This led to the observation that Pellino-2 changes intracellular localization in activated macrophages, compared to resting macrophages. While Pellino-2 is found in the cytoplasm of resting immune cells, when these become activated, Pellino-2 relocates to the site of the NLRP3 inflammasome.

Although the Pellino proteins were initially thought to have overlapping roles, the generation of knockout mice lacking one of the Pellinos proved that the proteins have distinct but overlapping functions. For instance, Pellino-1 expression has been shown to be upregulated by LPS treatment (51, 254), but we found that Pellino-2 protein levels are not affected by LPS treatment (249).

### 5.3. Pellino-2 is a K<sup>+</sup> sensor

Given that K<sup>+</sup> efflux has been widely recognized as a cellular event mediating the activation of the inflammasome, we hypothesized that intracellular K<sup>+</sup> concentration may influence Pellino-2 localization also in immune cells. Use of several K<sup>+</sup> channel blockers revealed that indeed, in THP-1 cells, Pellino-2 can change localization due to K<sup>+</sup> efflux, and that blocking K<sup>+</sup> channels inhibits Pellino-2 relocation, NLRP3 inflammasome maturation and IL-1 $\beta$  secretion.

Thus, we have shown that Pellino-2 intracellular localization is highly sensitive to K<sup>+</sup> efflux and the intracellular K<sup>+</sup> concentration. It is unclear how Pellino-2 can sense this event, of K<sup>+</sup> efflux, but it has been shown previously that K<sup>+</sup> ions are found in the enzymatic centers of functional ribosomes (143), suggesting the importance of metal ions for protein synthesis and/or function. It is conceivable that K<sup>+</sup> ions can also be

found in the 3D structure of Pellino-2 and that the depletion of intracellular  $K^+$  affects the structural integrity of Pellino-2 or alters its function. Of course, X-ray crystallography or cryo-electron microscopy may elucidate these hypotheses.

In non-immune cells, under non-physiological conditions, Pellino-2 relocates to the nucleus due to  $K^+$  efflux. The functional significance of this is still unclear, although it enables Pellino-2 to gain access to its nuclear interaction partners, NEK9 and cyclin F.

#### 5.4. Pellino-2 and novel interaction partners

A different direction of this thesis has been to identify novel protein-protein interactions involving Pellino-2. As a next step, we wanted to determine if any of these interactions were affected by the OPDKD-associated variant. A yeast two-hybrid screen identified 13 potential interactors of Pellino-2 and co-immunoprecipitation experiments confirmed the six top candidates: ROBO-1, IRS-1, DVL-2, TRAF7, cyclin F and NEK9. The wide range of intracellular signaling pathways in which these proteins are involved suggests that Pellino-2 is a more versatile protein than originally thought. Its classical function as E3 ubiquitin ligase remains to be explored in relation to all these newly identified interaction partners, however it is conceivable that Pellino-2 may exert other functions apart from ubiquitination.

The interplay between Pellino-2 and its interaction partners is a dynamic and complex process, and beyond the scope of the present study. In the following section, potential implications for these protein-protein interactions are briefly discussed.

IRS-1 and DVL-2 have been hypothesized to act in conjunction during epithelial-mesenchymal transitioning. IRS-1 is thought to impair the activity of a yet unknown E3 ubiquitin ligase thus leading to the blocking of DVL-2 poly-ubiquitination and degradation (255). Depending on which protein Pellino-2 binds to, it may facilitate (via IRS-1) or, quite the opposite, block epithelial-mesenchymal transition (via DVL-2).

Pellino-2 also interacts with NEK9 and cyclin F, both with nuclear localization and with roles in the cell division process. NEK9 is a kinase that initiates interphase progression, by phosphorylating histones and NEK6 and NEK7, thus controlling chromosome separation. Cyclin F is an E3 ubiquitin ligase that targets CCP110 during G2 phase for proteasomal degradation, thereby acting as an inhibitor of centrosome reduplication.

Again, depending on which protein Pellino-2 interacts with, it may act as a facilitator (via NEK9) or inhibitor (via cyclin F) of cell division.

TRAF7 belongs to the TNF receptor associated factor (TRAF) family of proteins, alongside TRAF6, a known interaction partner of Pellino-2. TRAF6-Pellino-2 interaction has been extensively characterized (32, 33, 61). TRAF7 also possesses E3 ubiquitin ligase activity and may target Pellino-2 for ubiquitination. Conversely, Pellino-2 may exert its E3 ubiquitin ligase activity on TRAF7, since no E3 ubiquitin ligases are known to target TRAF7 for ubiquitination. TRAF7 stands out from its TRAF family of proteins due to its structure: TRAF7 has only one TRAF-type ZINC finger domain (compared to two or three, like the other TRAFs). In addition, instead of a C-terminal TRAF domain, TRAF7 presents seven WD40 repeats (256). Therefore, it may be that Pellino-2 signaling via TRAF7 has novel implications for downstream signaling. Interestingly, TRAF7 interacts with ROBO-4, a member of the ROBO family of proteins (257).

Several interaction partners of Pellino-2 are known to be important in NLRP3 function. Activation of NLRP3 inflammasome has been shown to decrease IRS-1 expression levels (258), while the antidiabetic drug glyburide inhibits NLRP3 inflammasome activation, by blocking  $K^+$  channels and thus  $K^+$  efflux (156). Furthermore, the process of epithelial-to-mesenchymal transition, involving among others DVL-2, has been shown to occur downstream of the NLRP3 inflammasome activation (259). Another interesting recent finding is that NEK7, a nuclear kinase and a substrate of Pellino-2 newly identified interaction partner NEK9, is a crucial element in the activation of the NLRP3 inflammasome (178). Noteworthy, NLRP3 inflammasome activation and cell division (mitosis) are mutually exclusive events (177), therefore NEK7 activity during NLRP3 inflammasome activation must be different than its activity during cell division. We have shown that  $K^+$  efflux leads to Pellino-2 relocation during inflammasome activation (249). It has also been shown that NEK7 activity occurs downstream of  $K^+$  efflux, prior to inflammasome activation (139). We hypothesize that  $K^+$  efflux leads to Pellino-2 relocation, which activates its binding partner NEK9. Downstream of NEK9, NEK7 contributes to the activation of NLRP3 inflammasome. Further investigations are needed to confirm this. Also, it remains to be elucidated how  $K^+$  efflux (that leads



to Pellino-2 relocation) plays a role in such diverse intracellular signaling cascades like cell migration, epithelial-mesenchymal transition, insulin signaling, or cell division.

### 5.5. Pellino-2 in disease

As previously mentioned, this study into Pellino-2 was initiated after a likely disease-causing *PELI2* variant was found in a patient with OPDKD. Furthermore, bioinformatic predictors of mutation pathogenicity have indicated that the c.770C>T, p.(Thr257Ile) *PELI2* variant is likely to be damaging.

Initially, we wanted to investigate the effects of the OPDKD *PELI2* variant in patient macrophages. Unfortunately, the patient carrying this mutation lives in a remote mountainous area in Peru and we have only been able to obtain a skin biopsy from him. The alternative was to produce stably transfected THP-1 monocytes, that can easily be converted to macrophages. Transduction of THP-1 cells using shRNA constructs has been successful (260-262). However, we have been unable to transduce THP-1 cells with lentiviral vectors carrying full-length wild type or c.770C>T *PELI2* cDNA.

As an alternative, we chose to stably overexpress *PELI2* with a C-terminal HA tag in U87MG cells. U87MG cells are glioblastoma cells, originating from astrocytes. Alongside microglia, astrocytes also perform innate immune functions in the brain. The U87MG cells therefore contain NLRP3 inflammasome components, but the cells are different from immune cells in that expression of NLRP3 is not upregulated by bacterial components like LPS. The cells are relatively easy to transduce to make stably transfected cells (263).

In transgenic U87MG cells overexpressing the c.770C>T *PELI2* variant, we observed constitutive activation of the NLRP3 inflammasome, by measuring high levels of secreted IL-1 $\beta$  even in resting cells. This suggests that chronic inflammation may be important in *PELI2*-associated OPDKD development.

Multiple potential mechanisms have been hypothesized for the development of pterygium and keloids (oxidative stress, UV light, epigenetics) and several molecules related to proliferation, inflammation, angiogenesis and fibrosis are common biomarkers related to the development of these conditions (264, 265). The NLRP3 inflammasome has also been implicated in their pathogenesis, as both pterygium and

keloids seem to present with high levels of NLRP3 (191, 194), caspase-1 and IL-1 $\beta$  (181, 191).

We have shown by various methods in our first two publications that Pellino-2 can change localization depending on the intracellular concentration of K<sup>+</sup> ions: upon K<sup>+</sup> efflux, Pellino-2 is redistributed to different intracellular compartments. The fact that K<sup>+</sup> efflux leads to NLRP3 inflammasome activation has been known for some time (108). Our work has strengthened the connection between Pellino-2 and NLRP3 inflammasome assembly and activation, and further, that K<sup>+</sup> efflux is important in this process.

At the same time, we are reporting a novel *PELI2* variant associated with OPDKD. The mutation appears to be disease-causing via constitutive NLRP3 inflammasome activation. The variant did not affect the ability of Pellino-2 to relocate in response to K<sup>+</sup> efflux.

Genetic mutations of *NLRP3* that constitutively activate the NLRP3 inflammasome are well documented (187), for example c.61G>C, p.(Asp21His), a heterozygous pathogenic variant associated with keratitis fugax hereditaria (KFH) (200). There are several similarities between OPDKD and KFH, as well as some differences. Both conditions can manifest at an early age with corneal changes alone (KFH) or in combination with skin changes (OPDKD). On the other hand, KFH is an episodic disease, whereas OPDKD is a progressive disease. Further, *PDGFRB*-related OPDKD is caused by a temperature-sensitive variant, whereas KFH has not been linked to seasonal variations (188).

There are also *NLRP3* mutations that lead to NLRP3 inflammasome activation under cold conditions (203). We show that the activation of the NLRP3 inflammasome could be initiated, by simply culturing macrophages at lower temperatures. This is of particular interest as recently, a temperature-sensitive mutation in *PDGFRB* (MIM#173419) was found associated with OPDKD in a Norwegian family (208). This autosomal dominant variant NM\_002609.3 (*PDGFRB*): c.1996A>T, p.(Asn666Tyr) leads to ligand-independent autoactivation of the kinase at 32 °C, the physiological corneal temperature. As both cornea and digits have lower and more variable

temperatures than the core body temperature (242), this observation could be important for understanding why these body parts are most affected in the *PDGFRB*-associated OPDKD. It remains to be determined if the physiological corneal temperature is also important in *PELI2*-associated OPDKD.

Figure 7 summarizes the findings of this thesis and indicates mechanisms contributing to the development of *PELI2*-associated OPDKD.

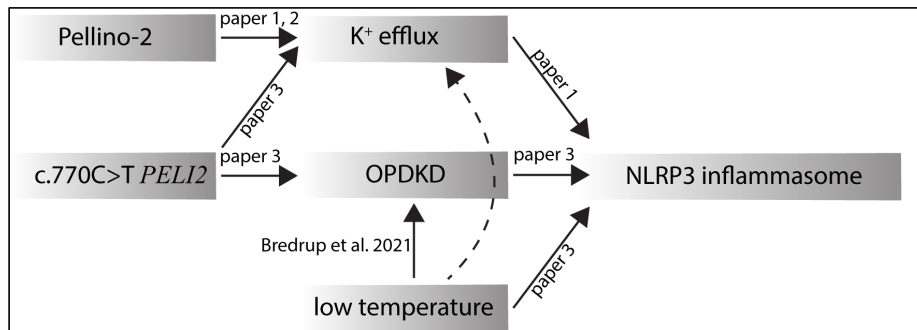


**Figure 7. Proposed mechanism for the development of inflammation mediated OPDKD.**

In the TLR pathways, TAK-1 is a well-known downstream interaction partner of Pellino-2: Pellino-2 is required for TAK1-dependent NF- $\kappa$ B activation (61). Four *de novo* mutations in *MAP3K7* encoding TAK-1 have been shown to cause frontometaphyseal dysplasia 2 (FMD2), a rare skeletal genetic disease associated with keloid development (266-268). The FMD2-associated *MAP3K7* mutations lead to increased TAK-1 autophosphorylation and activation of downstream signaling. It is conceivable that the OPDKD Pellino-2 mutation, acting upstream of TAK-1, activates similar intracellular signaling cascades that lead to abnormal cell proliferation as seen in keloids.

Also toll-like receptors have been implicated in the pathogenesis of both keloids and pterygium, the hallmarks of OPDKD. Pterygial conjunctival cells have increased expression of TLR3 in the superficial layers of the conjunctiva, compared to epithelial layers (214), while TLR6, 7 and 8 are highly upregulated in keloid scars (229). In addition, upregulation of TLR4 was shown in keloids, which led to increased connective tissue growth factor (CTGF) and collagen accumulation within keloids (230).

Together, these data suggest that *PELI2*-associated OPDKD could be caused by an excessive immune process that involves the NLRP3 inflammasome.

Therefore, NLRP3 inflammasome blocking could be a viable target in treatment. However, the identification of the molecular mechanism, via Pellino-2 and K<sup>+</sup> efflux, may provide multiple and more specific targets, in order to avoid off-target immunosuppressive side-effects. There are small molecules already in development against Pellino-1 (another member of the Pellino family) (269) and K<sup>+</sup> channel blockers glyburide and quinine, are commercially available drugs, that indirectly block the inflammasome activation. In addition, there are also drugs that target the inflammasome directly, pointed either at the components of the inflammasome (NLRP3 protein, ASC protein, pro-caspase 1 enzyme) or the end-products of inflammasome activation (IL-1 $\beta$ , IL-18).

## Conclusions and future perspectives

In this thesis, we focused on endogenous Pellino-2 in immune and non-immune cells and characterized multiple facets of this protein. We showed that Pellino-2 acts as a potential  $K^+$  sensor that changes intracellular localization following  $K^+$  efflux. In immune cells, Pellino-2 relocates to the activated NLRP3 inflammasome, and we have shown that Pellino-2 is essential for mediating the effect of  $K^+$  efflux on inflammasome activation. In non-immune cells, Pellino-2 relocates to the nucleus, but the functional significance of this is still unclear. Pellino-2 is constitutively expressed in non-immune cells and it readily responds to  $K^+$  efflux from these cells. This opens up for research into its  $K^+$  sensing ability and the functions and relevance of Pellino-2 in non-immune cells.

One proof of this was the expansion of the list of interaction partners of Pellino-2, to include ROBO-1, IRS-1, DVL-2, TRAF7, cyclin F and NEK9. Our project was exclusively aimed at studying protein-protein interactions in an overexpression system and confirmation of these findings are still needed for endogenously expressed proteins. Nevertheless, these findings open new avenues of research into Pellino-2, especially if these Pellino-interacting proteins are substrates for Pellino-induced ubiquitination. Our data suggest that Pellino-2 is a dynamic protein that can move within the cell to reach its interaction partners. With more Pellino-binding proteins being identified, it is not unlikely that these will also reveal new functions for Pellino-2 in signaling pathways mediated by these interaction partners.

Lastly, we reported a novel mutation in *PELI2* that appears to constitutively activate the NLRP3 inflammasome, a potential mechanism for inflammation and tissue overgrowth in OPDKD. The potential targeting of NLRP3 inflammasome in the treatment of *PELI2*-related OPDKD is subject to further research.



## References

1. Chen L, Deng H, Cui H, Fang J, Zuo Z, Deng J, et al. Inflammatory responses and inflammation-associated diseases in organs. *Oncotarget*. 2018;9(6):7204-18.
2. Kulkarni OP, Lichtnekert J, Anders HJ, Mulay SR. The Immune System in Tissue Environments Regaining Homeostasis after Injury: Is "Inflammation" Always Inflammation? *Mediators Inflamm*. 2016;2016:2856213.
3. Medzhitov R. Inflammation 2010: new adventures of an old flame. *Cell*. 2010;140(6):771-6.
4. Yamauchi T, Moroishi T. Hippo Pathway in Mammalian Adaptive Immune System. *Cells*. 2019;8(5):398.
5. Alishahi M, Farzaneh M, Ghaedrahmati F, Nejabatdoust A, Sarkaki A, Khoshnam SE. NLRP3 inflammasome in ischemic stroke: As possible therapeutic target. *International Journal of Stroke*. 2019;14(6):574-91.
6. Guttman JA, Finlay BB. Tight junctions as targets of infectious agents. *Biochim Biophys Acta*. 2009;1788(4):832-41.
7. Basset C, Holton J, O'Mahony R, Roitt I. Innate immunity and pathogen-host interaction. *Vaccine*. 2003;21 Suppl 2:S12-23.
8. Bouziat R, Jabri B. IMMUNOLOGY. Breaching the gut-vascular barrier. *Science*. 2015;350(6262):742-3.
9. Akashi K, Traver D, Miyamoto T, Weissman IL. A clonogenic common myeloid progenitor that gives rise to all myeloid lineages. *Nature*. 2000;404(6774):193-7.
10. Dunkelberger JR, Song WC. Complement and its role in innate and adaptive immune responses. *Cell research*. 2010;20(1):34-50.
11. Michallet MC, Rota G, Maslowski K, Guarda G. Innate receptors for adaptive immunity. *Curr Opin Microbiol*. 2013;16(3):296-302.
12. Medvedev AE, Murphy M, Zhou H, Li X. E3 ubiquitin ligases Pellinos as regulators of pattern recognition receptor signaling and immune responses. *Immunological reviews*. 2015;266(1):109-22.
13. Schwandner R, Dziarski R, Wesche H, Rothe M, Kirschning CJ. Peptidoglycan- and Lipoteichoic Acid-induced Cell Activation Is Mediated by Toll-like Receptor 2. *Journal of Biological Chemistry*. 1999;274(25):17406-9.
14. Hayashi F, Smith KD, Ozinsky A, Hawn TR, Yi EC, Goodlett DR, et al. The innate immune response to bacterial flagellin is mediated by Toll-like receptor 5. *Nature*. 2001;410(6832):1099-103.
15. Lund JM, Alexopoulou L, Sato A, Karow M, Adams NC, Gale NW, et al. Recognition of single-stranded RNA viruses by Toll-like receptor 7. *Proceedings of the National Academy of Sciences of the United States of America*. 2004;101(15):5598-603.
16. Ramadan A, Land WG, Paczesny S. Editorial: Danger Signals Triggering Immune Response and Inflammation. *Front Immunol*. 2017;8:979.
17. Lin SC, Lo YC, Wu H. Helical assembly in the MyD88-IRAK4-IRAK2 complex in TLR/IL-1R signalling. *Nature*. 2010;465(7300):885-90.
18. Ferrao R, Zhou H, Shan Y, Liu Q, Li Q, Shaw DE, et al. IRAK4 dimerization and trans-autophosphorylation are induced by Myddosome assembly. *Mol Cell*. 2014;55(6):891-903.
19. Moynagh PN. The roles of Pellino E3 ubiquitin ligases in immunity. *Nat Rev Immunol*. 2014;14(2):122-31.

20. Takaesu G, Ninomiya-Tsuji J, Kishida S, Li X, Stark GR, Matsumoto K. Interleukin-1 (IL-1) receptor-associated kinase leads to activation of TAK1 by inducing TAB2 translocation in the IL-1 signaling pathway. *Mol Cell Biol.* 2001;21(7):2475-84.
21. Grosshans J, Schnorrer F, Nusslein-Volhard C. Oligomerisation of Tube and Pelle leads to nuclear localisation of dorsal. *Mech Dev.* 1999;81(1-2):127-38.
22. Rich T, Allen RL, Lucas AM, Stewart A, Trowsdale J. Pellino-related sequences from *Caenorhabditis elegans* and *Homo sapiens*. *Immunogenetics.* 2000;52(1-2):145-9.
23. Resch K, Jockusch H, Schmitt-John T. Assignment of homologous genes, Peli1/PELI1 and Peli2/PELI2, for the Pelle adaptor protein Pellino to mouse chromosomes 11 and 14 and human chromosomes 2p13.3 and 14q21, respectively, by physical and radiation hybrid mapping. *Cytogenetics and cell genetics.* 2001;92(1-2):172-4.
24. Jensen LE, Whitehead AS. Pellino3, a novel member of the Pellino protein family, promotes activation of c-Jun and Elk-1 and may act as a scaffolding protein. *Journal of immunology (Baltimore, Md : 1950).* 2003;171(3):1500-6.
25. Schauvliege R, Janssens S, Beyaert R. Pellino proteins: novel players in TLR and IL-1R signalling. *J Cell Mol Med.* 2007;11(3):453-61.
26. Chang M, Jin W, Chang J-H, Xiao Y, Brittain GC, Yu J, et al. The ubiquitin ligase Peli1 negatively regulates T cell activation and prevents autoimmunity. *Nature immunology.* 2011;12(10):1002-9.
27. Strickson S, Emmerich CH, Goh ETH, Zhang J, Kelsall IR, Macartney T, et al. Roles of the TRAF6 and Pellino E3 ligases in MyD88 and RANKL signaling. *Proceedings of the National Academy of Sciences.* 2017;114(17):E3481.
28. Moynagh PN. The Pellino family: IRAK E3 ligases with emerging roles in innate immune signalling. *Trends in Immunology.* 2009;30(1):33-42.
29. Strelow A, Kollwe C, Wesche H. Characterization of Pellino2, a substrate of IRAK1 and IRAK4. *FEBS Letters.* 2003;547(1-3):157-61.
30. Butler MP, Hanly JA, Moynagh PN. Pellino3 is a novel upstream regulator of p38 MAPK and activates CREB in a p38-dependent manner. *J Biol Chem.* 2005;280(30):27759-68.
31. Butler MP, Hanly JA, Moynagh PN. Kinase-active interleukin-1 receptor-associated kinases promote polyubiquitination and degradation of the Pellino family: direct evidence for PELLINO proteins being ubiquitin-protein isopeptide ligases. *J Biol Chem.* 2007;282(41):29729-37.
32. Jensen LE, Whitehead AS. Pellino2 activates the mitogen activated protein kinase pathway. *FEBS Letters.* 2003;545(2-3):199-202.
33. Huoh YS, Ferguson KM. The pellino e3 ubiquitin ligases recognize specific phosphothreonine motifs and have distinct substrate specificities. *Biochemistry.* 2014;53(30):4946-55.
34. Lin CC, Huoh YS, Schmitz KR, Jensen LE, Ferguson KM. Pellino proteins contain a cryptic FHA domain that mediates interaction with phosphorylated IRAK1. *Structure.* 2008;16(12):1806-16.
35. Schauvliege R, Janssens S, Beyaert R. Pellino proteins are more than scaffold proteins in TLR/IL-1R signalling: a role as novel RING E3-ubiquitin-ligases. *FEBS Lett.* 2006;580(19):4697-702.
36. Durocher D, Jackson SP. The FHA domain. *FEBS Letters.* 2002;513(1):58-66.
37. Lorick KL, Jensen JP, Fang S, Ong AM, Hatakeyama S, Weissman AM. RING fingers mediate ubiquitin-conjugating enzyme (E2)-dependent ubiquitination. *Proceedings of the National Academy of Sciences of the United States of America.* 1999;96(20):11364-9.



38. Ordureau A, Smith H, Windheim M, Peggie M, Carrick E, Morrice N, et al. The IRAK-catalysed activation of the E3 ligase function of Pellino isoforms induces the Lys63-linked polyubiquitination of IRAK1. *Biochem J.* 2008;409(1):43-52.
39. Goldstein G, Scheid M, Hammerling U, Schlesinger DH, Niall HD, Boyse EA. Isolation of a polypeptide that has lymphocyte-differentiating properties and is probably represented universally in living cells. *Proceedings of the National Academy of Sciences of the United States of America.* 1975;72(1):11-5.
40. Strieter ER, Korasick DA. Unraveling the Complexity of Ubiquitin Signaling. *ACS Chemical Biology.* 2012;7(1):52-63.
41. Jiang X, Chen ZJ. The role of ubiquitylation in immune defence and pathogen evasion. *Nat Rev Immunol.* 2012;12(1):35-48.
42. Nakayama KI, Nakayama K. Ubiquitin ligases: cell-cycle control and cancer. *Nat Rev Cancer.* 2006;6(5):369-81.
43. Terrell J, Shih S, Dunn R, Hicke L. A function for monoubiquitination in the internalization of a G protein-coupled receptor. *Mol Cell.* 1998;1(2):193-202.
44. Petroski MD, Deshaies RJ. Context of multiubiquitin chain attachment influences the rate of Sic1 degradation. *Mol Cell.* 2003;11(6):1435-44.
45. Sadowski M, Suryadinata R, Tan AR, Roesley SN, Sarcevic B. Protein monoubiquitination and polyubiquitination generate structural diversity to control distinct biological processes. *IUBMB life.* 2012;64(2):136-42.
46. Endoh M, Endo TA, Endoh T, Isono K, Sharif J, Ohara O, et al. Histone H2A mono-ubiquitination is a crucial step to mediate PRC1-dependent repression of developmental genes to maintain ES cell identity. *PLoS genetics.* 2012;8(7):e1002774.
47. Wu K, Yan H, Fang L, Wang X, Pflieger C, Jiang X, et al. Mono-ubiquitination drives nuclear export of the human DCN1-like protein hDCN1. *J Biol Chem.* 2011;286(39):34060-70.
48. Xu P, Duong DM, Seyfried NT, Cheng D, Xie Y, Robert J, et al. Quantitative proteomics reveals the function of unconventional ubiquitin chains in proteasomal degradation. *Cell.* 2009;137(1):133-45.
49. Tenno T, Fujiwara K, Tochio H, Iwai K, Morita EH, Hayashi H, et al. Structural basis for distinct roles of Lys63- and Lys48-linked polyubiquitin chains. *Genes to cells : devoted to molecular & cellular mechanisms.* 2004;9(10):865-75.
50. Jiang Z, Johnson HJ, Nie H, Qin J, Bird TA, Li X. Pellino 1 is required for interleukin-1 (IL-1)-mediated signaling through its interaction with the IL-1 receptor-associated kinase 4 (IRAK4)-IRAK-tumor necrosis factor receptor-associated factor 6 (TRAF6) complex. *J Biol Chem.* 2003;278(13):10952-6.
51. Weighardt H, Jusek G, Mages J, Lang R, Hoebe K, Beutler B, et al. Identification of a TLR4- and TRIF-dependent activation program of dendritic cells. *Eur J Immunol.* 2004;34(2):558-64.
52. Chang M, Jin W, Sun S-C. Peli1 facilitates TRIF-dependent Toll-like receptor signaling and proinflammatory cytokine production. *Nature immunology.* 2009;10(10):1089-95.
53. Xiao Y, Jin J, Chang M, Chang J-H, Hu H, Zhou X, et al. Peli1 promotes microglia-mediated CNS inflammation by regulating Traf3 degradation. *Nat Med.* 2013;19(5):595-602.
54. Xiao H, Qian W, Staschke K, Qian Y, Cui G, Deng L, et al. Pellino 3b Negatively Regulates Interleukin-1-induced TAK1-dependent NFκB Activation. *The Journal of Biological Chemistry.* 2008;283(21):14654-64.
55. Siednienko J, Jackson R, Mellett M, Delagic N, Yang S, Wang B, et al. Pellino3 targets the IRF7 pathway and facilitates autoregulation of TLR3- and viral-induced expression of type I interferons. *Nature immunology.* 2012;13(11):1055-62.

56. Yang S, Wang B, Humphries F, Hogan AE, O'Shea D, Moynagh PN. The E3 ubiquitin ligase Pellino3 protects against obesity-induced inflammation and insulin resistance. *Immunity*. 2014;41(6):973-87.
57. Yu KY, Kwon HJ, Norman DAM, Vig E, Goebel MG, Harrington MA. Cutting Edge: Mouse Pellino-2 Modulates IL-1 and Lipopolysaccharide Signaling. *The Journal of Immunology*. 2002;169(8):4075-8.
58. Pennell S, Smerdon SJ. Pellino proteins splitting up the FHAmily! *Structure*. 2008;16(12):1752-4.
59. Cluxton CD, Caffrey BE, Kinsella GK, Moynagh PN, Fares MA, Fallon PG. Functional conservation of an ancestral Pellino protein in helminth species. *Sci Rep*. 2015;5:11687.
60. Smith H, Peggie M, Campbell DG, Vandermoere F, Carrick E, Cohen P. Identification of the phosphorylation sites on the E3 ubiquitin ligase Pellino that are critical for activation by IRAK1 and IRAK4. *Proceedings of the National Academy of Sciences of the United States of America*. 2009;106(12):4584-90.
61. Kim TW, Yu M, Zhou H, Cui W, Wang J, DiCorleto P, et al. Pellino 2 is critical for Toll-like receptor/interleukin-1 receptor (TLR/IL-1R)-mediated post-transcriptional control. *J Biol Chem*. 2012;287(30):25686-95.
62. Liu Y, Dong W, Chen L, Xiang R, Xiao H, De G, et al. BCL10 mediates lipopolysaccharide/toll-like receptor-4 signaling through interaction with Pellino2. *J Biol Chem*. 2004;279(36):37436-44.
63. Dong W, Liu Y, Peng J, Chen L, Zou T, Xiao H, et al. The IRAK-1-BCL10-MALT1-TRAF6-TAK1 cascade mediates signaling to NF-kappaB from Toll-like receptor 4. *J Biol Chem*. 2006;281(36):26029-40.
64. Humphries F, Bergin R, Jackson R, Delagic N, Wang B, Yang S, et al. The E3 ubiquitin ligase Pellino2 mediates priming of the NLRP3 inflammasome. *Nature communications*. 2018;9(1):1560.
65. Nogueira E, Ponciano VC, Naka EL, Marques GD, Cenedeze MA, Camara NO, et al. Toll-like receptors-related genes in kidney transplant patients with chronic allograft nephropathy and acute rejection. *International immunopharmacology*. 2009;9(6):673-6.
66. Yang S, Wang B, Humphries F, Jackson R, Healy ME, Bergin R, et al. Pellino3 ubiquitinates RIP2 and mediates Nod2-induced signaling and protective effects in colitis. *Nature immunology*. 2013;14(9):927-36.
67. Kim JJ, Hong YM, Yun SW, Han MK, Lee KY, Song MS, et al. Assessment of risk factors for Korean children with Kawasaki disease. *Pediatr Cardiol*. 2012;33(4):513-20.
68. Kim JJ, Hong YM, Sohn S, Jang GY, Ha KS, Yun SW, et al. A genome-wide association analysis reveals 1p31 and 2p13.3 as susceptibility loci for Kawasaki disease. *Human genetics*. 2011;129(5):487-95.
69. Xu F, Gao F. Liuwei Dihuang pill cures postmenopausal osteoporosis with kidney-Yin deficiency: Potential therapeutic targets identified based on gene expression profiling. *Medicine*. 2018;97(31):e11659.
70. Baines KJ, Simpson JL, Wood LG, Scott RJ, Gibson PG. Transcriptional phenotypes of asthma defined by gene expression profiling of induced sputum samples. *Journal of Allergy and Clinical Immunology*. 2011;127(1):153-60.e9.
71. You Q, Wang J, Jia D, Jiang L, Chang Y, Li W. MiR-802 alleviates lipopolysaccharide-induced acute lung injury by targeting Peli2. *Inflammation Research*. 2020;69(1):75-85.
72. Rednam CK, Wilson RL, Selvaraju V, Rishi MT, Thirunavukkarasu M, Coca-Soliz V, et al. Increased survivability of ischemic skin flap tissue in Flk-1(+/-) mice by Pellino-1 intervention. *Microcirculation*. 2017;24(6).

73. Thirunavukkarasu M, Selvaraju V, Joshi M, Coca-Soliz V, Tapias L, Saad I, et al. Disruption of VEGF Mediated Flk-1 Signaling Leads to a Gradual Loss of Vessel Health and Cardiac Function During Myocardial Infarction: Potential Therapy With Pellino-1. *J Am Heart Assoc.* 2018;7(18):e007601.
74. Selvaraju V, Thirunavukkarasu M, Joshi M, Oriowo B, Shaikh IA, Rishi MT, et al. Deletion of newly described pro-survival molecule Pellino-1 increases oxidative stress, downregulates cIAP2/NF- $\kappa$ B cell survival pathway, reduces angiogenic response, and thereby aggravates tissue function in mouse ischemic models. *Basic Res Cardiol.* 2020;115(4):45.
75. Zhang C, Jing L-w, Li Z-t, Chang Z-w, Liu H, Zhang Q-m, et al. Identification of a prognostic 28-gene expression signature for gastric cancer with lymphatic metastasis. *Bioscience Reports.* 2019;39(5).
76. Kim S, Lee SY, Bae S, Lee JK, Hwang K, Go H, et al. Pellino1 promotes chronic inflammatory skin disease via keratinocyte hyperproliferation and induction of the T helper 17 response. *Exp Mol Med.* 2020;52(9):1537-49.
77. Liu S, Gao S, Yang Z, Zhang P. miR-128-3p reduced acute lung injury induced by sepsis via targeting PEL12. *Open Med (Wars).* 2021;16(1):1109-20.
78. Lu A, Wu H. Structural mechanisms of inflammasome assembly. *Febs j.* 2015;282(3):435-44.
79. Sharma D, Kanneganti TD. The cell biology of inflammasomes: Mechanisms of inflammasome activation and regulation. *J Cell Biol.* 2016;213(6):617-29.
80. Fernandes-Alnemri T, Wu J, Yu JW, Datta P, Miller B, Jankowski W, et al. The pyroptosome: a supramolecular assembly of ASC dimers mediating inflammatory cell death via caspase-1 activation. *Cell Death & Differentiation.* 2007;14(9):1590-604.
81. Martinon F, Burns K, Tschopp J. The Inflammasome: A Molecular Platform Triggering Activation of Inflammatory Caspases and Processing of proIL- $\beta$ . *Molecular Cell.* 2002;10(2):417-26.
82. Franchi L, Warner N, Viani K, Nuñez G. Function of Nod-like receptors in microbial recognition and host defense. *Immunological reviews.* 2009;227(1):106-28.
83. Vajjhala PR, Mirams RE, Hill JM. Multiple binding sites on the pyrin domain of ASC protein allow self-association and interaction with NLRP3 protein. *J Biol Chem.* 2012;287(50):41732-43.
84. Duncan JA, Bergstralh DT, Wang Y, Willingham SB, Ye Z, Zimmermann AG, et al. Cryopyrin/NALP3 binds ATP/dATP, is an ATPase, and requires ATP binding to mediate inflammatory signaling. *Proceedings of the National Academy of Sciences.* 2007;104(19):8041.
85. Hamilton C, Anand PK. Right place, right time: localisation and assembly of the NLRP3 inflammasome. *F1000Res.* 2019;8.
86. Subramanian N, Natarajan K, Clatworthy MR, Wang Z, Germain RN. The adaptor MAVS promotes NLRP3 mitochondrial localization and inflammasome activation. *Cell.* 2013;153(2):348-61.
87. Zhang Z, Meszaros G, He WT, Xu Y, de Fatima Magliarelli H, Mailly L, et al. Protein kinase D at the Golgi controls NLRP3 inflammasome activation. *The Journal of experimental medicine.* 2017;214(9):2671-93.
88. Zhou R, Yazdi AS, Menu P, Tschopp J. A role for mitochondria in NLRP3 inflammasome activation. *Nature.* 2011;469(7329):221-5.
89. Misawa T, Takahama M, Kozaki T, Lee H, Zou J, Saitoh T, et al. Microtubule-driven spatial arrangement of mitochondria promotes activation of the NLRP3 inflammasome. *Nature immunology.* 2013;14(5):454-60.

90. Yang CS, Kim JJ, Kim TS, Lee PY, Kim SY, Lee HM, et al. Small heterodimer partner interacts with NLRP3 and negatively regulates activation of the NLRP3 inflammasome. *Nature communications*. 2015;6:6115.
91. Chen J, Chen ZJ. PtdIns4P on dispersed trans-Golgi network mediates NLRP3 inflammasome activation. *Nature*. 2018;564(7734):71-6.
92. Wang Y, Yang C, Mao K, Chen S, Meng G, Sun B. Cellular localization of NLRP3 inflammasome. *Protein & Cell*. 2013;4(6):425-31.
93. Franchi L, Muñoz-Planillo R, Núñez G. Sensing and reacting to microbes through the inflammasomes. *Nature immunology*. 2012;13(4):325-32.
94. Kanneganti T-D, Özören N, Body-Malapel M, Amer A, Park J-H, Franchi L, et al. Bacterial RNA and small antiviral compounds activate caspase-1 through cryopyrin/Nalp3. *Nature*. 2006;440(7081):233-6.
95. Martinon F, Pétrilli V, Mayor A, Tardivel A, Tschopp J. Gout-associated uric acid crystals activate the NALP3 inflammasome. *Nature*. 2006;440(7081):237-41.
96. Hornung V, Bauernfeind F, Halle A, Samstad EO, Kono H, Rock KL, et al. Silica crystals and aluminum salts activate the NALP3 inflammasome through phagosomal destabilization. *Nature immunology*. 2008;9(8):847-56.
97. Kelley N, Jeltema D, Duan Y, He Y. The NLRP3 Inflammasome: An Overview of Mechanisms of Activation and Regulation. *International Journal of Molecular Sciences*. 2019;20(13):3328.
98. Bauernfeind FG, Horvath G, Stutz A, Alnemri ES, MacDonald K, Speert D, et al. Cutting edge: NF- $\kappa$ B activating pattern recognition and cytokine receptors license NLRP3 inflammasome activation by regulating NLRP3 expression. *Journal of immunology* (Baltimore, Md : 1950). 2009;183(2):787-91.
99. Schroder K, Sagulenko V, Zamoshnikova A, Richards AA, Cridland JA, Irvine KM, et al. Acute lipopolysaccharide priming boosts inflammasome activation independently of inflammasome sensor induction. *Immunobiology*. 2012;217(12):1325-9.
100. Kim SJ, Cha JY, Kang HS, Lee JH, Lee JY, Park JH, et al. Corosolic acid ameliorates acute inflammation through inhibition of IRAK-1 phosphorylation in macrophages. *BMB Rep*. 2016;49(5):276-81.
101. Codolo G, Plotegher N, Pozzobon T, Brucale M, Tessari I, Bubacco L, et al. Triggering of inflammasome by aggregated  $\alpha$ -synuclein, an inflammatory response in synucleinopathies. *PloS one*. 2013;8(1):e55375.
102. Halle A, Hornung V, Petzold GC, Stewart CR, Monks BG, Reinheckel T, et al. The NALP3 inflammasome is involved in the innate immune response to amyloid-beta. *Nature immunology*. 2008;9(8):857-65.
103. Duewell P, Kono H, Rayner KJ, Sirois CM, Vladimer G, Bauernfeind FG, et al. NLRP3 inflammasomes are required for atherogenesis and activated by cholesterol crystals. *Nature*. 2010;464(7293):1357-61.
104. Murakami T, Ockinger J, Yu J, Byles V, McColl A, Hofer AM, et al. Critical role for calcium mobilization in activation of the NLRP3 inflammasome. *Proceedings of the National Academy of Sciences*. 2012;109(28):11282-7.
105. Vanden Abeele F, Bidaux G, Gordienko D, Beck B, Panchin YV, Baranova AV, et al. Functional implications of calcium permeability of the channel formed by pannexin 1. *Journal of Cell Biology*. 2006;174(4):535-46.
106. Brough D, Le Feuvre RA, Wheeler RD, Solovyova N, Hilfiker S, Rothwell NJ, et al. Ca<sup>2+</sup> stores and Ca<sup>2+</sup> entry differentially contribute to the release of IL-1 beta and IL-1 alpha from murine macrophages. *Journal of immunology* (Baltimore, Md : 1950). 2003;170(6):3029-36.

107. Katsnelson MA, Rucker LG, Russo HM, Dubyak GR. K<sup>+</sup> efflux agonists induce NLRP3 inflammasome activation independently of Ca<sup>2+</sup> signaling. *Journal of immunology* (Baltimore, Md : 1950). 2015;194(8):3937-52.
108. Muñoz-Planillo R, Kuffa P, Martínez-Colón G, Smith BL, Rajendiran TM, Núñez G. K<sup>+</sup> efflux is the common trigger of NLRP3 inflammasome activation by bacterial toxins and particulate matter. *Immunity*. 2013;38(6):1142-53.
109. Mao K, Chen S, Chen M, Ma Y, Wang Y, Huang B, et al. Nitric oxide suppresses NLRP3 inflammasome activation and protects against LPS-induced septic shock. *Cell research*. 2013;23(2):201-12.
110. Hernandez-Cuellar E, Tsuchiya K, Hara H, Fang R, Sakai S, Kawamura I, et al. Cutting Edge: Nitric Oxide Inhibits the NLRP3 Inflammasome. *The Journal of Immunology*. 2012;189(11):5113-7.
111. Verhoef PA, Kertesz SB, Lundberg K, Kahlenberg JM, Dubyak GR. Inhibitory Effects of Chloride on the Activation of Caspase-1, IL-1 $\beta$  Secretion, and Cytolysis by the P2X7 Receptor. *The Journal of Immunology*. 2005;175(11):7623-34.
112. Jung S-S, Moon J-S, Xu J-F, Ifedigbo E, Ryter SW, Choi AMK, et al. Carbon monoxide negatively regulates NLRP3 inflammasome activation in macrophages. *American Journal of Physiology-Lung Cellular and Molecular Physiology*. 2015;308(10):L1058-L67.
113. Cruz CM, Rinna A, Forman HJ, Ventura AL, Persechini PM, Ojcius DM. ATP activates a reactive oxygen species-dependent oxidative stress response and secretion of proinflammatory cytokines in macrophages. *J Biol Chem*. 2007;282(5):2871-9.
114. Bauernfeind F, Bartok E, Rieger A, Franchi L, Núñez G, Hornung V. Cutting Edge: Reactive Oxygen Species Inhibitors Block Priming, but Not Activation, of the NLRP3 Inflammasome. *The Journal of Immunology*. 2011;187(2):613.
115. Ichinohe T, Yamazaki T, Koshiba T, Yanagi Y. Mitochondrial protein mitofusin 2 is required for NLRP3 inflammasome activation after RNA virus infection. *Proceedings of the National Academy of Sciences of the United States of America*. 2013;110(44):17963-8.
116. Iyer SS, He Q, Janczy JR, Elliott EI, Zhong Z, Olivier AK, et al. Mitochondrial cardiolipin is required for Nlrp3 inflammasome activation. *Immunity*. 2013;39(2):311-23.
117. Nakahira K, Haspel JA, Rathinam VAK, Lee S-J, Dolinay T, Lam HC, et al. Autophagy proteins regulate innate immune responses by inhibiting the release of mitochondrial DNA mediated by the NALP3 inflammasome. *Nature immunology*. 2011;12(3):222-30.
118. Lupfer C, Thomas PG, Anand PK, Vogel P, Milasta S, Martinez J, et al. Receptor interacting protein kinase 2-mediated mitophagy regulates inflammasome activation during virus infection. *Nature immunology*. 2013;14(5):480-8.
119. Shi CS, Shenderov K, Huang NN, Kabat J, Abu-Asab M, Fitzgerald KA, et al. Activation of autophagy by inflammatory signals limits IL-1 $\beta$  production by targeting ubiquitinated inflammasomes for destruction. *Nature immunology*. 2012;13(3):255-63.
120. Harris J, Hartman M, Roche C, Zeng SG, O'Shea A, Sharp FA, et al. Autophagy controls IL-1 $\beta$  secretion by targeting pro-IL-1 $\beta$  for degradation. *J Biol Chem*. 2011;286(11):9587-97.
121. Weber K, Schilling JD. Lysosomes integrate metabolic-inflammatory cross-talk in primary macrophage inflammasome activation. *J Biol Chem*. 2014;289(13):9158-71.
122. Orłowski GM, Colbert JD, Sharma S, Bogyo M, Robertson SA, Rock KL. Multiple Cathepsins Promote Pro-IL-1 $\beta$  Synthesis and NLRP3-Mediated IL-1 $\beta$  Activation. *The Journal of Immunology*. 2015;195(4):1685.
123. Katsnelson MA, Lozada-Soto KM, Russo HM, Miller BA, Dubyak GR. NLRP3 inflammasome signaling is activated by low-level lysosome disruption but inhibited by

- extensive lysosome disruption: roles for K<sup>+</sup> efflux and Ca<sup>2+</sup> influx. *American Journal of Physiology-Cell Physiology*. 2016;311(1):C83-C100.
124. Gu T-T, Song L, Chen T-Y, Wang X, Zhao X-J, Ding X-Q, et al. Fructose downregulates miR-330 to induce renal inflammatory response and insulin signaling impairment: Attenuation by morin. *Molecular Nutrition & Food Research*. 2017;61(8):1600760.
125. Zhou Y, Lu M, Du R-H, Qiao C, Jiang C-Y, Zhang K-Z, et al. MicroRNA-7 targets Nod-like receptor protein 3 inflammasome to modulate neuroinflammation in the pathogenesis of Parkinson's disease. *Molecular Neurodegeneration*. 2016;11(1):28.
126. Wang Y, Han Z, Fan Y, Zhang J, Chen K, Gao L, et al. MicroRNA-9 Inhibits NLRP3 Inflammasome Activation in Human Atherosclerosis Inflammation Cell Models through the JAK1/STAT Signaling Pathway. *Cellular Physiology and Biochemistry*. 2017;41(4):1555-71.
127. Haneklaus M, Gerlic M, Kurowska-Stolarska M, Rainey A-A, Pich D, McInnes IB, et al. Cutting Edge: miR-223 and EBV miR-BART15 Regulate the NLRP3 Inflammasome and IL-1 $\beta$  Production. *The Journal of Immunology*. 2012;189(8):3795.
128. Pétrilli V, Papin S, Dostert C, Mayor A, Martinon F, Tschopp J. Activation of the NALP3 inflammasome is triggered by low intracellular potassium concentration. *Cell Death & Differentiation*. 2007;14(9):1583-9.
129. Stehlik C, Dorfleutner A. COPs and POPs: Modulators of Inflammasome Activity. *The Journal of Immunology*. 2007;179(12):7993.
130. Komune N, Ichinohe T, Ito M, Yanagi Y. Measles virus V protein inhibits NLRP3 inflammasome-mediated interleukin-1 $\beta$  secretion. *J Virol*. 2011;85(24):13019-26.
131. Young JL, Sukhova GK, Foster D, Kisiel W, Libby P, Schönbeck U. The serpin proteinase inhibitor 9 is an endogenous inhibitor of interleukin 1beta-converting enzyme (caspase-1) activity in human vascular smooth muscle cells. *The Journal of experimental medicine*. 2000;191(9):1535-44.
132. Beynon V, Quintana FJ, Weiner HL. Activated Human CD4<sup>+</sup>CD45RO<sup>+</sup> Memory T-Cells Indirectly Inhibit NLRP3 Inflammasome Activation through Downregulation of P2X7R Signalling. *PLoS one*. 2012;7(6):e39576.
133. Mitroulis I, Kambas K, Ritis K. Neutrophils, IL-1 $\beta$ , and gout: is there a link? *Seminars in Immunopathology*. 2013;35(4):501-12.
134. Guarda G, Dostert C, Staehli F, Cabalzar K, Castillo R, Tardivel A, et al. T cells dampen innate immune responses through inhibition of NLRP1 and NLRP3 inflammasomes. *Nature*. 2009;460(7252):269-73.
135. Guarda G, Braun M, Staehli F, Tardivel A, Mattmann C, Förster I, et al. Type I Interferon Inhibits Interleukin-1 Production and Inflammasome Activation. *Immunity*. 2011;34(2):213-23.
136. Walev I, Klein J, Husmann M, Valeva A, Strauch S, Wirtz H, et al. Potassium Regulates IL-1 $\beta$  Processing Via Calcium-Independent Phospholipase A2. *The Journal of Immunology*. 2000;164(10):5120-4.
137. Tang T, Lang X, Xu C, Wang X, Gong T, Yang Y, et al. CLICs-dependent chloride efflux is an essential and proximal upstream event for NLRP3 inflammasome activation. *Nature communications*. 2017;8(1):202.
138. Li C, Chen M, He X, Ouyang D. A mini-review on ion fluxes that regulate NLRP3 inflammasome activation. *Acta Biochim Biophys Sin (Shanghai)*. 2021;53(2):131-9.
139. He Y, Zeng MY, Yang D, Motro B, Nunez G. NEK7 is an essential mediator of NLRP3 activation downstream of potassium efflux. *Nature*. 2016;530(7590):354-7.
140. Zhao N, Li CC, Di B, Xu LL. Recent advances in the NEK7-licensed NLRP3 inflammasome activation: Mechanisms, role in diseases and related inhibitors. *J Autoimmun*. 2020;113:102515.

141. Groß CJ, Mishra R, Schneider KS, Médard G, Wettmarshausen J, Dittlein DC, et al. K(+) Efflux-Independent NLRP3 Inflammasome Activation by Small Molecules Targeting Mitochondria. *Immunity*. 2016;45(4):761-73.
142. Meng G, Zhang F, Fuss I, Kitani A, Strober W. A mutation in the *Nlrp3* gene causing inflammasome hyperactivation potentiates Th17 cell-dominant immune responses. *Immunity*. 2009;30(6):860-74.
143. Rozov A, Khusainov I, El Omari K, Duman R, Mykhaylyk V, Yusupov M, et al. Importance of potassium ions for ribosome structure and function revealed by long-wavelength X-ray diffraction. *Nature communications*. 2019;10(1):2519.
144. McDonough AA, Youn JH. Potassium Homeostasis: The Knowns, the Unknowns, and the Health Benefits. *Physiology*. 2017;32(2):100-11.
145. Feraïlle E, Dizin E. Coordinated Control of ENaC and Na<sup>+</sup>,K<sup>+</sup>-ATPase in Renal Collecting Duct. *J Am Soc Nephrol*. 2016;27(9):2554-63.
146. Taura J, Kircher DM, Gameiro-Ros I, Slesinger PA. Comparison of K(+) Channel Families. *Handb Exp Pharmacol*. 2021.
147. Ewart HS, Klip A. Hormonal regulation of the Na<sup>(+)</sup>-K<sup>(+)</sup>-ATPase: mechanisms underlying rapid and sustained changes in pump activity. *American Journal of Physiology-Cell Physiology*. 1995;269(2):C295-C311.
148. Cang C, Aranda K, Seo YJ, Gasnier B, Ren D. TMEM175 Is an Organelle K(+) Channel Regulating Lysosomal Function. *Cell*. 2015;162(5):1101-12.
149. Feng X, Zhao Z, Li Q, Tan Z. Lysosomal Potassium Channels: Potential Roles in Lysosomal Function and Neurodegenerative Diseases. *CNS Neurol Disord Drug Targets*. 2018;17(4):261-6.
150. Kuum M, Veksler V, Kaasik A. Potassium fluxes across the endoplasmic reticulum and their role in endoplasmic reticulum calcium homeostasis. *Cell Calcium*. 2015;58(1):79-85.
151. Zhu J, Yan J, Thornhill WB. The Kv1.3 potassium channel is localized to the cis-Golgi and Kv1.6 is localized to the endoplasmic reticulum in rat astrocytes. *The FEBS Journal*. 2014;281(15):3433-45.
152. Jang SH, Byun JK, Jeon WI, Choi SY, Park J, Lee BH, et al. Nuclear localization and functional characteristics of voltage-gated potassium channel Kv1.3. *J Biol Chem*. 2015;290(20):12547-57.
153. Garlid KD, Paucek P. Mitochondrial potassium transport: the K(+) cycle. *Biochim Biophys Acta*. 2003;1606(1-3):23-41.
154. Herrera R, Álvarez María C, Gelis S, Ramos J. Subcellular potassium and sodium distribution in *Saccharomyces cerevisiae* wild-type and vacuolar mutants. *Biochemical Journal*. 2013;454(3):525-32.
155. Langendorf H, Siebert G, Kesselring K, Hannover R. High Nucleo-cytoplasmic Concentration Gradient of Chloride in Rat Liver. *Nature*. 1966;209(5028):1130-1.
156. Zahid A, Li B, Kombe AJK, Jin T, Tao J. Pharmacological Inhibitors of the NLRP3 Inflammasome. *Frontiers in Immunology*. 2019;10(2538).
157. Lamkanfi M, Mueller JL, Vitari AC, Misaghi S, Fedorova A, Deshayes K, et al. Glyburide inhibits the Cryopyrin/Nalp3 inflammasome. *J Cell Biol*. 2009;187(1):61-70.
158. Di A, Xiong S, Ye Z, Malireddi RKS, Kometani S, Zhong M, et al. The TWIK2 Potassium Efflux Channel in Macrophages Mediates NLRP3 Inflammasome-Induced Inflammation. *Immunity*. 2018;49(1):56-65.e4.
159. Liu W, Guo W, Wu J, Luo Q, Tao F, Gu Y, et al. A novel benzo[d]imidazole derivative prevents the development of dextran sulfate sodium-induced murine experimental colitis via inhibition of NLRP3 inflammasome. *Biochemical pharmacology*. 2013;85(10):1504-12.

160. Juliana C, Fernandes-Alnemri T, Wu J, Datta P, Solorzano L, Yu J-W, et al. Anti-inflammatory Compounds Parthenolide and Bay 11-7082 Are Direct Inhibitors of the Inflammasome\*. *Journal of Biological Chemistry*. 2010;285(13):9792-802.
161. Youm YH, Nguyen KY, Grant RW, Goldberg EL, Bodogai M, Kim D, et al. The ketone metabolite  $\beta$ -hydroxybutyrate blocks NLRP3 inflammasome-mediated inflammatory disease. *Nat Med*. 2015;21(3):263-9.
162. Coll RC, Hill JR, Day CJ, Zamoshnikova A, Boucher D, Massey NL, et al. MCC950 directly targets the NLRP3 ATP-hydrolysis motif for inflammasome inhibition. *Nature Chemical Biology*. 2019;15(6):556-9.
163. Jiang H, He H, Chen Y, Huang W, Cheng J, Ye J, et al. Identification of a selective and direct NLRP3 inhibitor to treat inflammatory disorders. *Journal of Experimental Medicine*. 2017;214(11):3219-38.
164. Mortimer L, Moreau F, MacDonald JA, Chadee K. NLRP3 inflammasome inhibition is disrupted in a group of auto-inflammatory disease CAPS mutations. *Nature immunology*. 2016;17(10):1176-86.
165. Song N, Liu Z-S, Xue W, Bai Z-F, Wang Q-Y, Dai J, et al. NLRP3 Phosphorylation Is an Essential Priming Event for Inflammasome Activation. *Molecular Cell*. 2017;68(1):185-97.e6.
166. Spalinger MR, Kasper S, Gottier C, Lang S, Atrott K, Vavricka SR, et al. NLRP3 tyrosine phosphorylation is controlled by protein tyrosine phosphatase PTPN22. *The Journal of Clinical Investigation*. 2016;126(5):1783-800.
167. Stutz A, Kolbe C-C, Stahl R, Horvath GL, Franklin BS, van Ray O, et al. NLRP3 inflammasome assembly is regulated by phosphorylation of the pyrin domain. *Journal of Experimental Medicine*. 2017;214(6):1725-36.
168. Barry R, John SW, Liccardi G, Tenev T, Jaco I, Chen CH, et al. SUMO-mediated regulation of NLRP3 modulates inflammasome activity. *Nature communications*. 2018;9(1):3001.
169. Bose S, Segovia JA, Somarajan SR, Chang TH, Kannan TR, Baseman JB. ADP-ribosylation of NLRP3 by *Mycoplasma pneumoniae* CARDS toxin regulates inflammasome activity. *mBio*. 2014;5(6).
170. Lopez-Castejon G, Luheshi NM, Compan V, High S, Whitehead RC, Flitsch S, et al. Deubiquitinases regulate the activity of caspase-1 and interleukin-1 $\beta$  secretion via assembly of the inflammasome. *J Biol Chem*. 2013;288(4):2721-33.
171. Py BF, Kim MS, Vakifahmetoglu-Norberg H, Yuan J. Deubiquitination of NLRP3 by BRCC3 critically regulates inflammasome activity. *Mol Cell*. 2013;49(2):331-8.
172. Han S, Lear TB, Jerome JA, Rajbhandari S, Snavely CA, Gulick DL, et al. Lipopolysaccharide Primes the NALP3 Inflammasome by Inhibiting Its Ubiquitination and Degradation Mediated by the SCFFBXL2 E3 Ligase. *Journal of Biological Chemistry*. 2015;290(29):18124-33.
173. Yan Y, Jiang W, Liu L, Wang X, Ding C, Tian Z, et al. Dopamine Controls Systemic Inflammation through Inhibition of NLRP3 Inflammasome. *Cell*. 2015;160(1):62-73.
174. Song H, Liu B, Huai W, Yu Z, Wang W, Zhao J, et al. The E3 ubiquitin ligase TRIM31 attenuates NLRP3 inflammasome activation by promoting proteasomal degradation of NLRP3. *Nature communications*. 2016;7(1):13727.
175. Kawashima A, Karasawa T, Tago K, Kimura H, Kamata R, Usui-Kawanishi F, et al. ARIH2 Ubiquitinates NLRP3 and Negatively Regulates NLRP3 Inflammasome Activation in Macrophages. *Journal of immunology (Baltimore, Md : 1950)*. 2017;199(10):3614-22.
176. Sharif H, Wang L, Wang WL, Magupalli VG, Andreeva L, Qiao Q, et al. Structural mechanism for NEK7-licensed activation of NLRP3 inflammasome. *Nature*. 2019;570(7761):338-43.



177. Shi H, Wang Y, Li X, Zhan X, Tang M, Fina M, et al. NLRP3 activation and mitosis are mutually exclusive events coordinated by NEK7, a new inflammasome component. *Nature immunology*. 2016;17(3):250-8.
178. Schmid-Burgk JL, Chauhan D, Schmidt T, Ebert TS, Reinhardt J, Endl E, et al. A Genome-wide CRISPR (Clustered Regularly Interspaced Short Palindromic Repeats) Screen Identifies NEK7 as an Essential Component of NLRP3 Inflammasome Activation. *J Biol Chem*. 2016;291(1):103-9.
179. Gimenez F, Bhela S, Dogra P, Harvey L, Varanasi SK, Jaggi U, et al. The inflammasome NLRP3 plays a protective role against a viral immunopathological lesion. *Journal of leukocyte biology*. 2016;99(5):647-57.
180. Vinaik R, Abdullahi A, Barayan D, Jeschke MG. NLRP3 inflammasome activity is required for wound healing after burns. *Translational Research*. 2020;217:47-60.
181. Vinaik R, Barayan D, Auger C, Abdullahi A, Jeschke MG. Regulation of glycolysis and the Warburg effect in wound healing. *JCI Insight*. 2020;5(17).
182. Liu D, Zeng X, Li X, Cui C, Hou R, Guo Z, et al. Advances in the molecular mechanisms of NLRP3 inflammasome activators and inactivators. *Biochemical pharmacology*. 2020;175:113863.
183. Chi W, Li F, Chen H, Wang Y, Zhu Y, Yang X, et al. Caspase-8 promotes NLRP1/NLRP3 inflammasome activation and IL-1 $\beta$  production in acute glaucoma. *Proceedings of the National Academy of Sciences*. 2014;111(30):11181.
184. Tseng WA, Thein T, Kinnunen K, Lashkari K, Gregory MS, D'Amore PA, et al. NLRP3 Inflammasome Activation in Retinal Pigment Epithelial Cells by Lysosomal Destabilization: Implications for Age-Related Macular Degeneration. *Investigative Ophthalmology & Visual Science*. 2013;54(1):110-20.
185. Xu Q, Zhang J, Qin T, Bao J, Dong H, Zhou X, et al. The role of the inflammasomes in the pathogenesis of uveitis. *Experimental Eye Research*. 2021;208:108618.
186. Kim EH, Park M-J, Park S, Lee E-S. Increased expression of the NLRP3 inflammasome components in patients with Behçet's disease. *Journal of Inflammation*. 2015;12(1):41.
187. Louvrier C, Assrawi E, El Khouri E, Melki I, Copin B, Bourrat E, et al. NLRP3-associated autoinflammatory diseases: Phenotypic and molecular characteristics of germline versus somatic mutations. *J Allergy Clin Immunol*. 2020;145(4):1254-61.
188. Turunen JA, Wedenoja J, Repo P, Järvinen RS, Jäntti JE, Mörtenhumer S, et al. Keratoendotheliitis Fugax Hereditaria: A Novel Cryopyrin-Associated Periodic Syndrome Caused by a Mutation in the Nucleotide-Binding Domain, Leucine-Rich Repeat Family, Pyrin Domain-Containing 3 (NLRP3) Gene. *Am J Ophthalmol*. 2018;188:41-50.
189. Moshirfar M, Hastings J, Ronquillo Y, Patel BC. Keratoendotheliitis Fugax Hereditaria. *StatPearls*. Treasure Island (FL): StatPearls Publishing Copyright © 2021, StatPearls Publishing LLC.; 2021.
190. Zheng Q, Ren Y, Reinach PS, Xiao B, Lu H, Zhu Y, et al. Reactive oxygen species activated NLRP3 inflammasomes initiate inflammation in hyperosmolarity stressed human corneal epithelial cells and environment-induced dry eye patients. *Exp Eye Res*. 2015;134:133-40.
191. Sun N, Zhang H. Pyroptosis in pterygium pathogenesis. *Biosci Rep*. 2018;38(3).
192. Kistowska M, Gehrke S, Jankovic D, Kerl K, Fettelschoss A, Feldmeyer L, et al. IL-1 $\beta$  drives inflammatory responses to propionibacterium acnes in vitro and in vivo. *J Invest Dermatol*. 2014;134(3):677-85.
193. Li ZJ, Choi DK, Sohn KC, Seo MS, Lee HE, Lee Y, et al. Propionibacterium acnes activates the NLRP3 inflammasome in human sebocytes. *J Invest Dermatol*. 2014;134(11):2747-56.

194. Lee S, Kim SK, Park H, Lee YJ, Park SH, Lee KJ, et al. Contribution of Autophagy-Notch1-Mediated NLRP3 Inflammasome Activation to Chronic Inflammation and Fibrosis in Keloid Fibroblasts. *Int J Mol Sci.* 2020;21(21).
195. Karmakar M, Katsnelson MA, Dubyak GR, Pearlman E. Neutrophil P2X7 receptors mediate NLRP3 inflammasome-dependent IL-1 $\beta$  secretion in response to ATP. *Nature communications.* 2016;7:10555.
196. Karmakar M, Katsnelson M, Malak HA, Greene NG, Howell SJ, Hise AG, et al. Neutrophil IL-1 $\beta$  processing induced by pneumolysin is mediated by the NLRP3/ASC inflammasome and caspase-1 activation and is dependent on K<sup>+</sup> efflux. *Journal of immunology (Baltimore, Md : 1950).* 2015;194(4):1763-75.
197. Liu D, Yang P, Gao M, Yu T, Shi Y, Zhang M, et al. NLRP3 activation induced by neutrophil extracellular traps sustains inflammatory response in the diabetic wound. *Clinical Science.* 2019;133(4):565-82.
198. Wang Y, Wan L, Zhang Z, Li J, Qu M, Zhou Q. Topical calcitriol application promotes diabetic corneal wound healing and reinnervation through inhibiting NLRP3 inflammasome activation. *Experimental Eye Research.* 2021;209:108668.
199. Niu L, Li L, Xing C, Luo B, Hu C, Song M, et al. Airborne particulate matter (PM<sub>2.5</sub>) triggers cornea inflammation and pyroptosis via NLRP3 activation. *Ecotoxicology and Environmental Safety.* 2021;207:111306.
200. Turunen JA, Immonen AT, Järvinen RS, Kawan S, Repo P, Korsbäck A, et al. In Vivo Corneal Confocal Microscopy and Histopathology of Keratitis Fugax Hereditaria From a Pathogenic Variant in NLRP3. *Am J Ophthalmol.* 2020;213:217-25.
201. Ruusuvaara P, Setälä K. Keratoendotheliitis fugax hereditaria. *Acta Ophthalmologica.* 1987;65(2):159-69.
202. Welzel T, Kuemmerle-Deschner JB. Diagnosis and Management of the Cryopyrin-Associated Periodic Syndromes (CAPS): What Do We Know Today? *J Clin Med.* 2021;10(1).
203. Booshehri LM, Hoffman HM. CAPS and NLRP3. *J Clin Immunol.* 2019;39(3):277-86.
204. Lachmann HJ. Periodic fever syndromes. *Best Practice & Research Clinical Rheumatology.* 2017;31(4):596-609.
205. Kuemmerle-Deschner JB, Verma D, Endres T, Broderick L, de Jesus AA, Hofer F, et al. Clinical and Molecular Phenotypes of Low-Penetrance Variants of NLRP3: Diagnostic and Therapeutic Challenges. *Arthritis Rheumatol.* 2017;69(11):2233-40.
206. Agostini L, Martinon F, Burns K, McDermott MF, Hawkins PN, Tschopp J. NALP3 forms an IL-1 $\beta$ -processing inflammasome with increased activity in Muckle-Wells autoinflammatory disorder. *Immunity.* 2004;20(3):319-25.
207. Rosengren S, Mueller JL, Anderson JP, Niehaus BL, Misaghi A, Anderson S, et al. Monocytes from familial cold autoinflammatory syndrome patients are activated by mild hypothermia. *J Allergy Clin Immunol.* 2007;119(4):991-6.
208. Bredrup C, Cristea I, Safieh LA, Di Maria E, Gjertsen BT, Tveit KS, et al. Temperature-dependent autoactivation associated with clinical variability of PDGFRB Asn666 substitutions. *Hum Mol Genet.* 2021.
209. Abarca H, Mellgren AE, Trubnykova M, Haugen OH, Hovding G, Tveit KS, et al. Ocular pterygium--digital keloid dysplasia. *Am J Med Genet A.* 2014;164a(11):2901-7.
210. Van Acker SI, Van den Bogerd B, Haagdoorens M, Siozopoulou V, S ND, Pintelon I, et al. Pterygium-The Good, the Bad, and the Ugly. *Cells.* 2021;10(7).
211. Islam SI, Wagoner MD. Pterygium in young members of one family. *Cornea.* 2001;20(7):708-10.

212. Campagna G, Adams M, Wang L, Khandelwal S, Al-Mohtaseb Z. Comparison of Pterygium Recurrence Rates Among Different Races and Ethnicities After Primary Pterygium Excision by Surgeons in Training. *Cornea*. 2018;37(2):199-204.
213. Lan W, Petznick A, Heryati S, Rifada M, Tong L. Nuclear Factor- $\kappa$ B: Central Regulator in Ocular Surface Inflammation and Diseases. *The Ocular Surface*. 2012;10(3):137-48.
214. Lai C-C, Tseng S-H, Hsu S-M, Huang Y-T, Shieh C-C. Conjunctival Expression of Toll-Like Receptor 3 Plays a Pathogenic Role in the Formation of Ultraviolet Light-Induced Pterygium. *Investigative Ophthalmology & Visual Science*. 2021;62(10):6-.
215. Yamada K, Ueta M, Sotozono C, Yokoi N, Inatomi T, Kinoshita S. Upregulation of Toll-like receptor 5 expression in the conjunctival epithelium of various human ocular surface diseases. *Br J Ophthalmol*. 2014;98(8):1116-9.
216. Tong L, Lan W, Lim RR, Chaurasia SS. S100A Proteins as Molecular Targets in the Ocular Surface Inflammatory Diseases. *The Ocular Surface*. 2014;12(1):23-31.
217. Donato R, Cannon BR, Sorci G, Riuzzi F, Hsu K, Weber DJ, et al. Functions of S100 proteins. *Curr Mol Med*. 2013;13(1):24-57.
218. Gross SR, Sin CG, Barraclough R, Rudland PS. Joining S100 proteins and migration: for better or for worse, in sickness and in health. *Cellular and molecular life sciences : CMLS*. 2014;71(9):1551-79.
219. Oesterle A, Bowman MA. S100A12 and the S100/Calgranulins: Emerging Biomarkers for Atherosclerosis and Possibly Therapeutic Targets. *Arterioscler Thromb Vasc Biol*. 2015;35(12):2496-507.
220. Dassan P, Keir G, Brown MM. Criteria for a clinically informative serum biomarker in acute ischaemic stroke: a review of S100B. *Cerebrovasc Dis*. 2009;27(3):295-302.
221. Bertheloot D, Latz E. HMGB1, IL-1 $\alpha$ , IL-33 and S100 proteins: dual-function alarmins. *Cellular & Molecular Immunology*. 2017;14(1):43-64.
222. Rohde D, Schön C, Boerries M, Didrihsone I, Ritterhoff J, Kubatzky KF, et al. S100A1 is released from ischemic cardiomyocytes and signals myocardial damage via Toll-like receptor 4. *EMBO Mol Med*. 2014;6(6):778-94.
223. Riau AK, Wong TT, Beuerman RW, Tong L. Calcium-binding S100 protein expression in pterygium. *Mol Vis*. 2009;15:335-42.
224. Zhou L, Beuerman RW, Ang LPK, Chan CM, Li SFY, Chew FT, et al. Elevation of Human  $\alpha$ -Defensins and S100 Calcium-Binding Proteins A8 and A9 in Tear Fluid of Patients with Pterygium. *Investigative Ophthalmology & Visual Science*. 2009;50(5):2077-86.
225. Guo Q, Li X, Cui M-N, Liang Y, Li X-P, Zhao J, et al. Low-Dose Mitomycin C Decreases the Postoperative Recurrence Rate of Pterygium by Perturbing NLRP3 Inflammatory Signalling Pathway and Suppressing the Expression of Inflammatory Factors. *Journal of Ophthalmology*. 2019;2019:9472782.
226. Elsaie ML. Update on management of keloid and hypertrophic scars: A systemic review. *J Cosmet Dermatol*. 2021.
227. Kim SW. Management of keloid scars: noninvasive and invasive treatments. *Arch Plast Surg*. 2021;48(2):149-57.
228. Haugen OH, Bertelsen T. A new hereditary conjunctivo-corneal dystrophy associated with dermal keloid formation. Report of a family. *Acta Ophthalmol Scand*. 1998;76(4):461-5.
229. Bagabir RA, Syed F, Rautemaa R, McGrouther DA, Paus R, Bayat A. Upregulation of Toll-Like Receptors (TLRs) 6, 7, and 8 in Keloid Scars. *Journal of Investigative Dermatology*. 2011;131(10):2128-30.
230. Chen J, Zeng B, Yao H, Xu J. The effect of TLR4/7 on the TGF- $\beta$ -induced Smad signal transduction pathway in human keloid. *Burns*. 2013;39(3):465-72.

231. Lei R, Li J, Liu F, Li W, Zhang S, Wang Y, et al. HIF-1 $\alpha$  promotes the keloid development through the activation of TGF- $\beta$ /Smad and TLR4/MyD88/NF- $\kappa$ B pathways. *Cell Cycle*. 2019;18(23):3239-50.
232. Suetake T, Sasai S, Zhen Y-X, Ohi T, Tagami H. Functional Analyses of the Stratum Corneum in Scars: Sequential Studies After Injury and Comparison Among Keloids, Hypertrophic Scars, and Atrophic Scars. *Archives of Dermatology*. 1996;132(12):1453-8.
233. Zhong A, Xu W, Zhao J, Xie P, Jia S, Sun J, et al. S100A8 and S100A9 Are Induced by Decreased Hydration in the Epidermis and Promote Fibroblast Activation and Fibrosis in the Dermis. *The American Journal of Pathology*. 2016;186(1):109-22.
234. Zhao J, Zhong A, Friedrich EE, Jia S, Xie P, Galiano RD, et al. S100A12 Induced in the Epidermis by Reduced Hydration Activates Dermal Fibroblasts and Causes Dermal Fibrosis. *Journal of Investigative Dermatology*. 2017;137(3):650-9.
235. Vincent AS, Phan TT, Mukhopadhyay A, Lim HY, Halliwell B, Wong KP. Human skin keloid fibroblasts display bioenergetics of cancer cells. *J Invest Dermatol*. 2008;128(3):702-9.
236. Penttinen M, Niemi KM, Vinkka-Puhakka H, Johansson R, Aula P. New progeroid disorder. *Am J Med Genet*. 1997;69(2):182-7.
237. Zufferey F, Hadj-Rabia S, De Sandre-Giovannoli A, Dufier J-L, Leheup B, Schweitzer C, et al. Acro-osteolysis, keloid like-lesions, distinctive facial features, and overgrowth: Two newly recognized patients with premature aging syndrome, penttinen type. *American Journal of Medical Genetics Part A*. 2013;161(7):1786-91.
238. Bredrup C, Stokowy T, McGaughran J, Lee S, Sapkota D, Cristea I, et al. A tyrosine kinase-activating variant Asn666Ser in PDGFRB causes a progeria-like condition in the severe end of Penttinen syndrome. *Eur J Hum Genet*. 2019;27(4):574-81.
239. Johnston JJ, Sanchez-Contreras MY, Keppler-Noreuil KM, Sapp J, Crenshaw M, Finch NA, et al. A Point Mutation in PDGFRB Causes Autosomal-Dominant Penttinen Syndrome. *Am J Hum Genet*. 2015;97(3):465-74.
240. Xu L, Jensen H, Johnston JJ, Di Maria E, Kloth K, Cristea I, et al. Recurrent, Activating Variants in the Receptor Tyrosine Kinase *DDR2* Cause Warburg-Cinotti Syndrome. *The American Journal of Human Genetics*. 2018;103(6):976-83.
241. Cheung YH, Gayden T, Campeau PM, LeDuc CA, Russo D, Nguyen VH, et al. A recurrent PDGFRB mutation causes familial infantile myofibromatosis. *Am J Hum Genet*. 2013;92(6):996-1000.
242. Slettedal JK, Ringvold A. Correlation between corneal and ambient temperature with particular focus on polar conditions. *Acta Ophthalmologica*. 2015;93(5):422-6.
243. He C, Medley SC, Kim J, Sun C, Kwon HR, Sakashita H, et al. STAT1 modulates tissue wasting or overgrowth downstream from PDGFR $\beta$ . *Genes Dev*. 2017;31(16):1666-78.
244. Sannerud R, Marie M, Nizak C, Dale HA, Pernet-Gallay K, Perez F, et al. Rab1 defines a novel pathway connecting the pre-Golgi intermediate compartment with the cell periphery. *Mol Biol Cell*. 2006;17(4):1514-26.
245. McKenna A, Hanna M, Banks E, Sivachenko A, Cibulskis K, Kernysky A, et al. The Genome Analysis Toolkit: a MapReduce framework for analyzing next-generation DNA sequencing data. *Genome Res*. 2010;20(9):1297-303.
246. Van der Auwera GA, Carneiro MO, Hartl C, Poplin R, Del Angel G, Levy-Moonshine A, et al. From FastQ data to high confidence variant calls: the Genome Analysis Toolkit best practices pipeline. *Curr Protoc Bioinformatics*. 2013;43(1110):11.0.1-.0.33.
247. Danecek P, Auton A, Abecasis G, Albers CA, Banks E, DePristo MA, et al. The variant call format and VCFtools. *Bioinformatics*. 2011;27(15):2156-8.
248. Wang K, Li M, Hakonarson H. ANNOVAR: functional annotation of genetic variants from high-throughput sequencing data. *Nucleic Acids Res*. 2010;38(16):e164.

249. Cristea I, Bruland O, Rødahl E, Bredrup C. K<sup>+</sup> regulates relocation of Pellino-2 to the site of NLRP3 inflammasome activation in macrophages. *FEBS Letters*. 2021;n/a(n/a).
250. Pear WS, Nolan GP, Scott ML, Baltimore D. Production of high-titer helper-free retroviruses by transient transfection. *Proceedings of the National Academy of Sciences of the United States of America*. 1993;90(18):8392-6.
251. Swift S, Lorens J, Achacoso P, Nolan GP. Rapid production of retroviruses for efficient gene delivery to mammalian cells using 293T cell-based systems. *Curr Protoc Immunol*. 2001;Chapter 10:Unit 10.7C.
252. Daigneault M, Preston JA, Marriott HM, Whyte MKB, Dockrell DH. The Identification of Markers of Macrophage Differentiation in PMA-Stimulated THP-1 Cells and Monocyte-Derived Macrophages. *PLoS one*. 2010;5(1):e8668.
253. Liu X, Lin Z, Xu Y. Pellino1 promoted inflammation in lung injury model of sepsis by TRAF6/ NF- $\kappa$ B signal pathway. *J Inflamm (Lond)*. 2021;18(1):11.
254. Hughes BM, Burton CS, Reese A, Jabeen MF, Wright C, Willis J, et al. Pellino-1 Regulates Immune Responses to Haemophilus influenzae in Models of Inflammatory Lung Disease. *Front Immunol*. 2019;10:1721.
255. Geng Y, Ju Y, Ren F, Qiu Y, Tomita Y, Tomoeda M, et al. Insulin receptor substrate 1/2 (IRS1/2) regulates Wnt/beta-catenin signaling through blocking autophagic degradation of dishevelled2. *J Biol Chem*. 2014;289(16):11230-41.
256. Zotti T, Scudiero I, Vito P, Stilo R. The Emerging Role of TRAF7 in Tumor Development. *Journal of Cellular Physiology*. 2017;232(6):1233-8.
257. Shirakura K, Ishiba R, Kashio T, Funatsu R, Tanaka T, Fukada SI, et al. The Robo4-TRAF7 complex suppresses endothelial hyperpermeability in inflammation. *J Cell Sci*. 2019;132(1).
258. Cho KA, Kang PB. PLIN2 inhibits insulin-induced glucose uptake in myoblasts through the activation of the NLRP3 inflammasome. *Int J Mol Med*. 2015;36(3):839-44.
259. Alyaseer AAA, de Lima MHS, Braga TT. The Role of NLRP3 Inflammasome Activation in the Epithelial to Mesenchymal Transition Process During the Fibrosis. *Frontiers in Immunology*. 2020;11(883).
260. Maeß MB, Wittig B, Lorkowski S. Highly efficient transfection of human THP-1 macrophages by nucleofection. *J Vis Exp*. 2014(91):e51960.
261. Schulze F, Hengst E, Winkler S, Rösen-Wolff A. A transgenic in vitro cell model for the analysis of proinflammatory effects of naturally occurring genetic variants of caspase-1. *Pediatr Rheumatol Online J*. 2015;13(Suppl 1):P18-P.
262. Guzova JA, Primiano MJ, Jiao A, Stock J, Lee C, Winkler AR, et al. Optimized protocols for studying the NLRP3 inflammasome and assessment of potential targets of CP-453,773 in undifferentiated THP1 cells. *J Immunol Methods*. 2019;467:19-28.
263. Li Z, Du L, Li C, Wu W. Human chorionic gonadotropin  $\beta$  induces cell motility via ERK1/2 and MMP-2 activation in human glioblastoma U87MG cells. *J Neurooncol*. 2013;111(3):237-44.
264. Wanzeler ACV, Barbosa IAF, Duarte B, Borges D, Barbosa EB, Kamiji D, et al. Mechanisms and biomarker candidates in pterygium development. *Arq Bras Oftalmol*. 2019;82(6):528-36.
265. Wang Z-C, Zhao W-Y, Cao Y, Liu Y-Q, Sun Q, Shi P, et al. The Roles of Inflammation in Keloid and Hypertrophic Scars. *Frontiers in Immunology*. 2020;11(3185).
266. Wade EM, Daniel PB, Jenkins ZA, McInerney-Leo A, Leo P, Morgan T, et al. Mutations in MAP3K7 that Alter the Activity of the TAK1 Signaling Complex Cause Frontometaphyseal Dysplasia. *Am J Hum Genet*. 2016;99(2):392-406.


267. Wade EM, Jenkins ZA, Daniel PB, Morgan T, Addor MC, Adés LC, et al. Autosomal dominant frontometaphyseal dysplasia: Delineation of the clinical phenotype. *Am J Med Genet A*. 2017;173(7):1739-46.
268. Costantini A, Wallgren-Pettersson C, Mäkitie O. Expansion of the clinical spectrum of frontometaphyseal dysplasia 2 caused by the recurrent mutation p.Pro485Leu in MAP3K7. *Eur J Med Genet*. 2018;61(10):612-5.
269. Lee G, Lee Y, Chang M, Kang SUK, Ryou J-H, Lim J-J, et al. P120 BBT-401 IS A SELECTIVE PELLINO-1 PROTEIN-PROTEIN INTERACTION INHIBITOR IN CLINICAL DEVELOPMENT TARGETING A FIRST-IN-CLASS DRUG FOR UC TREATMENT. *Gastroenterology*. 2019;156(3):S82.

## Appendix

*PELI2* sequence and location of the mutation c.C770T

ATGTTTTCCCTGGCCAGGAGGAACACTGCGCCCCAATAAGGAGCCAGTGAAA  
TACGGGGAGCTGGTGGTGCTCGGGTACAATGGTGCTTACCCAATGGAGATAGA  
GGACGGAGGAAAAGTAGATTTGCCCTCTACAAGCGGCCCAAGGCAAATGGTGTC  
AAACCCAGCACCGTCCATGTGATATCCACGCCCCAGGCATCCAAGGCTATCAGCT  
GCAAAGGTCAACACAGTATATCCTACACTTTGTCAAGGAATCAGACTGTGGTGGT  
GGAGTACACACATGATAAGGATACGGATATGTTTCAGGTGGGCAGATCAACAGA  
AAGCCCTATCGACTTCGTTGTCACAGACACGATTTCTGGCAGCCAGAACACGGAC  
GAAGCCCAGATCACACAGAGCACCATATCCAGGTTGCGCTGCAGGATCGTGTGC  
GACAGGAATGAACCTTACACAGCACGGATATTCGCCGCCGGATTTGACTCTTCCA  
AAAACATATTTCTTGAGAAAAGGCAGCAAAGTGGAAAAACCCCGACGGCCACA  
TGGATGGGCTCACTACTAATGGCGTCCTGGTGTGCATCCACGAGGGGGCTTAC  
CGAGGAGTCCCAGCCGGGTCTGGCGCGAGATCTCTGTCTGTGGAGATGTGTA  
CACCTTGCGAGAAACCAGGTCGGCCCAGCAACGAGGAAAGCTGGTGGAAAGTG  
AGACCAACGTCCTGCAGGACGGCTCCCTCATTGACCTGTGTGGGGCCACTCTCCT  
CTGGAGAACAGCAGATGGGCTTTTTCATACTCCAACTCAGAAGCACATAGAAGC  
CCTCCGGCAGGAGATTAACGCCGCCCGGCCTCAGTGTCTGTGGGGCTCAACACC  
CTGGCCTTCCCAGCATCAACAGGAAAGAGGTGGTGGAGGAGAAGCAGCCCTGG  
GCATATCTCAGTTGTGGCCACGTGCACGGGTACCACAACCTGGGGCCATCGGAGT  
GACACGGAGGCCAACGAGAGGGAGTGTCCCATGTGCAGGACTGTGGGGCCCTAT  
GTGCCTCTCTGGCTTGGCTGTGAGGCAGGATTTTATGTAGACGCAGGACCGCCAA  
CTCATGCTTTCACTCCCTGTGGACACGTGTGCTCGGAGAAGTCTGCAAAATACTG  
GTCTCAGATCCCGTTGCCTCATGGAACCTCATGCATTTACGCTGCTTGCCTTTCT  
GTGCTACACAGCTGGTTGGGGAGCAAACTGCATCAAATTAATTTTCCAAGGTCC  
AATTGACTGA

# K<sup>+</sup> regulates relocation of Pellino-2 to the site of NLRP3 inflammasome activation in macrophages

 Ileana Cristea<sup>1</sup> , Ove Bruland<sup>2</sup> , Eyvind Rødahl<sup>1,3</sup>  and Cecilie Bredrup<sup>1,3</sup> 

1 Department of Clinical Medicine, University of Bergen, Norway

2 Department of Medical Genetics, Haukeland University Hospital, Bergen, Norway

3 Department of Ophthalmology, Haukeland University Hospital, Bergen, Norway

## Correspondence

C. Bredrup, Department of Ophthalmology, Haukeland University Hospital, Jonas Lies vei 72B, Bergen, 5021, Norway  
 Tel: (+47) 55974171  
 E-mail: Cecilie.Bredrup@uib.no

Eyvind Rødahl and Cecilie Bredrup contributed equally to this work.

(Received 22 March 2021, revised 16 July 2021, accepted 8 August 2021)

doi:10.1002/1873-3468.14176

Edited by Wilfried Ellmeier

**Pellino proteins are E3 ubiquitin ligases involved in the innate immune system. Recently, Pellino-2 was reported to modulate the activation of the mouse Nlrp3 inflammasome. We examined the intracellular localization of human Pellino-2 in THP1-derived macrophages during activation with LPS and ATP. We observed that Pellino-2 changed intracellular localization and colocalized with the inflammasome proteins NLRP3 and ASC late in the assembly of the inflammasome. Colocalization with NLRP3 and ASC was also seen in cells maintained in potassium-free medium. The colocalization and inflammasome activation were abrogated by several potassium channel inhibitors, supporting a role for potassium efflux in modulating intracellular localization of Pellino-2. The data suggest that Pellino-2 is essential for mediating the effect of potassium efflux on inflammasome activation.**

**Keywords:** ASC; inflammasome; NLRP3; PELI2; potassium efflux

The four mammalian Pellinos (Pellino-1, Pellino-2, and the two isoforms Pellino-3a and Pellino-3b) have been described as key E3 ubiquitin ligases that mediate innate immune responses [1]. Pellino-2 associates with several signaling proteins involved in the Toll-like receptor (TLR) pathway and functions as a positive regulator of NF- $\kappa$ B activation, leading to the upregulation of pro-inflammatory transcripts IL-6, IL-8, and TNF $\alpha$  [2]. Although the Pellino proteins seem to play distinct roles in immune signaling cascades [3–7], the mechanisms that selectively recruit Pellino-2 remain elusive.

The NLRP3 inflammasome is a cytosolic multiprotein complex that regulates the innate inflammatory response [8]. Its activation is a two-step process, beginning with ‘priming’. In this phase, TLRs are activated by extracellular ligands, leading to increased protein synthesis of components of the inflammasome and precursors of pro-inflammatory cytokines, among them pro-IL-1 $\beta$  [9]. In the second step, ‘activation’, the inflammasome is assembled, cleaving inactive precursors to active pro-inflammatory molecules, such as mature IL-1 $\beta$  [10]. A common intracellular response, potassium (K<sup>+</sup>) efflux [11,12], triggered by a variety of

## Abbreviations

ASC, apoptosis-associated speck-like protein; CO<sub>2</sub>, carbon dioxide; DMEM, Dulbecco’s modified Eagle’s medium; ELISA, enzyme-linked immunosorbent assay; fps, frames per second; HRP, horseradish peroxidase; IgG, immunoglobulin G; IL-1 $\beta$ , interleukin 1 beta; IL-6, interleukin 6; IL-8, interleukin 8; IRAK-1, interleukin 1 receptor-associated kinase 1; K<sup>+</sup>, potassium ions; KCl, potassium chloride; LDS, lithium dodecyl sulfate; LPS, lipopolysaccharide; Lys, lysine; NaCl, sodium chloride; NF- $\kappa$ B, nuclear factor kappa B; NLRP3, NLR family pyrin domain containing 3; PB, phosphate buffer; PFA, paraformaldehyde; PMSF, phenylmethylsulfonyl fluoride; pro-IL-1 $\beta$ , precursor of interleukin 1 beta; s.e.m., standard error of the mean; TLR, Toll-like receptor; TNF $\alpha$ , tumor necrosis factor alpha.



danger signals, like viral DNA, bacterial toxins, and nanoparticles [13,14], leads to the activation of the NLRP3 inflammasome. The effect of K<sup>+</sup> efflux is supported by studies showing that (a) depletion of cytosolic K<sup>+</sup> in response to ATP or nigericin mediates IL-1 $\beta$  maturation, (b) K<sup>+</sup> efflux alone can activate the NLRP3 inflammasome, and (c) high extracellular K<sup>+</sup> concentrations inhibit the activation of the NLRP3 inflammasome [11,15,16].

Recently, Pellino-2 was found to be involved in the activation of the mouse Nlrp3 inflammasome [17]. In a Pellino-2 constitutive knockout mouse model, Humphries and co-workers showed that Pellino-2 is essential in the priming step for the activation of the canonical pathway of the mouse Nlrp3 inflammasome. At the same time, they showed that Pellino-2 did not directly induce poly-ubiquitination of Nlrp3, thus suggesting that Pellino-2 may exert its effects on Nlrp3 in an indirect manner [17].

Although the function of Pellino-2 has been characterized to some extent, a detailed examination of the intracellular localization of Pellino-2 has not been reported. Therefore, in this study, we examined the intracellular localization of Pellino-2 in a human macrophage cell line, with particular emphasis on its interaction with the NLRP3 inflammasome. We show that Pellino-2 colocalizes with the inflammasome proteins NLRP3 and ASC in activated THP1-derived macrophages. This effect is abrogated when pharmacological K<sup>+</sup> channel blockers are used. Although NLRP3 appears to change localization for inflammasome activation, blocking of the K<sup>+</sup> channels prevents the relocation of Pellino-2 and thus the assembly and maturation of the inflammasome. Our findings indicate a significant effect of K<sup>+</sup> efflux on Pellino-2 localization and point to an essential role of Pellino-2 relocation in the activation of the NLRP3 inflammasome.

## Materials and methods

### Expression vectors

Human *PELI2* cDNA encoding full-length human Pellino-2 (UniProt ID: Q9HAT8) was subcloned from a pLenti-Peli2-myc-DDK vector (RC203409L1, OriGene, Rockville, USA) into a pQCXIH/pQCXIP retroviral expression vector (Clontech, California, USA), using BamHI and EcoRI restriction enzymes. An N-terminal GFP tag was inserted containing a linker between the GFP and Pellino-2, consisting of six amino acids (Ser-Gly-Leu-Arg-Ser-Ala) [18]. An additional plasmid was generated by inserting a C-terminal HA tag. All constructs were subsequently verified by Sanger sequencing.

### Transient transfection and cell lysis

For transient transfection, 8  $\mu$ L Lipofectamine 2000 reagent (Invitrogen, Waltham, Massachusetts, USA) and 2  $\mu$ g plasmid DNA encoding HA-tagged or GFP-tagged human Pellino-2 were added to HEK293 cells upon 60–70% confluency in 10-cm plates. Cells were harvested after 40 h. The cells were lysed in 50 mM Tris-HCl pH 7.4, 200 mM NaCl, 5 mM EDTA, 0.1% NP-40, 0.5% Tween-20, 1 mM PMSF and supplemented with complete protease inhibitors (Roche Diagnostics, Mannheim, Germany, #11-836-145-001). Cell lysates were centrifuged to remove cell debris. Bolt LDS sample buffer (Thermo Fisher, Waltham, MA, USA, #B0007) and Bolt sample reducing agent (Thermo Fisher, #B0009) were added before immunoblot analysis.

### Immunoblot analysis

Proteins were separated and transferred onto nitrocellulose membranes using the Bolt<sup>®</sup> Bis-Tris Plus electrophoresis and transfer system (Thermo Fisher Scientific). Membranes were incubated overnight at 4 °C with primary antibodies. The immunodetection of Pellino-2 (1 : 1000 dilution, Sigma-Aldrich, St. Louis, MO, USA, #HPA053182), the HA tag on Pellino-2 (1 : 500 dilution, Thermo Scientific, #71-5500), the GFP tag on Pellino-2 (1 : 500 dilution, Clontech, clone JL-8, #632381), and GAPDH (1 : 10 000 dilution, Sigma-Aldrich, #G9545) was performed according to Cell Signaling Technologies instructions (details in [Supporting information](#)). HRP-linked anti-rabbit IgG antibody (Cell Signaling, Danvers, MA, USA, #7074) at 1 : 2000 dilution was used as secondary antibody (detailed description in [Supporting information](#)).

To test for binding specificity of the Pellino-2 antibody, a blocking peptide PrEST antigen PELI2 (Sigma-Aldrich, #APREST83881) was used at 1 : 1000 dilution. Incubation with the blocking peptide and Pellino-2 antibody was performed in parallel with overnight incubation with the Pellino-2 antibody only.

### THP-1 cell differentiation into macrophages

THP-1 cells (ATCC TIB-202<sup>TM</sup>) were cultured in RPMI-1640 medium, supplemented with 10% FBS, 100 U·mL<sup>-1</sup> penicillin, 100  $\mu$ g·mL<sup>-1</sup> streptomycin, 2 mM L-glutamine, and 0.05 mM 2-mercapto-ethanol. Cells were cultured for no longer than 15 passages.

THP-1 monocytes were gradually transitioned for cultivation in Dulbecco's modified Eagle's medium (DMEM), high glucose (4500 mg·L<sup>-1</sup>), supplemented with 10% fetal bovine serum (FBS), 100 U·mL<sup>-1</sup> penicillin, 100  $\mu$ g·mL<sup>-1</sup> streptomycin, 2 mM L-glutamine, and 0.05 mM 2-mercapto-ethanol.

THP-1 monocytes were differentiated into adherent macrophages, as previously described [19], using 200 nM phorbol-12-myristate-13-acetate (PMA, Cell Signaling, #4174S) for 3 days, followed by a 5-day resting period (THP1PMA cells).

### Treatment of THP1PMA macrophages

Following differentiation into macrophages, the THP1PMA cells were primed with 100 ng·mL<sup>-1</sup> LPS (*E. coli* O111 : B4, Sigma-Aldrich, #LPS25) for 4 h and activated with 5 mM ATP (Thermo Scientific, #R0441) for 15 min, before fixation.

In order to block the activation of the NLRP3 inflammasome, THP1PMA cells were treated with either 10 μM quinine (Abcam, Cambridge, England, #ab141247), 30 mM KCl (Sigma-Aldrich, #1049360500) or 50 μM glyburide (Cayman Chem, Ann Arbor, MI, USA, #15009) for 30 min, before priming with LPS and activation with ATP, as described above.

THP-1 monocytes were also gradually transitioned for cultivation in complete DMEM culture medium, for immunofluorescence experiments involving potassium-free (K<sup>+</sup>-free) culture medium. Before fixation, the cell culture medium was changed for 3 h to DMEM without potassium chloride (KCl) (Cell Culture Technologies, custom-made).

### Immunofluorescence

Cells were seeded at a density of 75 000 cells/well in 12-well dishes on 18-mm glass coverslips coated with 0.1 mg·mL<sup>-1</sup> poly-L-lysine. The staining procedure was performed in accordance with Sannerud and co-workers (2008) (see [Supporting information](#) for details) [20]. The fixation step was performed at room temperature for 30 min using prewarmed 3% PFA in either PBS pH 7.4 or 0.1 M phosphate buffer (PB) pH 7.2.

Double-labeling immunofluorescence analysis was performed in THP1PMA macrophages, using antibodies against Pellino-2 (Sigma-Aldrich, #HPA053182), NLRP3 (Enzo, #ALX-804-819-C100), and ASC (Santa Cruz, #sc-514414). Goat anti-rabbit IgG Alexa Fluor® 488 and goat anti-mouse IgG Alexa Fluor® 594 (#111-546-144 and #115-586-146, both from Jackson Laboratories) were used as secondary antibodies.

### Quantification of secreted IL-1β upon NLRP3 inflammasome activation

THP-1 cells were seeded in 96-well tissue-culture plates (Corning Costar, #9018) at a density of 50 000 cells/well in 100 μL of THP-1 culture medium, supplemented with 200 nM of phorbol-myristate acetate (PMA, Cell Signaling, #4174S), and incubated for 3 days. The medium was replaced with THP-1 culture medium without PMA, and the cultures were allowed to rest for 5 days in the CO<sub>2</sub> incubator.

On the day of the assay, cells were primed with 100 ng·mL<sup>-1</sup> LPS (*E. coli* O111 : B4, #LPS25, Sigma-Aldrich) for 4 h to upregulate genes necessary for NLRP3 inflammasome activation and activated with 5 mM ATP (Thermo Scientific, #R0441) for 15 min. Wherever indicated, THP1PMA cells were also treated with either 10 μM quinine (Abcam, #ab141247), 30 mM KCl (Sigma-Aldrich, #1049360500), or 50 μM glyburide (Cayman Chem, #15009) for 30 min, before priming with LPS and activation with ATP, as described above.

After incubation, supernatants were collected and assayed for IL-1β release using a human IL-1β ELISA kit (Thermo Fisher, #88-7261-88) according to the manufacturer's protocol. Briefly, after precoating with a specific IL-1β antibody, the plates were blocked and incubated overnight with cell culture media from THP1PMA cells. After being washed, the plates were incubated with biotinylated detection antibody, avidin-HRP, and developed by chemiluminescence (see [Supporting information](#) for details).

### Cell viability assay

Cell proliferation/viability following NLRP3 inflammasome activation in THP1PMA cells was assessed by WST-1 assay. Twenty-four hours after inflammasome activation, the WST-1 reagent (Roche, #5015944001) was added into the wells at a 1 : 10 dilution and incubated at 37 °C for 4 h. The optical density (OD) was measured at wavelength 440 nm with correction at 650 nm, using a BioTek Synergy™ HT microplate reader.

### Image acquisition and analysis

Images were acquired using Leica SP5 and SP8 confocal laser scanning microscopes (Leica Microsystems). The Z-stack function was used to enhance resolution and allow for 3D examination, in order to confirm colocalization. Scale bar is 20 μm and the video frame rate 5 fps. Postprocessing of images was performed using the integrated adaptive deconvolution module Lightning (Leica Microsystems).

### Statistical analysis and reproducibility

Two-way ANOVA, followed by Tukey's multiple comparisons test, was performed for statistical analysis. All results have been replicated in at least 3 independent experiments.

## Results

### Validating Pellino-2 antibody specificity

In order to validate the commercial rabbit polyclonal Pellino-2 antibody used in this paper (targeting a C-terminal amino acid sequence NRKEVVEEKQPWA

YLSCGHVHGYHN), we first examined HEK293 cells transiently transfected with plasmids containing Pellino-2 tagged with either an HA tag or a GFP tag. Cell lysates were analyzed by immunoblotting using anti-Pellino-2 antibody, as well as anti-HA, anti-GFP, and anti-GAPDH antibodies (Fig. S1A). The anti-Pellino-2 antibody revealed endogenous Pellino-2 (MW 46 kDa), as well as the overexpressed HA-tagged Pellino-2 (MW 50 kDa) and GFP-tagged Pellino-2 (MW 73 kDa) at expected molecular weights. The overexpressed protein was also identified with anti-HA and anti-GFP antibodies. Next, we used a blocking peptide against the Pellino-2 antibody, PrEST antigen PELI2 (Fig. S1B), and we showed that binding of the antibody was effectively blocked by this antigen.

In immunofluorescence experiments, the anti-Pellino-2 antibody recognized both endogenous and overexpressed FLAG-tagged Pellino-2 (Fig. S1C). We

thereby concluded that the antibody was specific for Pellino-2.

### Pellino-2 colocalization with NLRP3 and ASC in primed and activated THP-1 derived macrophages

Given the recent report indicating that Pellino-2 influences Nlrp3 inflammasome activation in mouse macrophages, we investigated the localization of Pellino-2 in the human-derived immune cell line THP-1. We differentiated THP-1 monocytes into adherent macrophages (THP1PMA) using phorbol-12-myristate-13-acetate (PMA), followed by priming and activation, to initiate inflammasome assembly and release of mature pro-inflammatory cytokines.

In THP1PMA cells under resting conditions (Fig. 1), Pellino-2 was constitutively expressed and

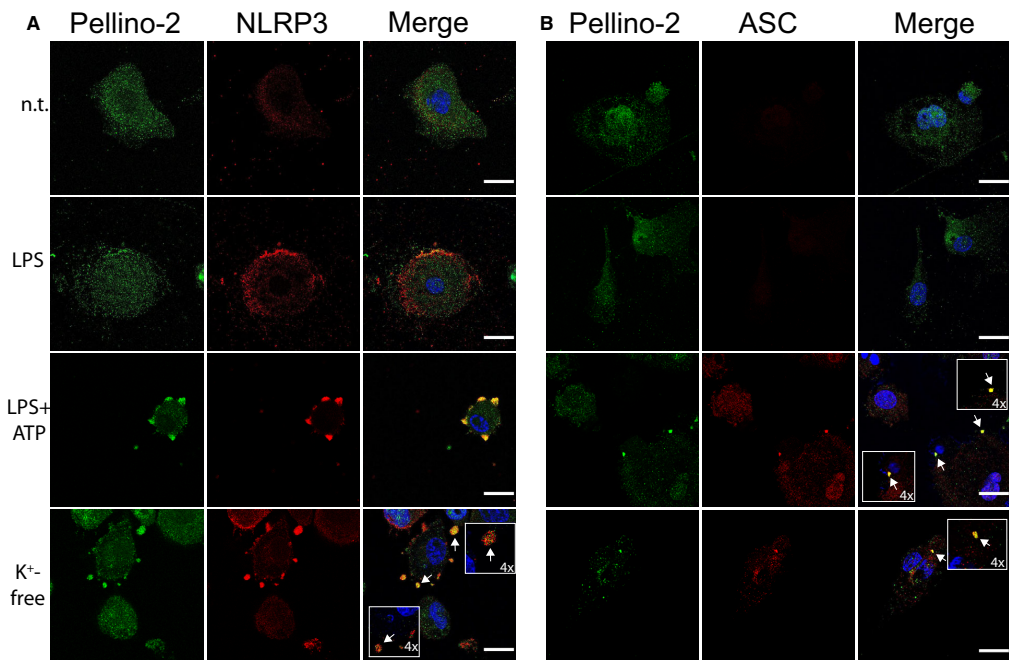


**Fig. 1.** Pellino-2 colocalizes with NLRP3 and ASC in primed and activated macrophages. THP-1 monocytes were differentiated into adherent macrophages using 200 nM phorbol-12-myristate-13-acetate (PMA) for 3 days, followed by a 5-day resting period. THP1PMA macrophages were subjected to indirect immunofluorescence, using PBS as fixation buffer for the fixative agent (3% PFA) without any prior treatment (n.t.), primed with 100 ng·mL<sup>-1</sup> LPS for 4 h (LPS), primed with 100 ng·mL<sup>-1</sup> LPS for 4 h and stimulated with 5 mM ATP for 15 min (LPS+ATP), or cultivated in potassium-free DMEM medium for 3 h (K<sup>+</sup>-free). The fluorescent images show endogenous Pellino-2, endogenous NLRP3 (A) or endogenous ASC (B) and nuclei (DAPI). The insets represent a 4 times magnification of the original images, postprocessed using the deconvolution module Lightning. Scale bar: 20 μm.

located in the cytoplasm, while expression of the NLRP3 protein was minimal.

Upon priming with LPS, upregulation of NLRP3 protein expression was seen, with a more specific and restricted localization close to the plasma membrane, indicating early stages of inflammasome activation. This was confirmed by the levels of secreted IL-1 $\beta$  in LPS-primed THP1PMA cells (Fig. 2). After activation with ATP, Pellino-2 changed location and became colocalized with the inflammasome protein NLRP3 (Fig. 1A) and with the adaptor protein ASC (Fig. 1B).

Thus, Pellino-2 changed its intracellular localization, depending on the activation status of the macrophages: In resting macrophages, Pellino-2 was spread diffusely in the cytoplasm, whereas during activation with ATP after priming with LPS, Pellino-2 concentrated at the site of the inflammasome and colocalized with NLRP3 and ASC.

### Extracellular K<sup>+</sup> ions influence localization of endogenous Pellino-2 and the activation of the inflammasome

Due to the role of K<sup>+</sup> efflux in NLRP3 inflammasome activation [11], we wanted to examine whether extracellular K<sup>+</sup> levels influence the localization of Pellino-2.

We first cultivated THP1PMA cells in K<sup>+</sup>-free medium for 3 h and performed immunofluorescence analysis using antibodies against Pellino-2, NLRP3, and ASC. In these cells, which had not been treated with LPS and ATP, restricted localization of the NLRP3 protein at the plasma membrane (Fig. 1A: K<sup>+</sup>-free), as well as ASC speck formation (Fig. 1B: K<sup>+</sup>-free), was seen, indicating activation of the inflammasome. In addition, relocation of Pellino-2 from the cytoplasm to the site of NLRP3 inflammasome activation (Fig. 1) and colocalization with the NLRP3 protein (Video S1)

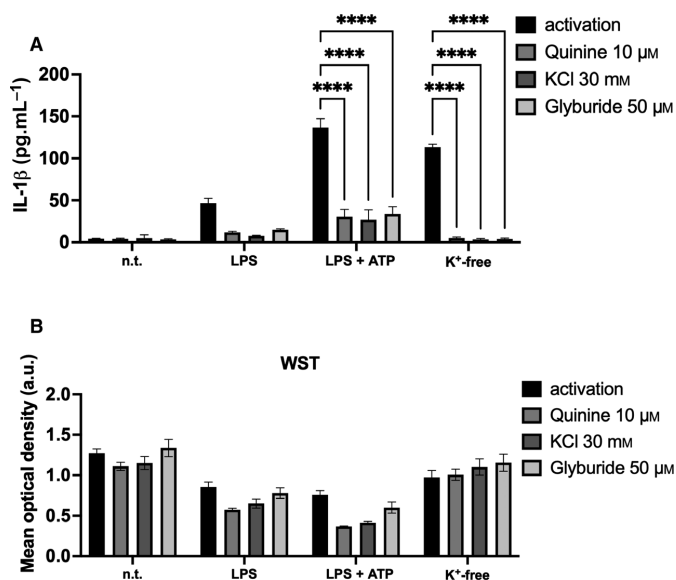


**Fig. 2.** NLRP3 inflammasome activation, measured in the levels of secreted IL-1 $\beta$ , followed by cell viability assay. (A) THP1PMA cells were left without any treatment (n.t.), or were primed with 100 ng mL<sup>-1</sup> LPS for 4 h (LPS), primed with 100 ng mL<sup>-1</sup> LPS for 4 h and stimulated with 5 mM ATP for 15 min (LPS+ATP) or cultivated in potassium-free DMEM medium for 3 h (K<sup>+</sup>-free), to induce NLRP3 inflammasome activation. Additionally, the cells were incubated with either 10  $\mu\text{M}$  quinine, 30 mM KCl, or 50  $\mu\text{M}$  glyburide for 30 min, before priming with LPS and activation with ATP, as described above. Supernatants were harvested, and the measurement of secreted IL-1 $\beta$  was performed by ELISA analysis. Data are shown as mean  $\pm$  s.e.m. of 3 biological replicates, each with 2 technical replicates. Statistical analysis was performed using two-way ANOVA, followed by Tukey's test. \*\*\*\*  $P < 0.0001$ . (B) The viability of the cells was measured 24 h after NLRP3 inflammasome activation, using the WST-1 assay. The WST-1 reagent was added in 1 : 10 dilution to the cells and further incubated for 4 h at 37  $^{\circ}\text{C}$ . Data are shown as mean  $\pm$  s.e.m. of 3 biological replicates. The cell viability assay performed 24 h after activation of the THP1PMA macrophages showed that the NLRP3 inflammasome activation affects the cells' viability.

and ASC protein (Video S2) were seen. This was similar to our findings in cells activated with ATP at physiological K<sup>+</sup> concentration. We used the Lightning deconvolution tool to achieve confocal super-resolution down to 120 nm: Pellino-2 was detected in very close proximity to both NLRP3 and ASC. The data suggested that low levels of extracellular K<sup>+</sup> alone are sufficient to activate the NLRP3 inflammasome and also to initiate the interaction of Pellino-2 with NLRP3 and ASC.

We next proceeded to study several known pharmacological K<sup>+</sup> channel inhibitors. We blocked the efflux of K<sup>+</sup> ions from THP1PMA-derived macrophages by incubating them with quinine (Fig. 3A), KCl (Fig. 3B), or glyburide (Fig. 3C) prior to their activation. Upon treatment with these compounds, Pellino-2 did not change localization even upon activation with LPS plus ATP or by cultivation in K<sup>+</sup>-free medium. Pellino-2 continued to show only a punctate cytoplasmic localization, indicating that Pellino-2 localization is directly sensitive to K<sup>+</sup> efflux from the cells.

In contrast, in cells treated with quinine, KCl, or glyburide, activation with LPS plus ATP or cultivation in K<sup>+</sup>-free medium resulted in a change of NLRP3 localization (Fig. 3). However, while in activated cells, the NLRP3 inflammasome is normally present as large aggregates close to the plasma membrane, in cells treated with K<sup>+</sup> channel blockers, NLRP3 was seen as multiple, small protein collections along the plasma membrane. We also found significantly reduced levels of IL-1 $\beta$  secretion (Fig. 2), suggesting that the final stages of NLRP3 inflammasome assembly had not been fully completed.

### The effect of K<sup>+</sup> ions in the fixation buffer

Since we observed an effect of K<sup>+</sup> efflux on Pellino-2 intracellular localization, it was of interest to examine the consequences of removing K<sup>+</sup> from the fixation buffer. The fixation buffer used in the immunofluorescence experiments was PBS (Figs 1 and 3), which contains 2.7 mM KCl and 1.8 mM KH<sub>2</sub>PO<sub>4</sub>. In immunofluorescence experiments, PBS is frequently interchanged with PB, which does not contain K<sup>+</sup>.

In PB-fixed THP1PMA cells, Pellino-2 was localized to the cytoplasm (Fig. 4). However, in THP1PMA cells primed with LPS before PB-fixation, Pellino-2 presented in the nucleus. Otherwise, priming and activation of the NLRP3 inflammasome, as well as relocation of Pellino-2 intracellularly and its colocalization with NLRP3 after culturing the cells in K<sup>+</sup>-free culture medium, were similar in PB- and PBS-fixed cells (Figs 1 and 4). Thus, the absence of K<sup>+</sup> in the fixation

buffer may influence the localization of Pellino-2 under certain circumstances.

## Discussion

Relocation of the Pellino protein has been reported in smaller organisms such as *Drosophila* [21]. In this study, we aimed to characterize the intracellular localization of Pellino-2 in a human macrophage cell line, with particular emphasis on its relation to the NLRP3 inflammasome. We showed that Pellino-2 colocalizes with the inflammasome proteins NLRP3 and ASC in activated THP1-derived macrophages. In addition to the activation status of the macrophages, the absence or presence of K<sup>+</sup> in the extracellular environment also determined the intracellular localization of Pellino-2, suggesting that Pellino-2 may translocate between various intracellular compartments in response to K<sup>+</sup> efflux, a common intracellular mechanism that leads to NLRP3 inflammasome activation.

The colocalization of Pellino-2 with the NLRP3 inflammasome is in line with previous reports of Pellino-2 assisting in NLRP3 inflammasome activation [17]. Humphries and co-workers suggested that Pellino-2 participates in the inflammasome activation, by indirectly promoting Lys-63-linked poly-ubiquitination of NLRP3 in the priming step. They demonstrated that LPS induces a time-dependent interaction of Pellino-2 with NLRP3 [17]. While they did not see a direct binding of Pellino-2 to NLRP3 in immunoprecipitation experiments, Pellino-2 coimmunoprecipitated with IRAK1. This suggested that ubiquitination could occur by counteracting the inhibitory effect of the Pellino-2 interaction partner IRAK1 on NLRP3. Our observation, that Pellino-2 colocalized with the inflammasome proteins NLRP3 and ASC after activation with ATP, is consistent with an indirect effect of Pellino-2 on the NLRP3 inflammasome during the priming phase, but also suggests that Pellino-2 could also have a more direct effect during the activation phase.

The presence of activated NLRP3 inflammasomes was indicated by the restricted localization of the NLRP3 protein (Fig. 1A) and the speck formation of ASC (Fig. 1B), as well as the increased secretion of IL-1 $\beta$  in the supernatants of the cell culture (Fig. 2A). While resting or primed macrophages displayed typical morphological characteristics of macrophages, such as increased cytoplasmic volume, activated macrophages by LPS plus ATP treatment had a smaller cellular volume, presumably, at least in part, due to K<sup>+</sup> ions efflux. It is in these smaller cells that we observed colocalization between Pellino-2 and NLRP3 and ASC (Fig. 1).

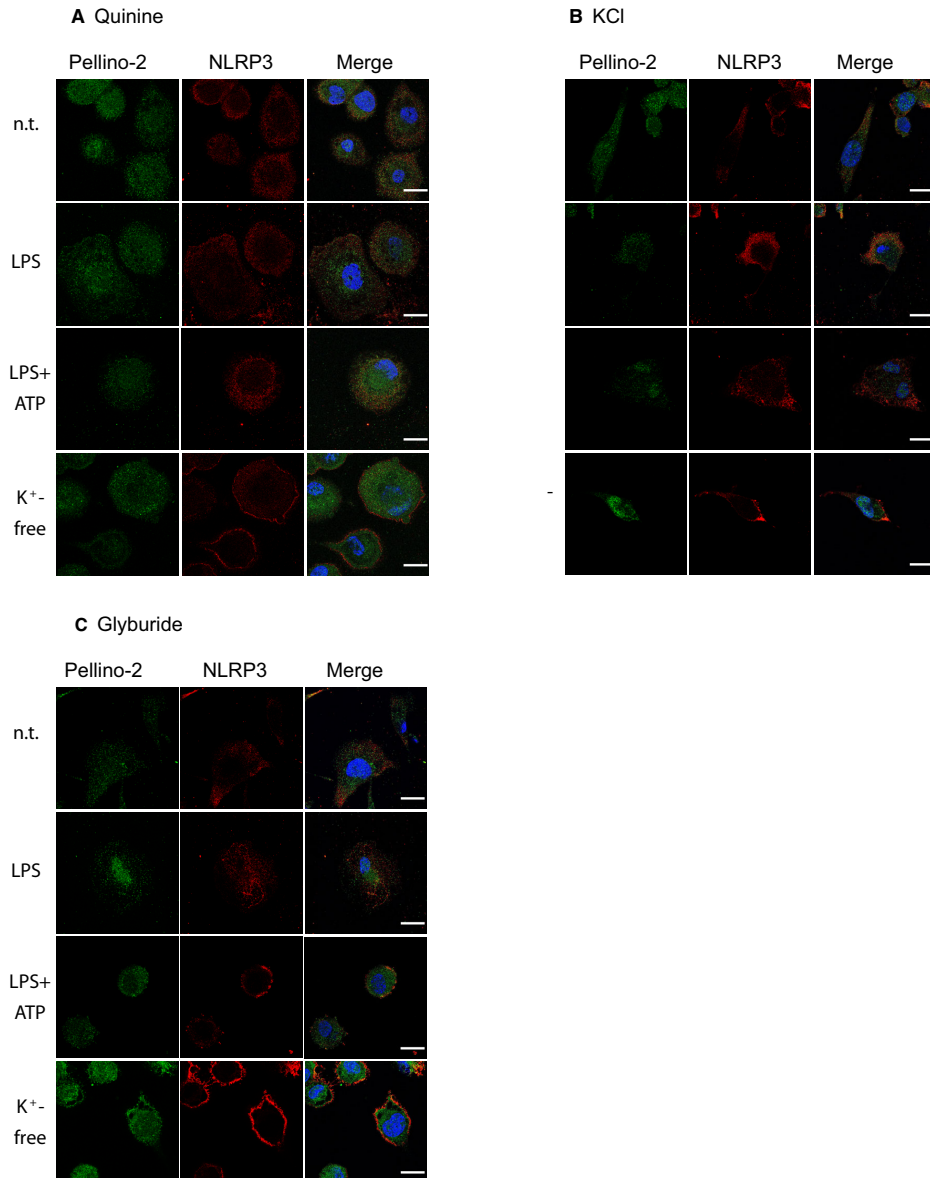


**Fig. 3.** Blocking the activation of the NLRP3 inflammasome abrogates colocalization between Pellino-2 and NLRP3. THP-1 monocytes were differentiated into adherent macrophages using 200 nM phorbol-12-myristate-13-acetate (PMA) for 3 days, followed by a 5-day resting period. THP1PMA macrophages were subjected to indirect immunofluorescence, using PBS as fixation buffer for the fixative agent (3% PFA). The cells were incubated for 30 min with 10  $\mu\text{M}$  quinine (A), 30 mM KCl (B), or 50  $\mu\text{M}$  glyburide (C), followed by no treatment (n.t.), priming with 100  $\text{ng}\cdot\text{mL}^{-1}$  LPS for 4 h (LPS), priming with 100  $\text{ng}\cdot\text{mL}^{-1}$  LPS for 4 h and stimulation with 5 mM ATP for 15 min (LPS+ATP), or cultivation in potassium-free DMEM medium for 3 h (K<sup>+</sup>-free). The fluorescent images show endogenous Pellino-2, endogenous NLRP3, and nuclei (DAPI). Scale bar: 20  $\mu\text{m}$ .

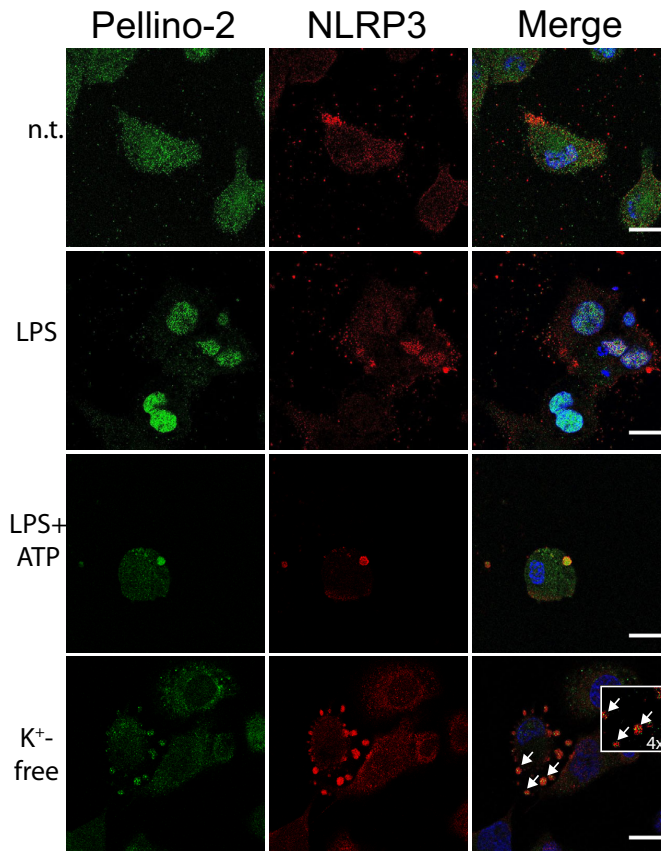


**Fig. 4.** The fixation buffer influences Pellino-2 localization in primed and activated macrophages. THP-1 monocyte cells were differentiated into adherent macrophages using 200 nM PMA for 3 days, followed by a 5-day resting period. THP1PMA macrophages (A) without any prior treatment (n.t.), (B) primed with 100 ng·mL<sup>-1</sup> LPS for 4 h (LPS), (C) primed with 100 ng·mL<sup>-1</sup> LPS for 4 h and stimulated with 5 mM ATP for 15 min (LPS+ATP), or (D) cultivated in potassium-free DMEM medium for 3 h ( $K^+$ -free) were fixed using 3% PFA in 0.1 M phosphate buffer, pH = 7.2 and subjected to indirect immunofluorescence. The fluorescent images show endogenous Pellino-2, endogenous NLRP3, and nuclei (DAPI). The inset represents a 4 times magnification of the original image, postprocessed using the deconvolution module Lightning. Scale bar: 20  $\mu$ m.

In experiments using  $K^+$ -depleted culture medium, we showed that low extracellular level of  $K^+$  alone can activate the inflammasome protein NLRP3 and initiate the interaction of Pellino-2 with NLRP3, pointing to an essential role of Pellino-2 relocation in the activation of the inflammasome. Similar observations of the effect of  $K^+$  efflux on NLRP3 inflammasome activation have been reported by Muñoz-Planillo and co-workers [11]. They showed that a reduction in cytosolic levels of  $K^+$  is both a necessary and sufficient step for activating the NLRP3 inflammasome in mice. However, the  $K^+$  response of Pellino-2 in our hands

was different from that of NLRP3, in that it occurred later in the inflammasome assembly and was completely blocked by several known blockers of the NLRP3 inflammasome.

While the canonical pathway for activating the NLRP3 inflammasome consists of two signals, priming and activation, in cells cultured in  $K^+$ -free medium this process seems to be reduced to a single step consisting only of  $K^+$  efflux. Our findings suggest that Pellino-2 is a sensor for  $K^+$  efflux that can subsequently trigger intracellular signaling downstream of TLR in the absence of a ligand.

NLRP3 inflammasome activation can be blocked by various chemicals. Quinine has been shown to inhibit K<sup>+</sup> efflux via the two-pore domain potassium channel TWIK2 [22]; high concentrations of extracellular K<sup>+</sup> ions inhibit the K<sup>+</sup> efflux necessary for activation of the NLRP3 inflammasome [11]; glyburide inhibits LPS plus ATP-induced caspase-1 activation, IL-1 $\beta$  secretion, and macrophage death [23]. We found that upon treatment with any of these blockers, signs of early activation of the NLRP3 inflammasome were present, albeit to a much lesser extent than in untreated cells. While NLRP3 relocated to the edge of the cells (Fig. 3), the levels of secreted IL-1 $\beta$  were significantly reduced (Fig. 2). Pellino-2, on the other hand, did not change intracellular localization when K<sup>+</sup> efflux was blocked with quinine, KCl, or glyburide (Fig. 3). It appears that NLRP3 can be partially activated, even in the presence of NLRP3 inflammasome blockers, suggesting that the blockers do not directly affect the NLRP3 protein. In contrast, blocking K<sup>+</sup> efflux prevents Pellino-2 relocation, and this could be the reason full inflammasome activation does not occur.

Paraformaldehyde is a common fixative used in immunofluorescence experiments and both PB and PBS are used as fixation buffers. Since Pellino-2 was observed to relocate in the cells in the absence of extracellular K<sup>+</sup>, we compared Pellino-2 localization using the two buffers. When using K<sup>+</sup>-free fixation buffer in primed immune cells, Pellino-2 surprisingly relocated to the nucleus (Fig. 4: LPS). While the significance of this finding for physiological conditions is not clear, it is important in future studies to use a K<sup>+</sup>-containing fixation buffer to maintain physiological conditions and avoid inconsistent results.

In summary, we show that Pellino-2 colocalizes with the inflammasome proteins NLRP3 and ASC in THP1-derived activated macrophages at a late stage of the inflammasome assembly. In immunofluorescence experiments, Pellino-2 is found in different intracellular compartments, depending on the absence or presence of K<sup>+</sup> in the extracellular environment, indicating a role for K<sup>+</sup> efflux in modulating intracellular transport of Pellino-2. When blocking K<sup>+</sup> efflux, the relocation of Pellino-2 is abrogated, as well as the activation of the NLRP3 inflammasome. Thus, our results indicate that Pellino-2 localization is directly sensitive to K<sup>+</sup> efflux from the cells and modulates the activation of the NLRP3 inflammasome.

## Acknowledgments

We would like to thank Unni Larsen for technical assistance, and we express our gratitude to prof.

Jaakko Saraste for valuable discussions regarding the immunofluorescence analysis. The immunofluorescence imaging was performed at the Molecular Imaging Center (MIC), Department of Biomedicine, University of Bergen, Norway. The work was supported by grants from the Western Norway Regional Health Authority (911977 and 912161), Inger Holm's Memory Foundation, and Dr. Jon S. Larsen's Foundation.

## Data accessibility

The data that support the findings of this study are available in the supplementary material of this article.

## Author contributions

ER and CB conceived and supervised the study. IC and OB performed the experiments. IC, ER, and CB wrote the manuscript. IC, OB, ER, and CB designed experiments, analyzed data, and reviewed the manuscript.

## References

- 1 Moynagh PN (2014) The roles of Pellino E3 ubiquitin ligases in immunity. *Nat Rev Immunol* **14**, 122–131.
- 2 Kim TW, Yu M, Zhou H, Cui W, Wang J, DiCorleto P, Fox P, Xiao H and Li X (2012) Pellino 2 Is critical for Toll-like Receptor/Interleukin-1 Receptor (TLR/IL-1R)-mediated Post-transcriptional Control. *J Biol Chem* **287**, 25686–25695.
- 3 Jiang Z, Johnson HJ, Nie H, Qin J, Bird TA and Li X (2003) Pellino 1 is required for interleukin-1 (IL-1)-mediated signaling through its interaction with the IL-1 receptor-associated kinase 4 (IRAK4)-IRAK-tumor necrosis factor receptor-associated factor 6 (TRAF6) complex. *J Biol Chem* **278**, 10952–10956.
- 4 Chang M, Jin W, Chang J-H, Xiao Y, Brittain GC, Yu J, Zhou X, Wang Y-H, Cheng X, Li P *et al.*, (2011) The ubiquitin ligase Peli1 negatively regulates T cell activation and prevents autoimmunity. *Nat Immunol* **12**, 1002–1009.
- 5 Enesa K, Ordureau A, Smith H, Barford D, Cheung PCF, Patterson-Kane J, Arthur JSC and Cohen P (2012) Pellino1 Is required for interferon production by viral double-stranded RNA. *J Biol Chem* **287**, 34825–34835.
- 6 Siednienko J, Jackson R, Mellett M, Delagic N, Yang S, Wang B, Tang LS, Callanan JJ, Mahon BP and Moynagh PN (2012) Pellino3 targets the IRF7 pathway and facilitates autoregulation of TLR3- and viral-induced expression of type I interferons. *Nat Immunol* **13**, 1055–1062.



- 7 Yang S, Wang B, Tang LS, Siednienko J, Callanan JJ and Moynagh PN (2013) Pellino3 targets RIP1 and regulates the pro-apoptotic effects of TNF- $\alpha$ . *Nat Commun* **4**, 2583.
- 8 Lu A and Wu H (2015) Structural mechanisms of inflammasome assembly. *Febs j* **282**, 435–444.
- 9 Bauernfeind FG, Horvath G, Stutz A, Alnemri ES, MacDonald K, Speert D, Fernandes-Alnemri T, Wu J, Monks BG, Fitzgerald KA *et al.*, (1950) (2009) Cutting edge: NF- $\kappa$ B activating pattern recognition and cytokine receptors license NLRP3 inflammasome activation by regulating NLRP3 expression. *J Immunol* **183**, 787–791.
- 10 Elliott EI and Sutterwala FS (2015) Initiation and perpetuation of NLRP3 inflammasome activation and assembly. *Immunol Rev* **265**, 35–52.
- 11 Munoz-Planillo R, Kuffa P, Martinez-Colon G, Smith BL, Rajendiran TM and Nunez G (2013) K(+) efflux is the common trigger of NLRP3 inflammasome activation by bacterial toxins and particulate matter. *Immunity* **38**, 1142–1153.
- 12 Lamkanfi M and Dixit VM (2014) Mechanisms and Functions of Inflammasomes. *Cell* **157**, 1013–1022.
- 13 Franchi L, Muñoz-Planillo R and Núñez G (2012) Sensing and reacting to microbes through the inflammasomes. *Nat Immunol* **13**, 325–332.
- 14 Hornung V, Bauernfeind F, Halle A, Samstad EO, Kono H, Rock KL, Fitzgerald KA and Latz E (2008) Silica crystals and aluminum salts activate the NALP3 inflammasome through phagosomal destabilization. *Nat Immunol* **9**, 847–856.
- 15 Walev I, Klein J, Husmann M, Valeva A, Strauch S, Wirtz H, Weichel O and Bhakdi S (2000) Potassium regulates IL-1 $\beta$  processing via calcium-independent phospholipase A2. *J Immunol* **164**, 5120–5124.
- 16 Pétrilli V, Papin S, Dostert C, Mayor A, Martinon F and Tschopp J (2007) Activation of the NALP3 inflammasome is triggered by low intracellular potassium concentration. *Cell Death Differ* **14**, 1583–1589.
- 17 Humphries F, Bergin R, Jackson R, Delagic N, Wang B, Yang S, Dubois AV, Ingram RJ and Moynagh PN (2018) The E3 ubiquitin ligase Pellino2 mediates priming of the NLRP3 inflammasome. *Nat Commun* **9**, 1560.
- 18 Sannerud R, Marie M, Nizak C, Dale HA, Pernet-Gallay K, Perez F, Goud B and Saraste J (2006) Rab1 defines a novel pathway connecting the pre-Golgi intermediate compartment with the cell periphery. *Mol Biol Cell* **17**, 1514–1526.
- 19 Daigneault M, Preston JA, Marriott HM, Whyte MKB and Dockrell DH (2010) The identification of markers of macrophage differentiation in PMA-stimulated THP-1 cells and monocyte-derived macrophages. *PLoS One* **5**, e8668.
- 20 Sannerud R, Marie M, Hansen BB and Saraste J (2008) Use of polarized PC12 cells to monitor protein localization in the early biosynthetic pathway. *Methods Mol Biol* **457**, 253–265.
- 21 Ji S, Sun M, Zheng X, Li L, Sun L, Chen D and Sun Q (2014) Cell-surface localization of Pellino antagonizes Toll-mediated innate immune signalling by controlling MyD88 turnover in Drosophila. *Nat Commun* **5**, 3458.
- 22 Di A, Xiong S, Ye Z, Malireddi RKS, Kometani S, Zhong M, Mittal M, Hong Z, Kanneganti T-D, Rehman J *et al.* (2018) The TWIK2 potassium efflux channel in macrophages mediates NLRP3 inflammasome-induced inflammation. *Immunity* **49**, 56–65.e4.
- 23 Lamkanfi M, Mueller JL, Vitari AC, Misaghi S, Fedorova A, Deshayes K, Lee WP, Hoffman AM and Dixit VM (2009) Glyburide inhibits the Cryopyrin/Nalp3 inflammasome. *J Cell Biol* **187**, 61–70.

## Supporting information

Additional supporting information may be found online in the Supporting Information section at the end of the article.

**Video S1.** Pellino-2 colocalizes with NLRP3 protein in activated macrophages. THP-1 monocytes were differentiated into adherent macrophages using 200 nM phorbol-12-myristate-13-acetate (PMA) for 3 days, followed by a 5-day resting period. THPIPMA macrophages were primed with 100 ng-mL LPS for 4 h and stimulated with 5 mM ATP for 15 min. The cells were subjected to indirect immunofluorescence, using PBS as fixation buffer for the fixative agent (3% PFA). The fluorescent images show endogenous Pellino-2, endogenous NLRP3 and nuclei (DAPI). Scale bar is 20  $\mu$ m and the video frame rate 5 fps.

**Video S2.** Pellino-2 colocalizes with ASC protein in activated macrophages. THP-1 monocytes were differentiated into adherent macrophages using 200 nM phorbol-12-myristate-13-acetate (PMA) for 3 days, followed by a 5-day resting period. THPIPMA macrophages were primed with 100 ng-mL LPS for 4 h and stimulated with 5 mM ATP for 15 min. The cells were subjected to indirect immunofluorescence, using PBS as fixation buffer for the fixative agent (3% PFA). The fluorescent images show endogenous Pellino-2, endogenous ASC and nuclei (DAPI). Scale bar is 20  $\mu$ m and the video frame rate 5 fps.

**Supplementary Material** Effect of K<sup>+</sup> ions on Pellino-2 intracellular localization.

**Fig. S1.** Anti-Pellino-2 antibody specifically recognizes endogenous and overexpressed Pellino-2 and is blocked by a specific blocking antigen.

## Errata

Page VII Article I has a different title: “Effect of K<sup>+</sup> ions on intracellular localization of Pellino-2” – corrected to “K<sup>+</sup> regulates relocation of Pellino-2 to the site of NLRP3 inflammasome activation in macrophages”

Page VII Misspelling in the title of Article II: “non-immune” – corrected to “nonimmune”

Page VII Article II was accepted for publication in FEBS Letters – doi.org/10.1002/1873-3468.14212

Page 26 Punctuation mistake: the comma before reference (92) should be placed after the reference: “during the priming step, (92)...” – corrected to “during the priming step (92), ...”

Page 28 Misspelling in the Abbreviations list of Table 3: “penumoniae” – corrected to “pneumoniae”

Page 49 Article I has a different title: “Effect of K<sup>+</sup> ions on intracellular localization of Pellino-2” – corrected to “K<sup>+</sup> regulates relocation of Pellino-2 to the site of NLRP3 inflammasome activation in macrophages”

Page 50 Misspelling in the title of Article II: “non-immune” – corrected to “nonimmune”

Page 57 Misspelling “blocking K<sup>+</sup> channels inhibit Pellino-2 relocation” – corrected to “blocking K<sup>+</sup> channels inhibits Pellino-2 relocation”

Page 59 Missing reference for the sentence “TRAF7 interacts with ROBO-4, a member of the ROBO family of proteins”

Shirakura K, Ishiba R, Kashio T, Funatsu R, Tanaka T, Fukada SI, Ishimoto K, Hino N, Kondoh M, Ago Y, Fujio Y, Yano K, Doi T, Aird WC, Okada Y. The Robo4-TRAF7 complex suppresses endothelial hyperpermeability in inflammation. *J Cell Sci.* 2019 Jan 2;132(1):jcs220228. doi: 10.1242/jcs.220228. PMID: 30510113.





Graphic design: Communication Division, UIB / Print: Skjipes Kommunikasjon AS



[uib.no](http://uib.no)

ISBN: 9788230865347 (print)  
9788230864494 (PDF)